THE HONG KONG
POLYTECHNIC UNIVERSITY
香港理工大學
Pao Yue-kong Library
包玉剛圖書館

Copyright Undertaking

This thesis is protected by copyright, with all rights reserved.

By reading and using the thesis, the reader understands and agrees to the following terms:

1. The reader will abide by the rules and legal ordinances governing copyright regarding the use of the thesis.
2. The reader will use the thesis for the purpose of research or private study only and not for distribution or further reproduction or any other purpose.
3. The reader agrees to indemnify and hold the University harmless from and against any loss, damage, cost, liability or expenses arising from copyright infringement or unauthorized usage.

IMPORTANT

If you have reasons to believe that any materials in this thesis are deemed not suitable to be distributed in this form, or a copyright owner having difficulty with the material being included in our database, please contact lbsys@polyu.edu.hk providing details. The Library will look into your claim and consider taking remedial action upon receipt of the written requests.

Pao Yue-kong Library, The Hong Kong Polytechnic University, Hung Hom, Kowloon, Hong Kong

http://www.lib.polyu.edu.hk

DEVELOPMENT OF HIGH-PERFORMANCE PREPLACED AGGREGATE CONCRETE

KUNAL KRISHNA DAS

PhD

The Hong Kong Polytechnic University

2022

The Hong Kong Polytechnic University

Department of Civil and Environmental Engineering

Development of High-Performance Preplaced Aggregate Concrete

Kunal Krishna Das

A thesis submitted in partial fulfilment of the requirements for the degree of Doctor of Philosophy

August 2021

CERTIFICATE OF ORIGINALITY

I hereby declare that this thesis is my own work and that, to the best of my knowledge and belief, it reproduces no material previously published or written, nor material that has been accepted for the award of any other degree or diploma, except where due acknowledgement has been made in the text.

_____ (Signed)

Kunal Krishna Das (Name of student)

To Maa and Deauta

for their constant love and support

ABSTRACT

Preplaced aggregate concrete ("PAC") is produced by pre-placing coarse aggregates into formwork and then injecting grout to fill in the voids between the coarse aggregates. Grout can be applied in two ways, i.e. gravity process and pumping process. In the gravity process, grout is applied from the top to flow under the action of gravity. In the pumping process, grout is pumped under pressure. Gravity process is limited to PAC having larger-size coarse aggregates. In most places including Hong Kong, size of commonly available coarse aggregates ranges from 10 mm to 20 mm, and this makes the pumping process inevitable. This requires the use of complex pumping equipment for grouting and results in underutilization of PAC, despite its high potentials. Further, to produce PAC using smaller-size coarse aggregates and through gravity process, grout needs to possess high performance such as high flowability and high cohesiveness (i.e. high resistance to bleeding) and this is achievable by optimizing the grout mix proportions.

For delivering a user-friendly approach towards the production of PAC, it is essential to investigate the feasibility of producing PAC with readily available resources, such as regular or smaller-size coarse aggregates and possible exclusion of pumping equipment. Incorporation of supplementary cementitious materials such as ground granulated blast furnace slag (GGBS) and silica fume (SF) in PAC can improve and impart desirable properties to PAC. Hence, experimental investigations were conducted to determine the effect of grout mix proportion, coarse aggregate size, and grouting process on mechanical properties and durability of PAC, for its sustainable application to repair works and small-scale constructions.

Experimental results have demonstrated that PAC can be produced successfully via gravity process, using traditional cement-sand grout with coarse aggregate size of 20 mm, displaying compatible performance to that of pumping process. For efficient penetrability of the grout through the coarse aggregate skeleton, flowability of the grout needs to be regulated within a suitable range (efflux time less than 20 seconds).

In terms of supplementary cementitious materials, GGBS enhances the flowability of grout, whereas SF improves the compressive strength of grout. By optimizing the composition of SF and GGBS, grout with suitable flowability and acceptable strength can be produced. GGBS and SF enhance the resistance to chloride ion penetration. PAC incorporating GGBS and SF (especially 40% GGBS and 10% SF) displays improved resistance to chloride ion penetration, and this is ascribed to high cement replacements. Given that production of cement alone contributes to the third-largest anthropogenic emission of CO_2, successful utilization of industrial by-products like GGBS and SF to form PAC helps to reduce the carbon footprint. In terms of drying shrinkage, low shrinkage PAC specimens can still be produced with incorporation of GGBS and SF.

While exclusion of sand from the grout improves the flowability and strength of grout, it reduces the strength, durability, and dimensional stability of PAC. With significant improvement in flowability of grout with the removal of sand, water to binder ratio and coarse aggregate size can be reduced. This subsequently improves the properties of PAC. An empirical relationship to predict the compressive strength of PAC is proposed through experimentally derived factorial design and statistical analysis of collectively obtained data and profound literature review.

LIST OF PUBLICATIONS

Das, K. K., Lam, E. S. S., and Tang, H. H. (2021). Partial replacement of cement by ground granulated blast furnace slag and silica fume in two-stage concrete (preplaced aggregate concrete). Structural Concrete, 22, 466-473.

Das, K. K. and Lam, E. S. S. (2019). Feasibility of producing two-stage (preplaced aggregate) concrete by gravity process. Structural Concrete, 21(3), 1157-1163.

Das, K. K. and Lam, E. S. S. (2021). Development of high-performance preplaced aggregate concrete. Poster presented at 23rd Young Researchers Conference (online), The Institution of Structural Engineers (IStructE).

Das, K. K. and Lam, E. S. S. (2019). Effect of coarse aggregate size and grouting process on properties of preplaced aggregate concrete. In Proceedings of the 4th World Congress on Civil, Structural, and Environmental Engineering (CSEE'19).

Das, K. K. and Lam, E. S. S. Effects of flowability and grout mix proportions constituting modified binders on the properties of preplaced aggregate concrete. In preparation.

Das, K. K., Lam, E. S. S., and Chau, Y. K. Preplaced aggregate concrete with modified binder- properties and prediction of compressive strength. In preparation.

ACKNOWLEDGEMENTS

First and foremost, I would like to express my heartfelt gratitude and sincere thanks to my supervisor, Dr. Eddie Siu-Shu Lam, for his valuable guidance and persistent support throughout my PhD study. I have been extremely lucky to have Dr. Lam as my supervisor who unreservedly provides me with help and assistance. His humble and caring nature has made my research experience interesting and stress-free.

I am grateful for the assistance by the technical staff of the Department of Civil and Environmental Engineering, The Hong Kong Polytechnic University, especially, Mr. King Her Wong, Mr. Chi Shing. Liu, Mr. John Chan, and Mr. Ho Yin Leung, just to name a few.

Next, I wish to express my deepest gratitude to the research team, Ms. Wing Sze Betsy Yip, Ms. Zhihang Xue, and Mr. Sohail Maqsood for their continued help and support throughout my study period. Contribution and support provided by final year project students, Mr. Ho Him Tang, Mr. Yu Kiu Chau, and Ms. Ching Tung Ip are greatly acknowledged. I had a great time working with them.

All my loving friends, especially Dr. Peichen Wu, Dr. Paola Pannuzzo, Mr. Nikolay Lyapunov, Mr. Fang Wang, Mr. Hanxiang Zhang, Mr. Daniel Sánchez Cazorla, Ms. Yibin Gou, Dr. Ryuichi Tani, Ms. Maria Victorowa, Mr. Gabriel Lee, Dr. Parth Shah, Mr. Partha Debnath, Mr Sushil Kumar, and Mr. Andrei Kvasov deserve appreciation for making my life in Hong Kong filled with warmth and joy. They are like my extended family who always makes me feel at home.

Further, I am indebted to my loving family, especially to my parents for their unconditional love and support. I would also like to take the opportunity to acknowledge my late grandmother who has always been an inspiration to me.

Last but not the least, I wish to acknowledge the financial support provided by The Hong Kong Polytechnic University for supporting my study and offering me the research environment.

TABLE OF CONTENTS

LIST OF FIGURES

LIST OF TABLES

CHAPTER 1

INTRODUCTION

1.1 Background of research

Preplaced aggregate concrete ("PAC") is produced by first pre-placing coarse aggregates and then injecting grout to fill in the voids between the coarse aggregates (illustrated in Figure 1.1). It is different from conventional concrete in two fundamental ways. Firstly, the coarse aggregates are placed into the formwork, and grout is then applied to fill in the voids. Secondly, the ratio of coarse aggregates in the mix proportion of PAC is substantially higher than that of conventional concrete. A typical value is about 60% as compared with 40% in conventional concrete (Najjar et al., 2014). As a result, only 30% to 40% of the total volume is filled by the grout. This substantially reduces the wet trades and exploitation of machinery and equipment on-site. Also, production of PAC consumes lesser energy as the coarse aggregates do not take part in the mixing process, making it more environmentally friendly. Further, PAC reduces the consumption of cement by 20% to 30% as compared with conventional concrete (Nowek et al., 2007).

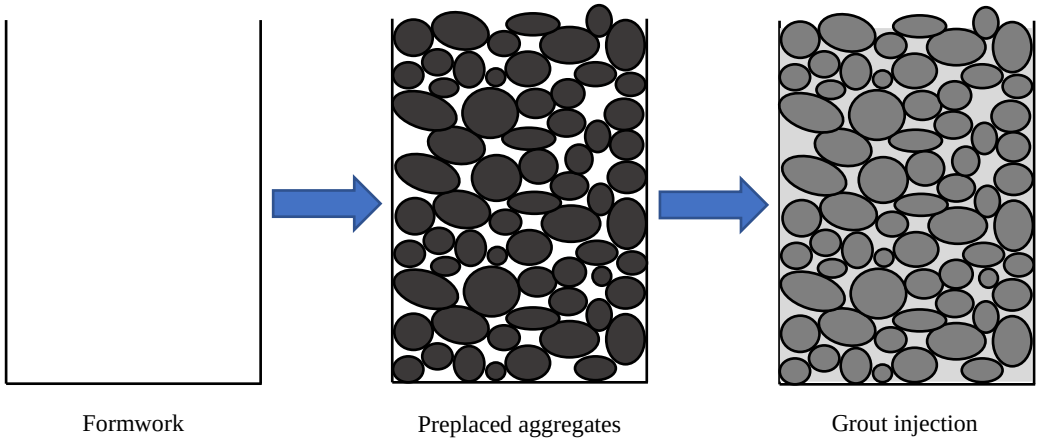

Figure 1.1 Production of PAC (Yoon et al., 2015)

Back to 1940s, PAC has found its applications in a wide range of structures including dams, bridges, and pavements (ACI 304.1). By forming PAC efficiently using pumping process and employing larger-sized coarse aggregates, properties such as low volume change and high bonding make PAC suitable for repair works and production of monolithic structures like mass concrete, attributing to its high density and low heat of hydration (ACI 304.1). PAC can be employed on sites with congested reinforcements, underwater constructions, etc. It has been successfully applied recently as part of the overall renovation and rehabilitation of Regency House Condominium Plaza parking garage, Phoenix, Arizona (ICRI Project Award, 2015). However, the use of PAC remains limited to mostly large-scale structures. Its application to small-scale repair and construction remains unpopular, attributing to the need for relatively larger-size coarse aggregates and sophisticated grouting equipment required for its production. Research on the mechanical, durable, and environmental potentials of PAC remains inadequate. A review reported by Najjar et al. (2014) has highlighted a lack of experimental data on the effect of admixtures and supplementary cementitious materials on the performance of PAC.

Because of the above drawbacks, there is a necessity to investigate the feasibility of producing PAC with readily available resources. Producing PAC with regular size coarse aggregates, if not smaller, is crucial for user-friendliness. Reducing reliance on sophisticated pumping equipment for efficient production of PAC is important for wider recognition. Incorporation of supplementary cementitious materials in PAC is vital to impart certain desired properties for application as an efficient repair and construction material.

1.2 Objectives

This study is mainly focused on developing high-performance PAC for application to structural repair and general constructions, necessitating superior durability and dimensional stability along with acceptable strength. Performance to be considered includes flowability and mechanical property of grout along with mechanical property, durability, and dimensional stability of PAC. The objectives of this study are shown as follows.

- Study the feasibility of producing PAC employing readily available coarse aggregates, without the use of grouting equipment.
- Include supplementary cementitious materials such as ground granulated blast furnace slag and silica fume as partial replacement of cement and optimize the grout mix proportion to produce PAC with improved properties.
- Examine the bond property of PAC as a repair material.
- Develop an empirical relationship to predict the compressive strength of PAC.

1.3 Project significance and value

This study provides thoughts on the feasibility of producing PAC with readily available resources. It implements a user-friendly approach to conveniently produce PAC for wider application and recognition. High-performance PAC employing regular and smaller-sized coarse aggregates, without the involvement of pumping machines is proposed. Grout mix proportions are optimized incorporating ground granulated blast furnace slag and silica fume to obtain enhanced properties along with environmental and economic benefits. The study also paves the way for future research on the incorporation of steel fibers in PAC, establishing its benefits and complexities. An empirical relationship to predict the compressive strength of PAC is proposed.

1.4 Layout of the thesis

This thesis comprises 8 chapters. An overview of the organization of study is elaborated in Figure 1.2.

Chapter 1 introduces PAC, its background, properties, and general application. This chapter articulates the objective and significance of this study.

Chapter 2 reviews current research on PAC and limitations including application, method of construction, properties, etc. Construction materials used by authors to produce PAC and conventional concrete are discussed.

Chapter 3 illustrates the methodology adopted in this study along with construction materials used. Tests and experiments performed in the entire study are elaborated.

Chapter 4 evaluates the properties of PAC against sizes of coarse aggregates and grouting process.

Chapter 5 investigates the performance of PAC produced by adding different supplementary cementitious materials to the grout. Effects of admixture dosage, sand to binder ratio, water to binder ratio, coarse aggregate size, adding steel fibers, adding ground granulated blast furnace slag, and adding silica fume are assessed.

Chapter 6 investigates the bond properties of PAC for different coarse aggregate sizes, with and without silica fume.

Chapter 7 formulates an empirical relationship statistically to predict compressive strength of PAC from the constituent materials.

Chapter 8 concludes the main achievements and findings of the study and provides recommendations for further study.

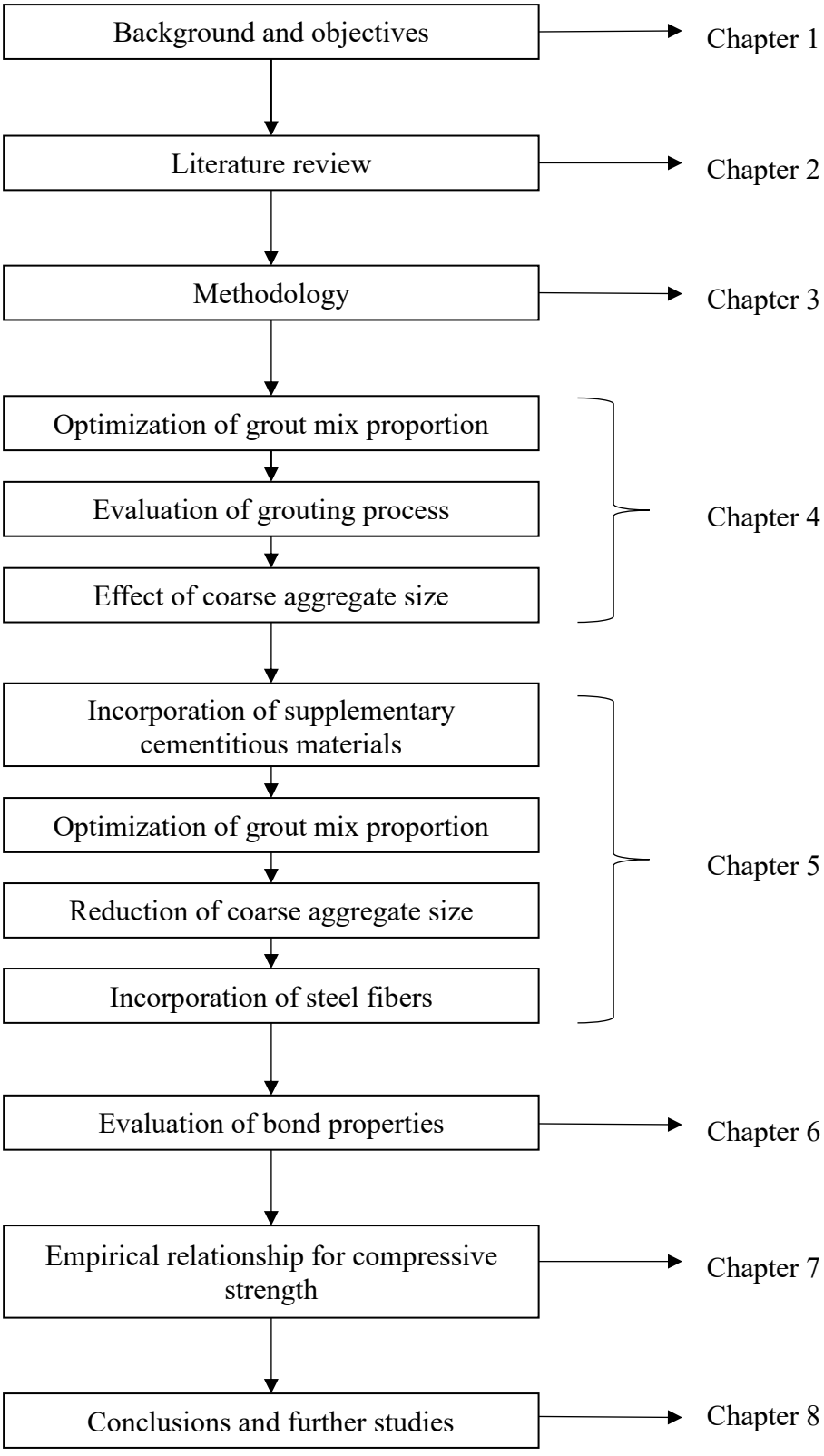

Figure 1.2 Organization of study

CHAPTER 2

LITERATURE REVIEW

2.1 Introduction

Preplaced aggregate concrete ("PAC") is produced by first placing coarse aggregates into the formwork and then applying grout to fill up the voids in between the coarse aggregates. Grouting in PAC can be achieved in two ways, i.e. gravity process and pumping process. In gravity process, the grout is applied from the top and is allowed to flow under the action of gravity. Whereas, in pumping process, the grout is pumped from the base until it rises to the desired depth (Najjar et al., 2014). PAC is known by various names such as Prepacked concrete (Abdul Awal, 1988), Polcrete (Abdelgader, 1995), Colcrete (Marke and Marke, 2010), Two-stage Concrete (Najjar et al., 2014), etc. Since the coarse aggregates are placed first, they occupy nearly 60% to 70% of the total volume (as compared with 40-50% in conventional concrete), leaving 30% to 40% of the voids in between the coarse aggregates to be filled by grout (Najjar et al., 2014). High content of coarse aggregates helps to reduce shrinkage by reducing the amount of cementitious material (Nowek et al., 2007) and introducing point-to-point contact between the coarse aggregates (Davis, 1960; Neville, 2011). The reduction in cementitious material by 30% to 40% as compared with that of conventional concrete reduces the heat of hydration, making the application of PAC suitable in mass construction (Bayer et al., 2019).

As, stress is transferred from the skeleton of coarse aggregates to hardened grout (Abdelgader, 1996), engineering properties of PAC, such as stress-strain relationships, are dominated by the properties of coarse aggregates (Abdelgader and Gorski, 2002). It is because efficient filling of voids by grout can provide PAC with higher strength

and durability. Thus, minimum size of coarse aggregates determines the maximum size of fine aggregates that can be used in the grout. By the same reason, larger-sized coarse aggregates (e.g., 50 mm) were extensively used to produce PAC in the 80s (Casson and Davies, 1986), as it enabled efficient filling of voids by grout.

Efficient filling up of voids by grout requires high penetrability of grout. Flowability of grout plays a significant role in the penetrability of grout through the preplaced coarse aggregates in PAC. Flowability of grout is governed by constituent materials and proportions, e.g., sand and water content, types and quantity of admixtures used, type and percentage replacements of supplementary cementitious materials, etc. With increasing plastic viscosity of the grout, efflux time increases (Roussel and Le Roy, 2005; Tuyan et al., 2020). Thus, plastic viscosity can be reflected by flowability, measured in terms of efflux time.

This chapter reviews the development of PAC and its application over time. Complexities and simplicities of different construction techniques and methods of producing PAC are discussed. Properties of PAC, such as mechanical properties, durability and dimensional stability are illustrated in contrast to conventional concrete. Drawbacks and shortfalls of PAC are identified and highlighted. Bond strength of concrete, being an important parameter for repair, is elaborated. A detailed review on various construction materials used in the study, such as coarse aggregates, fine aggregates, supplementary cementitious materials, admixtures, and fibers are included.

2.2 Application of PAC over time

In around 1937, PAC was used for the first time in the rehabilitation of Santa Fe Railroad tunnel near Martinez in California, USA, by Lee Turzillo and Louis S. Wertz (ACI 304.1). Large voids formed at the crown areas of the tunnel due to erosion were

filled with coarse aggregates first and then grouted. As grout consumption was reduced due to large volume being occupied by coarse aggregates, Professor Raymond E. Davis found it promising and thus developed the basis of PAC and grout proportions. In the 1940s, grout fluidifier (plasticizer) was used as admixtures and the use of PAC was restricted to repair of bridges and tunnel linings. With the growth in research and studies, PAC found its application in many large-scale projects (ACI 304.1). The following are some examples of applications of PAC.

In the early 1940s, large portion of an eroded backfill section of the spillway in Hoover Dam was repaired using PAC (Davis et al., 1955). As shown in Figure 2.1, 34 m long, 11 m deep, and 10 m wide section of the spillway was replaced using PAC. Afterwards, PAC was applied to other major projects. A classic example is the addition of an upstream face of a 52 m high dam in Nederland, Colorado in 1946. The front portion of the dam was anchored at 1.8 m from the surface by precast concrete slabs. During winter, when the reservoir was dry, the space between the original surface and the new face was filled with coarse aggregates. Later, grout was injected in the late spring by continuous pumping.

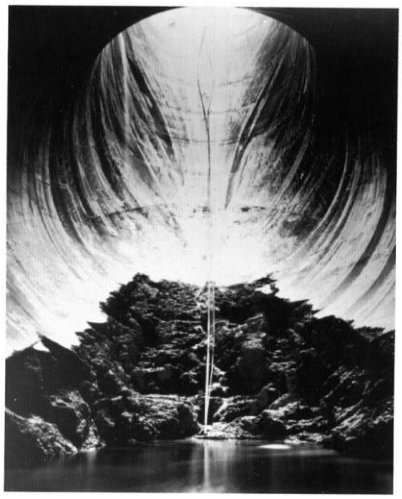

Figure 2.1 Eroded area in spillway at Hoover Dam (ACI 304.1)

In 1951, other structures along with embedment of turbine scroll cases were constructed using PAC by the U. S. Army Corps of Engineers. 380,000 m^3 of PAC was used to construct 34 piers of the Mackinac Bridge in 1951 (shown in Figure 2.2). In the 1970s, the Honshu-Shikoku Bridge Authority initiated extensive research to employ PAC in large-scale constructions (Davis and Haltenhoff, 1956; ACI 304.1). PAC soon found its application in a wide range of areas including hydroelectric power plants, biological shields around nuclear reactors and x-ray equipment, etc. Table 2.1 compiles some of the renowned projects employing PAC. In the past few decades, with intense research being accomplished, PAC gained new reputation, and application and scope of PAC widened (Du et al., 2017; Abdelgader et al., 2018; Cheng et al., 2019; Lv et al., 2020).

Figure 2.2 Construction of Mackinac Bridge (ACI 304.1)

Table 2.1 Renowned projects employing PAC

References	Project	Nature of work	Location
Davis et al. (1955)	Arizona spillway, Hoover Dam	Filling of cavity	Arizona-Nevada, USA
Davis et al. (1955)	Kenamo Penstock tunnel	Backfilling	British Colombia, Canada
Davis (1960)	Barker Dam	Repair	California, USA
Davis and Haltenhoff (1956); Waddell (1974)	Mackinac Bridge	Underwater casting of piers	Michigan, USA
Littlejohn and Crawley (1983)	KoRi Nuclear Plant	Construction	Pusan, South Korea
Littlejohn (1984)	Cromwell and Lauderdale Tower blocks	Underpinning	London, England
Littlejohn (1984)	Ninian Northern platform	Strengthening and stiffening of piers	North Sea, Scotland
Abdelgader (1996)	Cracow Dam	Repair	Cracow, Poland
Abdelgader (1996)	18 storied building	Construction of foundation	Gdansk, Poland
ACI 304.1	Lock wall	Construction	Pittsburgh, Pennsylvania, USA
ACI 304.1	Santa Fe railroad	Strengthening of tunnel	California, USA
ACI 304.1	West 6^{th} street Viaduct	Construction of columns	Erie, Pennsylvania, USA

Construction employing high-density coarse aggregates such as barite may lead to segregation of concrete as the coarse aggregates tend to settle at the bottom. Preplacing coarse aggregates offers an absolute solution to this complication (Narrow, 1954). PAC can also be employed for aesthetic preferences generated by leaving the coarse aggregate surface exposed (ACI 304.1). Greater dimensional stability makes PAC suitable for repair, ensuring relatively high bond with the adjacent surfaces (Warner, 2015).

Apart from the advantages mentioned above, the unique production technique of PAC also leads to certain shortfalls. With high volume of coarse aggregates being placed first, stronger formwork is required. To minimize leakage of grout and to withstand lateral pressure exerted by grout, formwork has to be watertight and strong. Stronger formwork incurs additional costs to the overall production process (REMR TN CS-MR-9.4, 1992; Najjar, 2014). Use of pumping equipment and machinery further upscales the production cost due to additional resources required for operation and maintenance of machinery (Abdelgader and Gorski, 2002; Nowek et al., 2007).

Advancement in PAC inspired the use of rocks as coarse aggregates with grout being replaced by self-consolidating concrete (SCC). This is known as rock-filled concrete (Huang et al., 2008). Rock-filled concrete gained wide acceptance in China, especially in recent years (Wang et al., 2019; Wei et al., 2019; Cheng et al., 2019). It found its application in more than 60 hydraulic engineering projects, like Changkeng third reservoir project in Guangdong, Shihe reservoir project in Hebei, Maopohe hydropower project in Yunnan, etc. (An et al., 2014). As rocks (size over 300 mm) are employed, the formworks are constructed out of brick masonry which makes it feasible for large-scale projects only.

SCC has the ability to flow readily under its own weight. It is essential for SCC to have high flowability (to efficiently fill all areas and corners) and superior passing ability (to pass through congested reinforcements without separation of the constituents or impeding the flow). Further, SCC has to display high resistance to segregation during and after placing and achieve full consolidation without compaction (ACI 237R-07). It has the benefits of reducing manpower, shortening time of construction, improving

productivity, enhancing quality, etc. (Kwan and Ng, 2010) and guarantees high durability by reducing the potential of poor compaction (Goodier, 2003).

The above-mentioned properties also hold for grouts used in PAC, especially to produce PAC using smaller-size coarse aggregates and through gravity process. As such, the small passages between coarse aggregates may cause blockage to grout. This can be avoided by increasing the flowability of grout, with decreasing segregation stability. Thus, it is necessary to achieve both high flowability and high segregation stability at the same time (Kwan and Ng, 2010).

2.3 Grouting

Grouting can be performed by gravity process or pumping process (shown in Figure 2.3). In gravity process, grout is applied from the top and is allowed to penetrate through the voids in between the coarse aggregates under the action of gravity. In pumping process, grout is pumped from the base under pressure and penetrated through the voids to reach the desired surface level (Awal, 1984). Gravity process is usually used for grouting thin sections, especially for depths less than 300 mm. For sections at greater depth, pumping process is suggested.

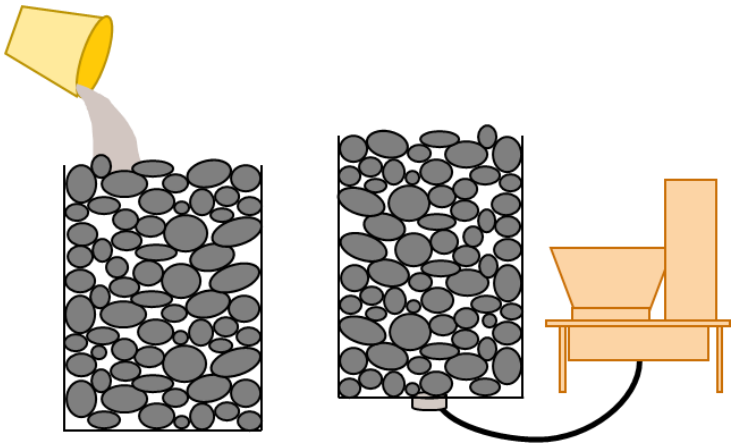

Figure 2.3 Grouting via gravity process (left) and pumping process (right)

Grouting process depends on the minimum size of coarse aggregates. When the minimum coarse aggregate size is 50 mm or above, gravity process can be successfully applied. Vice versa pumping process is recommended (Casson and Davies, 1986). Larger-size coarse aggregates offer larger and uninterrupted passages for grout to penetrate, leading to efficient filling of voids. Smaller-size coarse aggregates have the drawback of generating smaller passages. As a result, this may impede the flow of grout, form honeycombs and compromise the integrity of PAC (Najjar, 2017). This behaviour can be explained by Kozeny-Carman equation (Equation 2.1). As shown, pressure drop induced by flowing through a packed bed or particles, and pressure drop increases significantly when the particles get smaller.

$$\frac{\Delta p}{L} = -\frac{150\mu}{\phi_s^2 D_p^2}\frac{(1-\varepsilon)^2}{\varepsilon^3} v_s \qquad \text{Equation 2.1}$$

where,

Δp = pressure drop
L = total height of bed
v_s = superficial velocity
μ = viscosity of fluid
ε = porosity of bed
Φ_s = sphericity of the particles in the packed bed
D_p = diameter of the volume equivalent spherical particle

To inject grout using pumping process, pipes are inserted into the formwork. A single line of pipe extending from the pump to the formwork is more reliable than multiple lines of pipes supplying grout to two or more inserts, simultaneously. Flow of grout within the coarse aggregates may vary from insert to insert, resulting in uncertain grout distribution and clogged inserts (ACI 304.1). This requires sufficient pipe diameter at optimal velocity of pumping. Otherwise, it may result in energy wastage, and wear and

tear to the equipment. It is also essential for the entire grouting system to be watertight and being cleaned properly at regular intervals. This sophisticates the grouting process and upscales the resources required for the operation and maintenance of grouting equipment.

On the other hand, gravity process is simple and economical. Despite this, it is less developed and there are no definite guidelines and standards for the convenient production of PAC via gravity process. In some cases, pipes are inserted through the coarse aggregates and the grout is poured in through these pipes using funnels to direct the flow (O'Malley and Abdelgader, 2010; Abdelgader et al., 2013). This allows the grout to flow from the base to the surface. As size of coarse aggregates and flowability of grout govern the production of PAC via gravity process, research on efficient production of PAC in relation to the coarse aggregate size and flowability of grout is necessary.

2.4 Properties of PAC

2.4.1 Mechanical properties of PAC

Mechanical properties of PAC are unique from that of conventional concrete. In PAC, applied stress is transferred through the skeleton of coarse aggregates and the hardened grout after deformation (Abdelgader and Gorski, 2002). Type and size of coarse aggregates, grout composition, and grout properties have a strong influence on the mechanical properties of PAC. Although compressive strength of grout increases with increasing dosage of cement, it may reduce the compressive strength of PAC. This is attributed to formation of shrinkage cracks and contractions between the grout and the coarse aggregates, thereby compromising the strength of PAC (Abdelgader, 1996). Other factors influencing the compressive strength of PAC include interaction and

contact points between coarse aggregates, bonding between coarse aggregates, and properties of grout (Abdelgader, 1999). Mechanical interlocking between coarse aggregates and efficient bonding between grout and coarse aggregates are essential to produce PAC with superior compressive strength.

Tensile strength of PAC is influenced primarily by the water/cement ratio and secondarily by cement/sand ratio of grout. Similar to conventional concrete, tensile strength of PAC increases with increasing compressive strength of PAC (Awal, 1985; Abdelgader and Ben-Zeitun, 2005). Generally, tensile strength of PAC was found to be greater than that of conventional concrete of the same compressive strength, attributing to larger coarse aggregate content (Awal, 1985) and better mechanical interlocking between coarse aggregates (Najjar, 2014). Loading is initially transmitted to the coarse aggregate skeleton system and then to the grout, leading to efficient distribution of stress, as illustrated in Figure 2.4.

At the same grout content, PAC exhibited higher bond strength (Davis et al., 1955) and higher flexural strength (Marke and Marke, 2010) than that of conventional concrete. The combined effect of direct aggregate-to-aggregate contact and stronger bond strength provided by the grout has been recognised as the main factor enhancing the flexural strength of PAC.

The study above signifies the mechanism to enhance the strength of PAC. Although PAC can display higher strength than conventional concrete, research on PAC with compressive strength above 50 MPa is limited. Such strength development on PAC is yet to be addressed.

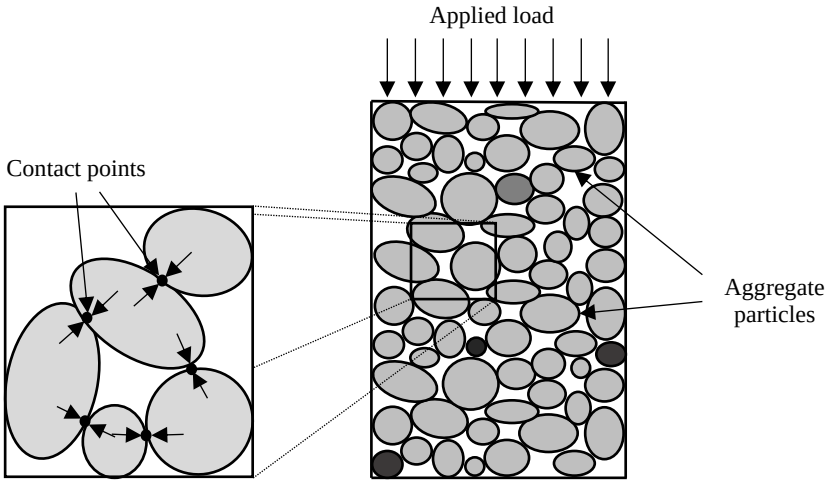

Figure 2.4 Interlocking of coarse aggregates in PAC (Najjar, 2014)

2.4.2 Durability of PAC

Durability of concrete refers to the ability to resist chemical attacks, weathering, and abrasion while sustaining its engineering properties. Generally, PAC exhibits high durability attributing to its dense structure and high coarse aggregate content. Davis (1960) prepared specimens for both conventional concrete and PAC to study the resistance against freezing and thawing. After 28 days of moist curing, the specimens were frozen in water at 18°F (-7.7°C) and thawed in water at 50°F (10°C). Any specimen losing 25% of its weight before reaching 300 cycles of freezing and thawing was regarded as unsatisfactory. As shown in Figure 2.5, conventional concrete lost 25% of its weight in 700 cycles, whereas PAC lost only 8% of its weight in 900 cycles. Both PAC and conventional concrete displayed satisfactory resistance to freezing and thawing. This indicates that PAC of suitable materials and good workmanship exhibit good resistance to weathering action due to freezing and thawing.

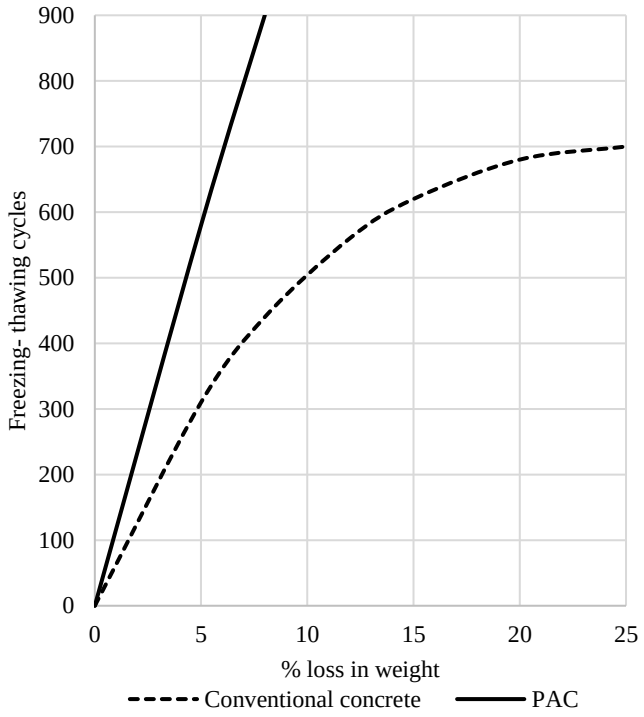

Figure 2.5 Durability of PAC versus conventional concrete at 60 days (Davis, 1960)

According to Najjar et al. (2014), structures constructed using PAC, such as dams, are less prone to thermal cracking ascribing to PAC's low heat of hydration as a result of lower cement content. PAC was found to have high resistance to aggressive environments. Inclusion of air-entrained admixtures in PAC further improved its frost resistance, displaying superior performance than that of conventional concrete. A field investigation conducted at the Tasman Bridge in Australia after 48 years of service revealed that the piles made of PAC displayed excellent durability (ACI 304.1).

In terms of supplementary cementitious materials, incorporation of ground granulated blast furnace slag and silica fume enhances the durability of concrete by improving the resistance to chloride ion penetration (Yildirim et al., 2011; Poon et al., 2006). Ground granulated blast furnace slag modifies the microstructure of cementitious paste with more capillary pores filled with C-S-H gel than normal concrete, resulting in lower

chloride ion penetration (Cheng et al., 2005). Presence of ground granulated blast furnace slag in concrete not only makes the cement matrix denser but also diminishes the pore size, reducing the chloride ion penetration (Yeau and Kim, 2005). Addition of silica fume improves durability of concrete by enhancing the interfacial transition zone (forming C-S-H at interface) and modifying the micro structure at interface (Siddique, 2011). Reduction in chloride ion permeability due to incorporation of silica fume is attributed to its pore size refinement mechanism (Khan and Siddique, 2011).

2.4.3 Dimensional stability of PAC

Shrinkage is an inherent property of concrete that leads to dimensional instability. It is a time-dependent strain or dimensional change at a constant temperature. Drying shrinkage and autogenous shrinkage are the two common types of shrinkage in concrete. Drying shrinkage is caused by loss of capillary water in concrete due to drying and autogenous shrinkage is caused due to internal consumption of water during hydration of cement. Generally, for conventional concrete total shrinkage is often referred to as drying shrinkage whereas autogenous shrinkage taking place at an early age (usually completed in the first 1 to 3 days) is negligible. Also, for most test programs, shrinkage is considered from the start of drying (ACI 209.2R). However, in the case of high strength concrete, both autogenous and drying shrinkage need to be identified, as the ratio of these shrinkages to total shrinkage varies with age and drying conditions (Sakata and Shimomura, 2004).

Shrinkage may lead to cracks, which is the most problematic flaw in concrete. As shrinkage is inevitable, efforts to reduce the magnitude of shrinkage is essential. Even low shrinkage repair materials may cause problems if the substrate is not able to respond appropriately (leading to differential shrinkage) and only material with high

dimensional stability is suitable for repair. When a repair material shrinks extensively, tensile stress develops at the interface between repair material and substrate. Ultimately, cracks develop at the interface leading to delamination of repair material at early age.

In the early days, magnitude of shrinkage was specified as high (unacceptable) and low (acceptable). Emmons (1993) took the liberty to classify shrinkage into low, moderate, and high. Acceptable shrinkage of normal-weight concrete has been considered as 500 microstrain (0.05%) at 30 days. Low shrinkage was assumed to be less than 500 microstrain. Shrinkage ranging between 500 microstrain (0.05%) and 1000 microstrain (0.10%) was considered as moderate shrinkage. Shrinkage exceeding 1000 microstrain (0.10%) was considered as high shrinkage. Figure 2.6 shows shrinkage recorded by the Alberta Concrete Patch Evaluation Program conducted as per ASTM C 157 in 1987, on repair concrete (Morgan, 1996). Shrinkage of 46 repair products was arranged in ascending order. Of all the repair products, only 15% were found to display drying shrinkage lower than that of normal-weight concrete. Over 50% displayed a drying shrinkage more than twice of normal-weight concrete, indicating plenty of room for the improvement of repair concrete products. Fu et al. (2016) compared restrained ring test with free shrinkage test of concrete and proposed free shrinkage limit of 450 microstrain at 28 days to ensure satisfactory resistance to cracking.

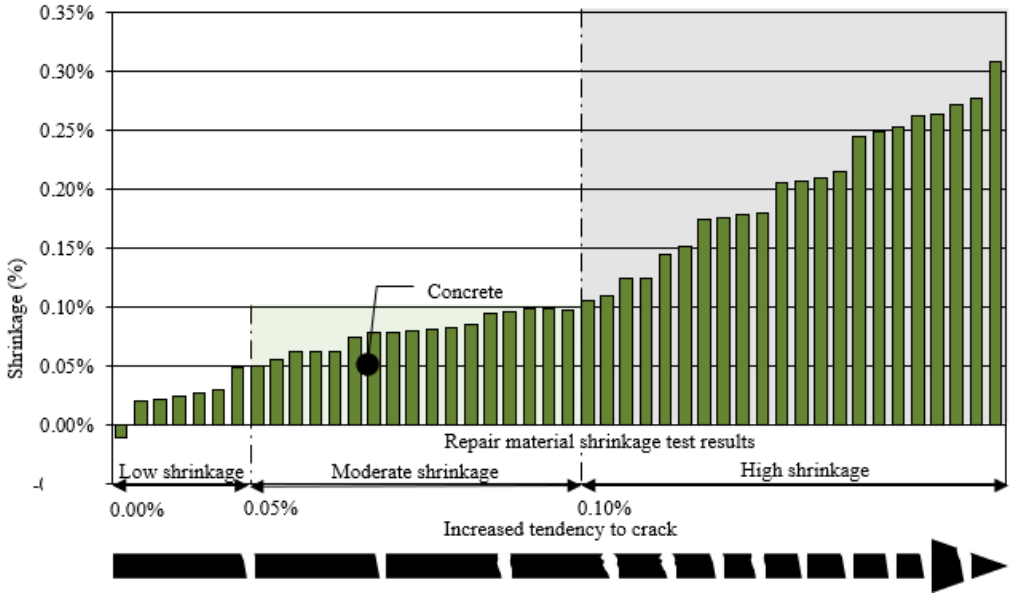

Figure 2.6 Shrinkage test results, Alberta Concrete Patch Evaluation Program (Morgan, 1996)

At one time, pumped mortars were extensively used for repair. However, their application was phased out because of relatively high drying shrinkage. This drawback could be overcome to a certain extent by applying grout to preplaced aggregates (forming PAC). Davis et al. (1955) observed that coarse aggregates in PAC were in direct contact with each other and that there was practically no shrinkage. A comparison between PAC and conventional concrete was conducted by Davis (1960), using the same quantity of cementitious material, sand, and water. The specimens were cured under standard moist conditions for 28 days. PAC and conventional concrete using the same maximum coarse aggregate size (1-1/2 inch) were compared. As shown in Figure 2.7, PAC exhibits a reduction in drying shrinkage by one third to that of conventional concrete. Neville (2011) reiterated that the initial point to point contact of coarse aggregates in PAC resulted in a reduced shrinkage, correspondingly reduced the tendency of concrete to crack. The above was further supposed by Abdelgader et al. (2016). This made PAC ideal for repair and patchwork.

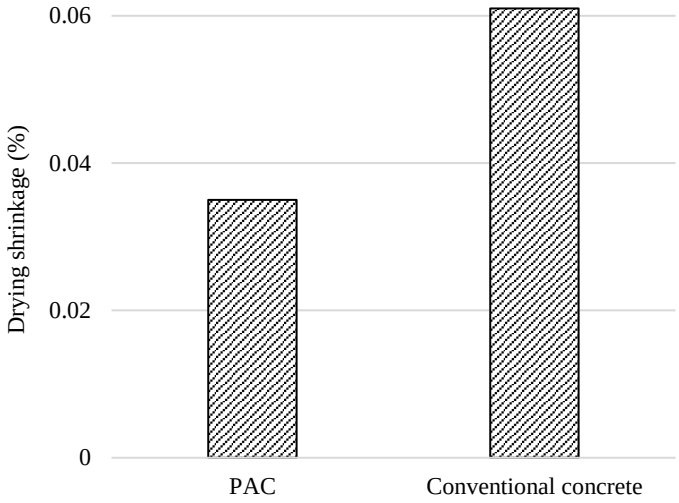

Figure 2.7 Drying shrinkage of PAC and conventional concrete at 60 days (Davis, 1960)

Drying shrinkage in PAC was also assessed beyond the walls of laboratories. PAC was employed to restore the backfill of a large, eroded section of a spillway in the Hoover Dam (ACI 304.1). After 3 years of repeated cycles of soaking wet in water and drying at 50% relative humidity and 70°F (21°C) temperature, drying shrinkage test was performed on PAC cores and conventional concrete cores extracted from the repair and the original tunnel lining, respectively. Based on the test results, PAC displayed a drying shrinkage at one third to that of conventional concrete.

2.5 Bond strength

Repair and strengthening of structures often include application of new concrete next to old concrete (substrate). Some of the most common examples are application of overlays on highways, patch repair of corroded or damaged concrete sections, retrofitting, and jacketing. For efficient repair and strengthening, adequate bonding between substrate and repair material is essential (Ali and Ambalavanan,1999; Oluokun and Haghayeghi, 1998). It also determines the efficiency and durability of repair

systems. As debonding is still not uncommon (Beushausen and Alexander, 2008), failure of a repair system remains high (Tayeh et al., 2013).

Silfwerbrand (1990) suggested that durability of bonding between substrate and repair material depends on several factors, and can be grouped into three main categories, i.e. (i) substrate characteristics, (ii) repair material characteristics and application technique, and (iii) environmental conditions (Silfwerbrand and Beushausen, 2005; Courard et al., 2014). Substrate characteristics include substrate properties, microcracks, roughness and cleanliness of substrate. Repair material characteristics and application technique include properties of repair material (such as strength, shrinkage, and durability), prewetting of substrate, bonding agents used, placement technique, and compaction. Environmental conditions include time of placement, workmanship, and the environment itself, i.e., temperature and humidity.

Among others, differential shrinkage between repair material and substrate is a major factor influencing bond strength and durability of repair (Talbot et al., 1994; Li et al., 1999; Delatte et al., 2000). This is significantly influenced by the characteristics and type of repair material used. Binder used in repair material is a vital factor that affects the performance of interfacial transition zone. Adding supplementary cementitious materials such as silica fume (Momayez, et al., 2005) and fly ash (Li, 2003) to binder improved bond properties of repair system. This was attributed to micro filler effect, which changed the microstructure at the interfacial transition zone of concrete (Cohen et al, 1914; Kuroda et al, 2000). Further, partial replacement of cement by fly ash enhances the long-term bond strength, attributing to the formation of dense C–S–H molecules at the interface, thereby eliminating air voids and other vacant spaces.

Bond strength between substrate and repair material can be measured in several ways, i.e. under tension, under shear, and under combination of compression and shear (Momayez, et al., 2005). Pull-off test and splitting prism test measures bond strength by applying tensile stress (Vizini et al., 2020). Bi-surface shear test measures bond strength by applying shear stress (Momayez et al., 2004). And slant shear test measures bond strength under combined compression and shear stress (Austin et al., 1999).

As mentioned in the previous sections, PAC displays high durability and superior dimensional stability. This indicates a high repair potential of PAC. As the casting technique of PAC is unique to that of conventional concrete, bond behaviour of PAC may be distinct to that of conventional concrete. Investigation on bond properties of PAC is essential to establish the benefits and complications of using PAC as a repair material.

2.6 Constitutive materials

Type and composition of raw materials used for the production of PAC play a vital role on fresh and hardened properties of PAC. A review on the construction materials used to produce PAC is discussed below.

2.6.1 Coarse aggregates

Type, size, and grading of coarse aggregates are crucial to the properties of concrete. Numerous investigations on the effects of coarse aggregates on properties of conventional concrete were conducted and copious information is available in the open literature. Generally, modulus of elasticity/plasticity decreases with increasing coarse aggregate size (Hughes et al. 1966). With increasing coarse aggregate size, compressive strength (Alexander and Wardlaw, 1960; Tumidajski and Gong; 2006) and flexural

strength (Ajamu and Lge, 2015) of concrete decreases. Concrete produced by using mixed coarse aggregates exhibited higher compressive strength attributing to its high packing density (Ede et al. 2016).

On the other hand, the effect of coarse aggregates on PAC is unique and distinct from that of conventional concrete. It is essential for the coarse aggregates to be washed and cleaned before use. Since coarse aggregates do not take part in mixing process, any fines or specks of dust on the surface of coarse aggregates may result in inefficient bonding between coarse aggregates and grout. Crushed stone or natural gravel, free of surface dust or fines, conforming to ASTM C 33 can be used as coarse aggregates for producing PAC. Maintaining a low void content in between coarse aggregates enables a reduction in cement content, contributing towards economy and limits temperature rise caused by heat of hydration. Voids between the coarse aggregates provide passage for grout to pass through. Hence, with the reduction in coarse aggregate size, voids between the coarse aggregates reduce and cause difficulties in applying grout.

There exist limited studies on the influence of types of coarse aggregates to the properties of PAC. Abdelgader (1999) studied the properties of PAC against coarse aggregates of different shapes, i.e. rounded, crushed, and mixed. As shown in Figure 2.8, PAC using mixed shape coarse aggregates exhibited superior results. This was ascribed to increased contact points between the coarse aggregate grains of mixed shape coarse aggregates, compared to crushed or rounded coarse aggregates. Similar observations were reported by Abdelgader and Gorski (2002).

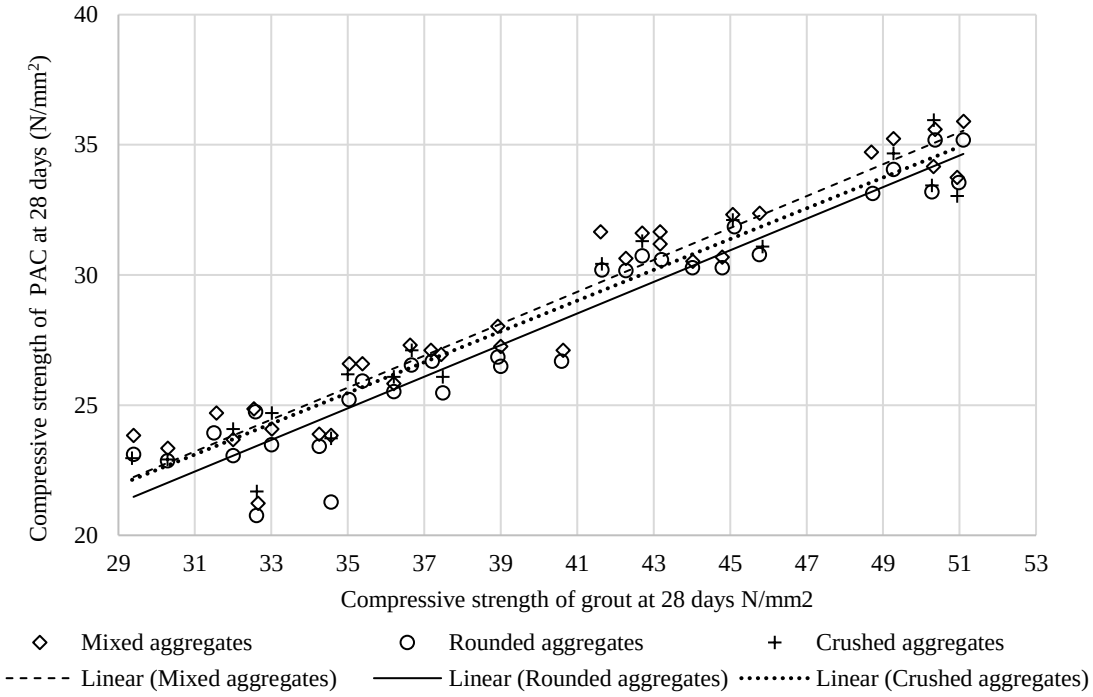

Figure 2.8 Relation between compressive strength of grout and compressive strength of PAC employing different types of coarse aggregates (Abdelgader, 1999)

Figure 2.9 shows compressive strength of PAC produced using rounded and crushed coarse aggregates (O'Malley and Abdelgader, 2010). PAC produced employing crushed coarse aggregates exhibited higher compressive strength than that produced employing rounded coarse aggregates. Crushed coarse aggregates provides better interlocking than rounded coarse aggregates. Rough texture of crushed coarse aggregates provides the grout with a better surface to bind on than that of smooth texture of rounded coarse aggregates.

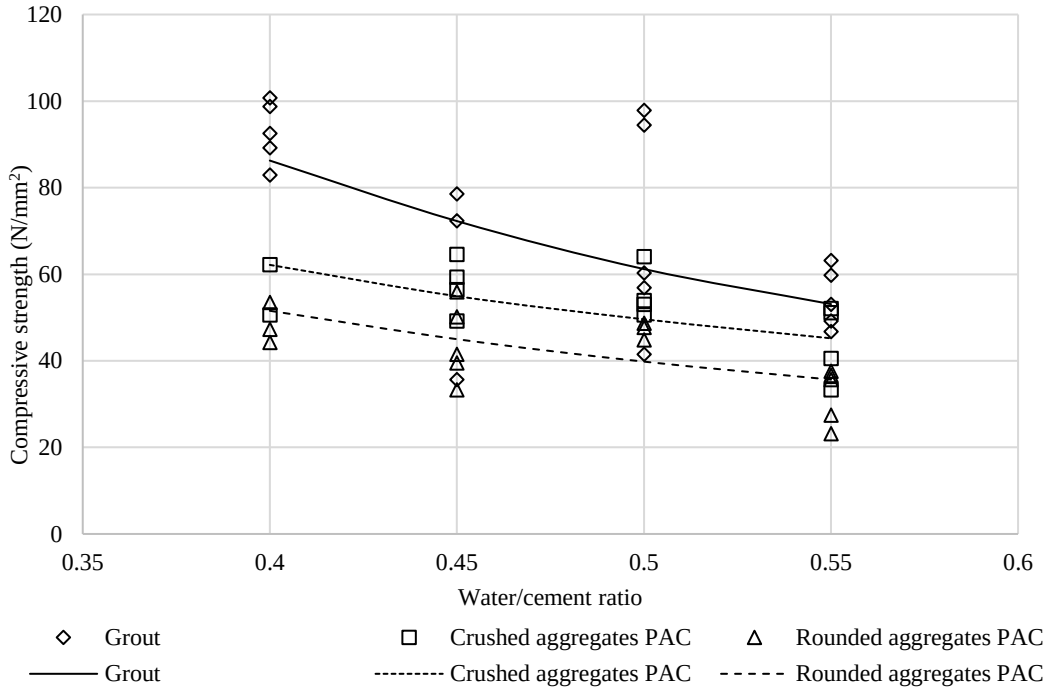

Figure 2.9 Compressive strength grouts and PAC (O'Malley and Abdelgader, 2009)

Marke and Marke (2010) compared flexural strength of conventional concrete and PAC. Coarse aggregates sizes included 47 mm, 50 mm, and 55 mm; with mix ratios of 1:2:4 and 1:3:6 (cement: fine aggregates: coarse aggregates). As shown in Figure 2.10 and Figure 2.11, flexural strength of PAC was higher than that of conventional concrete. Najjar et al. (2014) observed that bond strength in PAC was significantly affected by shape, texture, and mineralogy of coarse aggregates. Coarse aggregate shapes, such as bulky rounded or angular were preferred over flat or elongated ones. Use of flat or elongated coarse aggregates may narrow the path through which the grout flows, inhibiting penetration of grout, forming honeycombs and voids. PAC produced using rough-textured coarse aggregates were observed to exhibit higher strength than that produced using smooth-rounded ones as the former provided better surface for grout inter-keying.

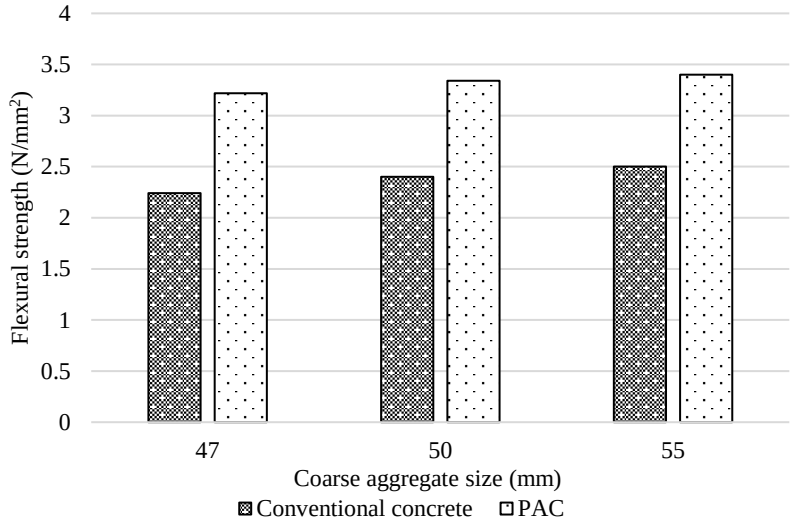

Figure 2.10 Flexural strength for PAC and conventional concrete for 1:2:4 nominal mix ratio (Marke and Marke, 2010)

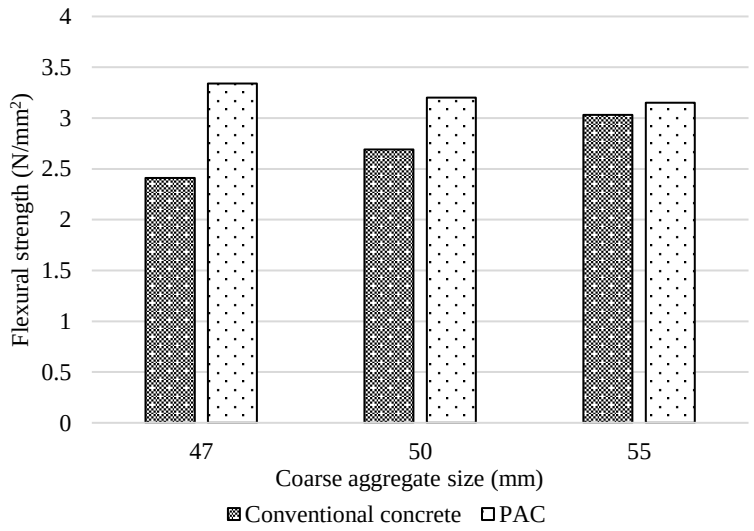

Figure 2.11 Flexural strength for PAC and conventional concrete for 1:3:6 nominal mix ratio (Marke and Marke, 2010)

Back in the 1950s, the recommended size of coarse aggregates in PAC was 38 mm (Champion and Davis, 1958). Coarse aggregates smaller than 20 mm were suggested to be eliminated as they might interrupt the grout flow. Later, Neville (1995) proposed to use coarse aggregates of sizes smaller than 38 mm, with the aggregates being gap-graded and of multiple sizes. Table 2.2 shows the grading limits for various minimum

size coarse aggregates recommended by ACI 304.1 to produce PAC. Generally, the grouting process and the grout determine the minimum size of coarse aggregates to be used or vice versa (Najjar, 2016).

Table 2.2 Grading limits of coarse aggregates for PAC (ACI 304.1)

Sieve size (mm)	Percentage passing (%)		
	Grading 1 For 12.5 mm minimum size coarse aggregate	Grading 2 For 19 mm minimum size coarse aggregate	Grading 3 For 38 mm minimum size coarse aggregate
37.5	95-100	-	0.5
25.0	40-80	-	-
19.0	20-45	0-10	-
12.5	0-10	0-2	-
9.5	0-2	0-1	-

2.6.2 Fine aggregates

In this study, the terms fine aggregates and sand are used interchangeably. For a suitable grout mix, fine aggregates should be hard, dense, durable, clean, and uncoated. In the case of PAC, grading of fine aggregates significantly influences the flowability of grout. Figure 2.12 compiles the grading of fine aggregates recommended by Neville and Brooks (1987) and ACI 304.1. In both gradings, fine aggregates with high fineness are recommended. Modulus of fineness quantifies the average size of the fine aggregates and plays an important role in compressive strength and drying shrinkage of PAC. Fine aggregates with a higher modulus of fineness increase water demand in the mix. With increasing water content, compressive strength decreases and drying shrinkage increases. An increase in the size of fine aggregates increases the risk of clogging in between the coarse aggregates and segregation within the grout. However, increase in the proportion of fine aggregates reduces the binder content, which

subsequently reduces the heat of hydration. Thus, proper optimization is essential as higher fine aggregate content may lead to a viscous grout, resulting in inefficient penetration.

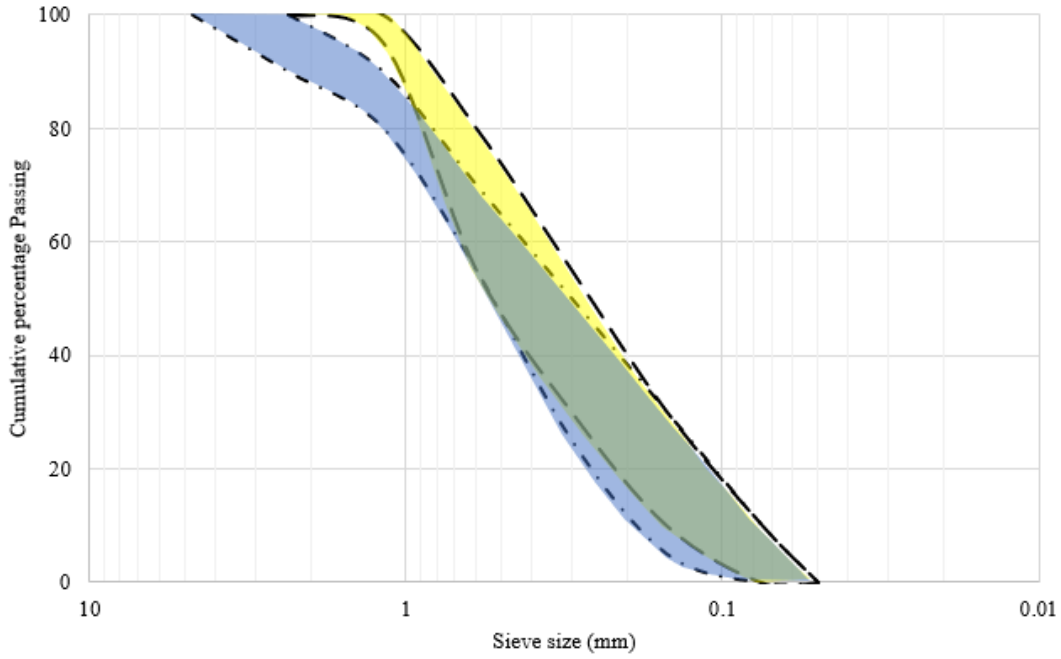

Figure 2.12 Grading of fine aggregates for PAC

Abdelgader (1996) observed that variation in sand content in grout did not have a significant influence on the strength of PAC. Mechanical properties of PAC were not affected by the amount of sand. However, change in sand quality resulted in change of physical properties e.g., sedimentation and fluidity. O'Malley and Abdelgader (2010) aimed to produce PAC on a small scale, using native Irish settings, without the use of any specialized plants. Grout was produced using 5 mm sand and was mixed in a slow-speed paddle mixer. Sedimentation was much higher than expected. Hence, it was concluded that combination of 5 mm sand and low-speed mixer was not suitable for successful production of PAC.

Abdelgader et al. (2013) investigated the fluidity, compressive strength, and flexural strength of PAC by varying water to cement ratios and sand to cement ratios. Table 2.3 shows the fluidity of grout. Fluidity of grout increases with sand to cement or water to cement ratio. Compressive strength of PAC and grout decreases with increasing water to cement ratio. Flexural strength of PAC was found to increase with increasing sand to cement ratio and decrease with increasing water to cement ratio. Coo and Pheeraphan (2015) observed that the efflux time of PAC was primarily influenced by the sand content in grout. Increasing sand content in the mix by 10% reduced slump of the mix by 20 mm.

Table 2.3 Fluidity of grout (Abdelgader et al., 2013)

Water/cement ratio	Sand/cement ratio	Fluidity	
		Flow cone (sec) (ASTM C 939)	Flow meter (cm) (ASTM C 230)
0.55	1.00	94	8
		90	9
0.80	2.00	40	15
		37	16

From the above, even though the influence of sand on mechanical properties of PAC is still in dispute, it has a prominent influence on the fresh properties of grout. Optimization of sand content to produce PAC is essential as it significantly influences the minimum size of coarse aggregates (ACI 304.1) and flowability of grout. Further investigation on sand content is vital to overcome the challenges on qualitative and quantitative assessment on effect of sand content to properties of PAC.

2.6.3 Supplementary cementitious materials

Use of supplementary cementitious materials as a partial replacement of cement reduces the weight of cement in concrete in addition to imparting certain desirable properties to it (Samad and Shah, 2017). Notwithstanding the above, supplementary cementitious materials such as fly ash, limestone powder, silica fumes, slag, metakaolin, etc. are scantly used in PAC. Partial replacement of cement by fly ash at 33% is recommended by ACI 304.1 for mass concrete, as it reduces the heat of hydration significantly. Addition of fly ash improved the flowability of grout, extended the grout handling time while reducing the water demand and bleeding (Najjar et al., 2014). With sufficient replacement of cement by fly ash, volume of paste increases, attributing to lower density of fly ash. This forms a lubricating layer between sand particles thereby reducing the friction and increasing the flowability of grout (Coo and Pheeraphan, 2015).

Research on PAC incorporating supplementary cementitious materials as partial replacement of cement to form grout is relatively limited compared to conventional concrete. Further, supplementary cementitious materials such as silica fume is rarely used in PAC as it increases the cohesion of grout, and subsequently induces voids in PAC. Some examples are compiled in Table 2.4. The following sub-section provides a review on supplementary cementitious materials used in this study, namely ground granulated blast furnace slag and silica fume.

Table 2.4 PAC incorporating supplementary cementitious materials by different authors

Reference	Pozzolan (% replacement of B)	HRWA (% by weight of B)	Efflux time (sec) (ASTM C 939)	28 days compressive strength (MPa)	
				Grout	PAC
Nehdi et al. (2017)	MK (10) FA (40)	0.35	35-40	-	25.10
Coo and Pheeraphan (2016)	FA (0-40) LP (0-50)	0.50	9.80-61.20	30.08-122.30	9.69-35.84
Mohammadhosseini et al. (2016)	POFA (0-30)	1.00	12.10-15.30	-	24.90-35.10
Najjar et al. (2016)	FA (0-50) SF (0-10) MK (0-10)	0.00-0.80	35.00-40.00	28.00-61.90	14.10-40.00
Coo and Pheeraphan (2015)	FA (0-40)	0.50	9.80-62.80	64.35-105.48	40.37-73.70
Abdelgader and El-Baden (2015)	SF (0-6)	0.00-2.00	-	-	8.29-25.65
O'Malley and Abdelgader (2010)	SF (6)	1.20	-	37.00-100.00	22.00-63.00
Vieira et al. (2010)	FA (60)	0.78-0.85	-	-	25.20-27.00
Nowek et al. (2007)	FA (0-25) SF (0-6)	0.70-1.00	-	37.50-73.30	22.10-42.60
Bayer (2004)	FA (0-50) GGBS (0-50)	1.00-2.00	-	-	10.60-28.40

W/B=Water to binder ratio, S/B=Sand to binder ratio, HRWRA=High range water reducing admixture, FA=Fly ash, GGBS=Ground granulated blast furnace slag, SF=Silica fume, MK=Metakaolin, POFA=Palm oil fuel ash.

2.6.3.1 Ground granulated blast furnace slag

Ground granulated blast furnace slag ("GGBS") has been used in composite cement and as a cementitious component of concrete for many years. Early industrial/commercial use of GGBS was to produce bricks. In the second half of the 19th century, cementitious properties of GGBS were discovered. By the end of the 19th

century, the first cement containing GGBS was produced. Since the late 1950s, GGBS has gained acceptance as a separate ground material added to concrete with Portland cement. In some countries, the term ‘slag cement’ is used for pure GGBS (Shumuye and Jun, 2018).

In warm weather, most concrete producers use GGBS as partial replacement of cementitious material by up to 50% to maintain high strength, achieve sulphate resistance or low-temperature rise. Under cold weather conditions, partial replacement of GGBS by not more than 20% to 30% is recommended to achieve early strengths for earlier release of formworks or when applied to thin sections at low temperatures. Generally, partial replacement of cement by GGBS reduces the cost of cementitious material, improves workability, reduces strength loss in hot weather conditions, and increases compressive and flexural strength. The use of GGBS in mortars and grouts improves its strength, permeability, flow, and cohesive characteristics (ACI 233R).

According to Cheng et al. (2005), GGBS modifies the pore structure in hardened cementitious material. It reacts with water in alkali environment and then with calcium hydroxide to form cement hydration product through pozzolanic reaction and forms extra C-S-H gel in the paste. With an increase in GGBS replacement, C-S-H content increases, forming a denser microstructure and lowers the porosity leading to superior durability. For instance, GGBS concrete beams were observed to have higher resistance to corrosion than plain concrete beams.

Khatib and Hibbert (2005) studied the influence of incorporating GGBS on concrete strength by partially replacing Portland cement with GGBS at 0%, 40%, 60%, and 80%. As shown in Figure 2.13, there was systematic decrease in compressive strength with increasing GGBS content. From 28 days to 90 days and beyond, the presence of GGBS

was highly beneficial at 40% to 60% replacement with strength exceeding that of control mix. However, a noticeable strength reduction at all ages was observed at 80% replacement of cement by GGBS. 90 days flexural strengths obtained from the mixes are shown in Figure 2.14. Flexural strength of concrete containing 60% GGBS was noticeably higher than that of control mix, whereas a slight decrease at 40% and marked decrease at 80% replacement of cement by GGBS were observed.

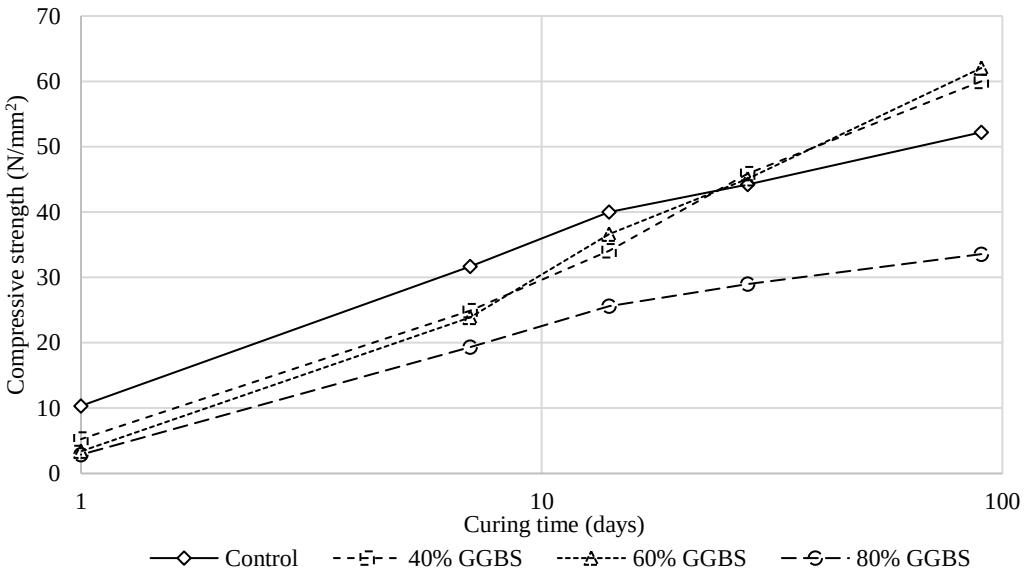

Figure 2.13 Effect of GGBS on compressive strength development (Khatib and Hibbert, 2005)

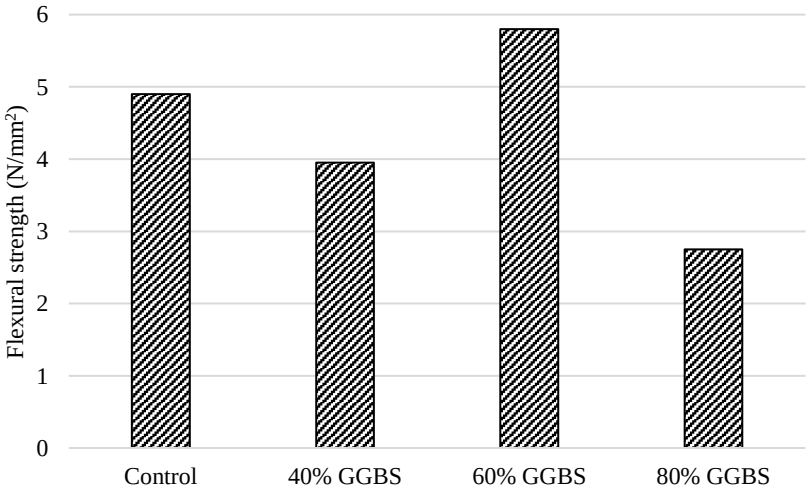

Figure 2.14 Effect of GGBS on flexural strength at 90 days (Khatib and Hibbert, 2005)

Yildirim et al. (2011) related cement types to resistance of concrete against chloride ion penetration. These included GGBS cement, sulphate resisting cement, and Portland cement blended with fly ash. The test results demonstrated that concretes produced using slag cement had substantially lower chloride ion permeability compared to that of other types of cement.

2.6.3.2 Silica fume

Silica fume ("SF") is also known as micro-silica, a non-crystalline polymorph of silicon dioxide. It is an ultrafine powder collected as a by-product of silicon and ferrosilicon alloy that consists of spherical particles with an average particle diameter of 150 nm. Its extreme fineness and high silica content make it a very effective pozzolanic material to improve the properties of concrete such as compressive strength, bond strength, abrasion resistance, etc. SF is used in two different ways: as a cement replacement to reduce the cement content, usually for economic reasons; and as an additive to improve concrete properties (in both fresh and hardened states). Generally, when SF is used as a partial replacement of cement in concrete, it enhances early strength (Poon et al., 2006) with no detrimental effect on the long-term strength and greatly improves the resistance to transportation of water and diffusion of harmful ions. As to the latter, concrete with SF exhibited lower total charges passed in chloride ion penetration test, than that of concrete without SF.

Nochaiya et al. (2010) studied the effects of SF and fly ash on conventional concrete. Mix proportions of cement paste with and without fly ash (at 5%, 10%, 20%, and 30% by weight of binder) and SF as an additive material (at 2.5%, 5%, and 10% by weight of binder), were produced. For all samples of Portland-fly ash cement pastes with SF, water requirements were higher than those mixes without SF. This was attributed to

higher surface areas of SF particles which increases the water requirement. Increasing SF content increased the compressive strength of concrete. This is because the particle size of SF is smaller than fly ash, leading to an increase in pozzolanic reaction between SiO_2 in SF and $Ca(OH)_2$ from hydration products. Strength development of Portland-fly ash cement paste without SF was found to be lower than that of Portland cement paste, especially in the mixes with greater fly ash content. High compressive strength of blended Portland-fly ash-SF concretes was attributed to both filler effect and pozzolanic reaction of SF, giving the cement matrix a denser microstructure and thereby resulting in a significant strength gain.

Research on the use of SF in PAC as an additive is limited. For instance, Nowek et al. (2007) found 6% and 10% partial replacement of cement by SF and fly ash, respectively, as the optimum percentage of replacement in PAC. PAC produced using grout incorporating SF exhibited superior physical properties than that of fly ash. Najjar and Abdelgader (2009) observed that on one hand, SF reduces the workability of grout, whereas, on the other hand, it increases the mechanical strength of PAC. Due to its fine particle size, it acts as a micro-filler material between cement and sand grain spaces, reducing the workability. SF chemically reacts with calcium hydroxide in the cement paste forming calcium silicate hydrate, delivering additional strength to the concrete.

Using SF in combination with superplasticizer exhibited enhanced compressive strength, compared to mixes without SF (Abdelgader and El-Baden, 2015). Fluidity of grout increases with the inclusion of superplasticizer, enabling the grout to efficiently fill up the voids between coarse aggregates. Pozzolanic activity of SF accelerates the hydration rate, leading to enhanced packing of microstructure.

2.6.4 Admixtures

Admixtures are ingredients added immediately before or during mixing to improve fresh and hardened properties. Admixtures such as superplasticizer ("SP"), grout fluidifier, expansive agent, air-entrained admixture, etc have been used to investigate the properties of PAC. Abdul Awal (1988) investigated the effects of SP and expansive additive on the compressive strength of PAC and conventional concrete. For mixes devoid of any admixtures and mixes containing only SP, conventional concrete displayed higher compressive strength than that of PAC. For mixes incorporating expansive additives, compressive strength of PAC was observed to be higher than that of conventional concrete.

ACI 304.1 recommends the use of grout fluidifier, usually at the rate of 1% by the weight of binder to counter the effects of bleeding water that generally tends to accumulate beneath the surface of coarse aggregates. It enables reduction in water to binder ratio, improves fluidity, retards stiffening of grout, and provides additional handling time. The use of air-entrained admixtures was observed to improve the frost resistance in PAC.

Incorporation of SP is essential to improve fresh properties of grout (Nowek et al., 2007). Abdelgader and Elgalhud (2008) studied the effects of SP and expansive agent (aluminium powder based) on the properties of PAC. Inclusion of SP in grout mixes with low water to cement ratio and high sand to cement ratio resulted in smooth surfaces at the sides and ends of hardened cylindrical specimens, attributing to the efficient filling of voids by grout in between the coarse aggregates. On the contrary to the above, the use of expansive agent reduced the compressive strength of PAC. This was ascribed to the formation of excessive air voids due to the release of hydrogen gas. Incorporation

of SP and expansive agent together produced PAC with high compressive strength. This was associated with high fluidity of grout due to incorporation of SP and minimized bleeding and settlement of grout due to incorporation of expansive agent. Expansion of grout removed the traces of bleed water that accumulates beneath the surface of coarse aggregates, eliminating any possible formation of weak zones.

Incorporating SP improves the fluidity of grout even at low water to binder ratios. However, over-dosage of SP may lead to excessive bleeding (Najjar et al., 2014). The use of SP in PAC can provide grout with the desired flowability without increasing the water content. Investigation on the use of SP is essential for successful production of PAC with superior properties.

2.6.5 Fibers

Fibers have been used in concrete to form fiber-reinforced concrete for decades (ACI 116 R). Applicable dosage of fibers varies depending on the type of fibers used. Figure 2.15 illustrates the types and amount of fibers recommended for fiber reinforced concrete. Various types of fibers have been successfully used in concrete, such as natural fibers (Kankam, 1997), steel fibers (Grunewald and Walraven, 2001), synthetic fibers (Trottier et al., 2002), glass fibers (Reis and Ferreira, 2003), etc. Fiber reinforced concrete has been studied and investigated extensively. As a result, a wide range of fibers are available commercially (Barr and El-Baden, 2003). Fibers improves ductility of concrete, especially in cases of high strength concrete which are significantly more brittle than normal strength concrete (Holschemacher et al., 2010). Type of fibers used influences the property of concrete. For instance, incorporation of nylon fibers at appropriate dosage reduces drying shrinkage of fiber reinforced concrete to one-fourth of that in plain concrete (Choi et al., 2011). Whereas incorporation of polyvinyl alcohol

fibers in concrete exhibits higher drying shrinkage than that of plain concrete (Noushini et al., 2014).

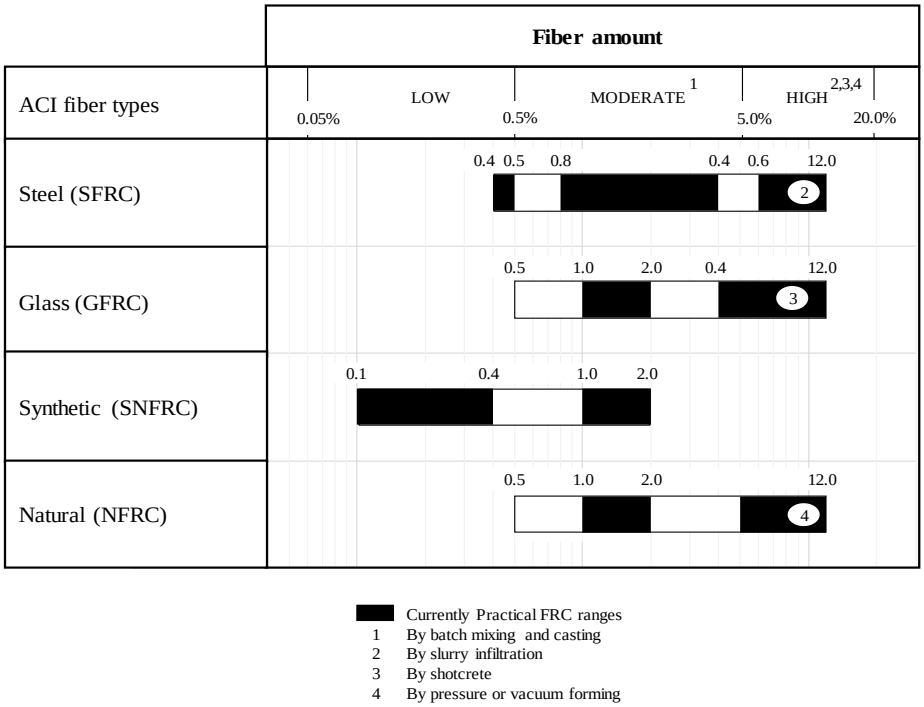

Figure 2.15 Fiber types and amount used by volume percent (Zollo, 1997)

Steel fibers have been extensively used in ground floor slabs, warehouses, etc., and represent a significant part of the fiber market. Steel fibers significantly reduce early age shrinkage in concrete. Hybrid concrete incorporating both macro and microfibers imparts superior crack-resistant properties as short fibers restrict micro-cracks and long fibers restrict macro cracks, enhancing the ductility and stiffness (Bentur and Mindess, 1990). With the increase in volume fraction of steel fibers, splitting tensile strength, flexural strength, and modulus of rupture improved significantly (Gao et al., 1997; Barr and El-Baden, 2003).

According to Song and Hwang (2004), compressive strength of concrete improved by 15.3% with incorporation of steel fibers at a dosage of 1.5% by volume fraction.

Increase in aspect ratio of fibers can significantly improve the mechanical properties of concrete (Suhad et al., 2018). As addition of fibers adversely effects on the workability of concrete (Barr and El-Baden, 2003), proper optimization of mix proportion is important. In PAC, fibers can be added with preplaced coarse aggregates to minimize the complications associated with workability. With proper optimization between coarse aggregate size and aspect ratio of fibers, fibers can remain trap in between the coarse aggregates without falling to the bottom of the volume of coarse aggregates, after grouting.

2.7 Summary

After PAC was discovered in 1937, it was applied to several large-scale projects. However, its application remains limited. This is probably ascribed to the complex pumping equipment required for grouting via pumping process. Gravity process is economical and user-friendly. However, it was limited to thin sections employing coarse aggregate size of 50 mm or above. This has resulted in underutilization of PAC, despite its high potentials.

Type and composition of raw material used to produce PAC play a vital role in determining its fresh and hardened properties. Coarse aggregate size and flowability of grout are factors influencing the penetrability of grout through the preplaced coarse aggregates that are still yet to be understood. Sand reduces flowability of grout significantly and its influence on the mechanical properties of PAC is still in dispute.

Use of mineral admixtures and pozzolans, for instance, slag, fly ash, SF or metakaolin in PAC have been scant compared to that of conventional concrete. Incorporation of supplementary cementitious materials as partial replacement of cement in grout may have positive effect to both grout and PAC properties. As the casting technique of PAC

is unique to that of conventional concrete, influence of supplementary cementitious materials to grout and in turn to PAC may not be similar to that of conventional concrete.

CHAPTER 3

METHODOLOGY

3.1 Introduction

As discussed in Chapter 2, fresh properties of grout play a vital role to the properties of PAC. The desirable flowability of grout depends on factors such as coarse aggregate size and gradation, grouting process, etc. The former influences the void content in between the coarse aggregates, thereby controlling the quantity of grout required to produce PAC. The latter includes gravity process and pumping process.

To start with the study, a preliminary experimental study was conducted to optimize grout proportions considering the flowability and compressive strength of grout. PAC was produced using different coarse aggregate sizes, employing both gravity and pumping process. The grout was subsequently modified using supplementary cementitious materials, i.e. GGBS and SF for different sand to binder ratios, water to binder ratios, and coarse aggregate sizes. Further, steel fibers were incorporated in different proportions to enhance the tensile properties and dimensional stability of PAC.

Bond strength between substrate and PAC (used as repair material) was evaluated. PAC was produced employing 10 mm and 20 mm coarse aggregates with and without SF. Further, an empirical relationship between compressive strength of PAC and its constituent components was developed through experimentally derived factorial design and statistical analysis of literature review.

In this chapter, properties of all constituent materials used in this study has been discussed. Testing procedures and methodologies applied to determine the fresh and hardened properties of PAC have been elaborated.

3.2 Materials

3.2.1 Cementitious materials

Ordinary Portland Cement of Type I conforming to ASTM C 150 was used. The mean particle size of cement was 0.0175 mm, determined by laser diffraction particle size analyser (LS13 320). GGBS and SF were obtained locally. To prevent GGBS and SF from exposure to moisture, they were packed in airtight bags. Chemical composition of cement, GGBS, and SF was analysed by X-ray fluorescence and are shown in Table 3.1. Cement and GGBS contained high percentage of CaO followed by SiO_2 and Al_2O_3. 90% of SF was composed of SiO_2. Particle size distribution of cement, GGBS and SF is shown in Figure 3.1.

Table 3.1 Chemical composition of cement, GGBS, and SF

Chemical composition	Mass%		
	Cement	GGBS	SF
MgO	0.59	6.88	2.25
Al_2O_3	5.73	16.90	0.48
SiO_2	19.10	31.70	90.30
P_2O_5	0.17	0.09	0.19
SO_3	4.40	2.45	0.61
Cl	0.01	-	0.02
K_2O	0.66	0.51	2.94
CaO	65.70	40.10	0.99
TiO_2	0.35	0.80	-
MnO	0.02	0.28	0.14
Fe_2O_3	3.14	0.27	1.24
ZnO	0.02	-	0.51
SrO	0.09	0.05	-
ZrO_2	-	0.04	-
PbO	-	-	0.15

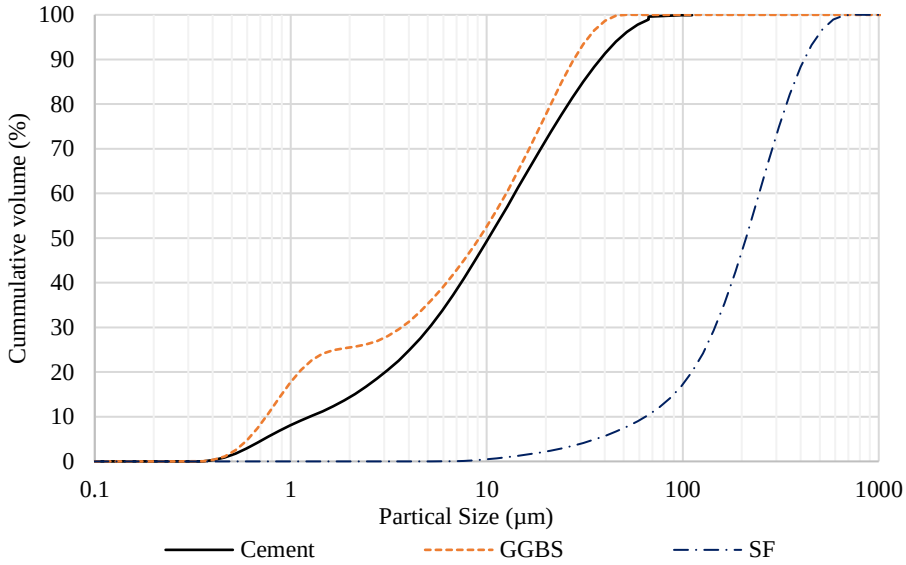

Figure 3.1 Particle size distribution of cement, GGBS, and SF

3.2.2 Fine aggregates

Natural river sand obtained locally having a specific gravity of 2.65 and fineness modulus of 2.41 and sieved as per ACI 304.1 (grading 3) was used as fine aggregates. The moisture content of sand was ranged between 1.5% to 2.4%. Sieve analysis was conducted as per ASTM C 136. The results based on three sets of sieve analysis are shown in Table 3.2 and Figure 3.2.

Table 3.2 Sieve analysis of sand

Sieve size (mm)	Weight retained (g)				Percentage retained (%)	Cumulative percentage retained (%)	Percentage passing (%)
	1	2	3	Average			
4.75	0.00	0.00	0.00	0.00	0.00	0.00	100
2.36	25.32	26.56	27.62	26.50	2.65	2.65	97.35
1.18	74.33	72.65	79.22	75.40	7.54	10.19	89.81
0.60	280.00	274.56	274.64	276.40	27.64	37.83	62.17
0.30	330.23	328.89	307.78	322.30	32.23	70.06	29.94
0.15	208.42	210.56	194.82	204.60	20.46	90.52	9.48
0.075	75.33	80.23	86.54	80.70	8.07	98.59	1.41

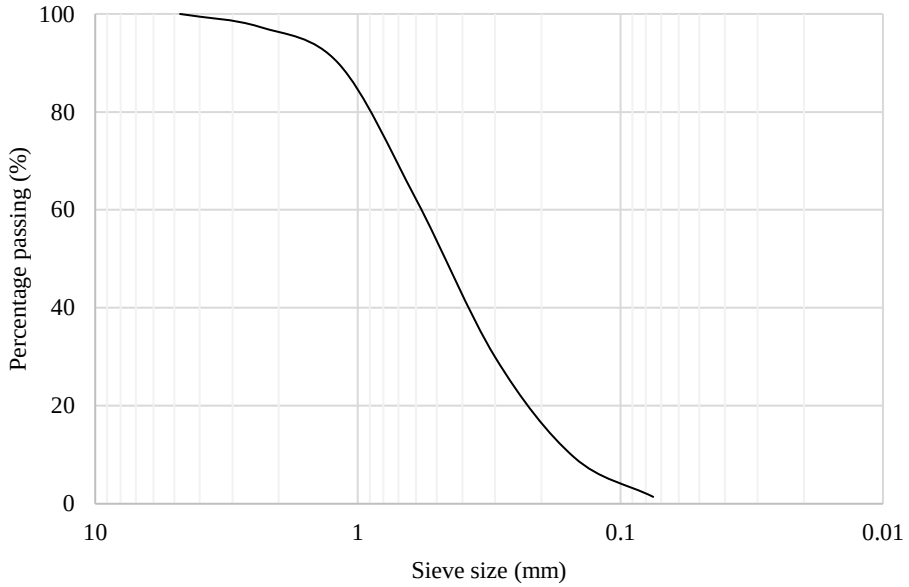

Figure 3.2 Grading of sand

3.2.3 Coarse aggregates

To obtain a wide range of coarse aggregate sizes, coarse aggregates were collected from a crushing plant in Tuen Mun, Hong Kong. They were sieved to uniform sizes of 14 mm, 20 mm, 37 mm, and 45 mm. Table 3.3 shows the gradation of coarse aggregates. Further, coarse aggregates of 10 mm and 20 mm sizes, readily available in the laboratory, were used. All coarse aggregates were crushed granite and of siliceous mineralogy. They were sieved to remove unwanted smaller particles. Three sets of sieve analysis as per ASTM C 136 for 10 mm and 20 mm coarse aggregates are shown in Table 3.4 and Table 3.5, respectively. Figure 3.3 shows coarse aggregate gradation for 10 mm and 20 mm coarse aggregates. It is essential for coarse aggregates to be washed and cleaned before use. Since coarse aggregates do not take part in the mixing process, any fines or specks of dust on the surface of coarse aggregates may result in inefficient bonding between coarse aggregates and grout. In this study, coarse aggregates were washed manually using a sieve. Coarse aggregates were sieved in small quantities and

washed under running tap water for around 5 to 8 minutes until clear water was observed passing through the sieves. Excess water was allowed to drain off and the coarse aggregates were spread on clean trays for air drying. Upon drying, coarse aggregates were stored in clean dry boxes (shown in Figure 3.4) and were used within one month of washing. Before producing PAC, a handful of coarse aggregates were examined for any dust or clay on its surface by visual inspection.

Table 3.3 Sieve analysis of coarse aggregates

Aggregate size (mm)	Sieve size (mm)	
	Passing	Retaining
45.00	50.00	45.00
37.00	45.00	37.50
20.00	37.50	20.00
14.00	20.00	14.00

Table 3.4 Sieve analysis of 10 mm coarse aggregates

Sieve size (mm)	Weight retained (g)				Percentage retained (%)	Cumulative percentage retained (%)	Percentage passing (%)
	1	2	3	Average			
45.00	0.00	0.00	0.00	0.00	0.00	0.00	100.00
37.50	0.00	0.00	0.00	0.00	0.00	0.00	100.00
20.00	0.00	0.00	0.00	0.00	0.00	0.00	100.00
14.00	39.35	0.00	44.65	28.00	2.80	2.80	97.20
10.00	320.12	323.21	275.36	306.23	30.62	33.42	66.58
5.00	637.62	669.95	678.28	661.95	66.20	99.62	0.38

Table 3.5 Sieve analysis of 20 mm coarse aggregates

Sieve size (mm)	Weight retained (g)				Percentage retained (%)	Cumulative percentage retained (%)	Percentage passing (%)
	1	2	3	Average			
45.00	0.00	0.00	0.00	0.00	0.00	0.00	100.00
37.50	0.00	97.00	42.11	46.37	4.64	4.64	95.36
20.00	831.12	720.25	839.05	796.81	15.25	19.89	80.11
14.00	162.21	178.32	117.07	152.53	79.68	99.57	0.43
10.00	0.00	0.00	0.00	0.00	0.00	99.64	0.36
5.00	0.00	0.00	0.00	0.00	0.00	99.64	0.36

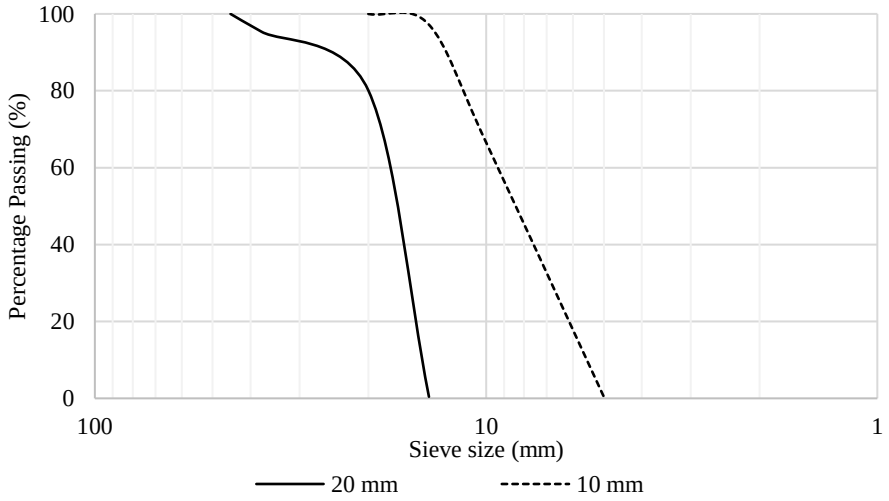

Figure 3.3 Grading of 10 mm and 20 mm coarse aggregates

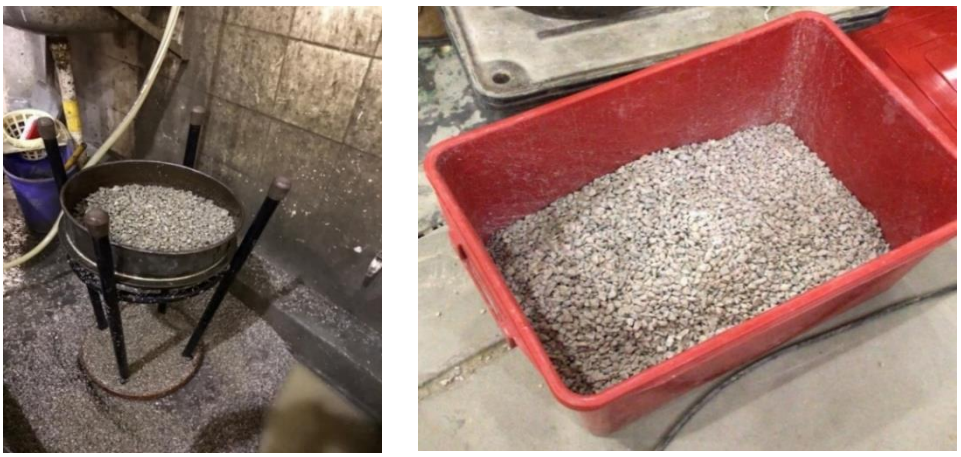

Figure 3.4 Preparation of coarse aggregates

3.2.4 Superplasticizer (“SP”)

SP was used to improve the flowability of grouts so as to enhance the penetrability of grout through the coarse aggregate skeleton. SP is a high range water reducing admixture that increases the flowability of grout without necessitating an increase in water content. SP used in the study was ADVA 109. It is based on polycarboxylate-type polymer technology and complies with BS EN 934-2. Dosage of SP is limited to 1.5% by weight of binder based on trial and error to avoid excessive bleeding of cement-sand grout. In this study, SP dosage it was limited to 1.5% by weight of binder.

3.2.5 Fibers

To improve tensile strength of PAC, locally available copper coated steel fibers (shown in Figure 3.5) were incorporated. Table 3.6 shows the specified detail of steel fibers used. This type of fiber is generally used to reinforce concrete on application to pavements, floors, bridges, etc.

Figure 3.5 Copper coated steel fibers

Table 3.6 Specified detail of steel fibers

Properties	Measurement
Type	Micro
Average length (L)	13 mm
Diameter (D)	0.18 mm
Aspect ratio (L/D)	72
Shape	Straight
Tensile strength	750-1250 MPa

3.3 Testing methodologies

ASTM C 29 was modified to estimate the **void content** of coarse aggregates. Void content refers to the space in between the coarse aggregate skeleton that would be occupied by grout. To estimate the void content, cylinders of 150 mm diameter x 300 mm height were filled with coarse aggregates of specific sizes. Water was then added to occupy the space in between the coarse aggregates. Volume of water (shown in Equation 3.1) represents the volume of grout required to fill in the voids between coarse aggregates. Equation 3.2 computes the void content of the coarse aggregates. The procedure was performed three times for each coarse aggregate gradation and the average was considered. Table 3.7 shows the void content of single-sized coarse aggregates (sieve analysis given in Table 3.3). As shown in Figure 3.6, variation of void content against coarse aggregates follows a linear relationship. Table 3.8 shows the void content of 10 mm and 20 mm coarse aggregates (sieve analysis shown in Table 3.4 and Table 3.5). There could be wall effects arising from confinement of coarse aggregates in cylinders. As diameter of cylinders is small compared to size of formworks used in the construction of PAC structures, void content may not be the same. In this study, cylinders used for producing specimens were of similar size, and this suggests similar void contents for all specimens.

$$\text{Volume of water} = \frac{B - A}{\rho_w} \quad \text{Equation 3.1}$$

$$\text{Void Content } (\%) = \frac{\text{Volume of water}}{V_t} x100 \quad \text{Equation 3.2}$$

where,

V_t = volume of cylinder considered

A = weight of coarse aggregates and mould

B = weight of coarse aggregates, mould, and water

ρ_w = density of water

Table 3.7 Void content of coarse aggregates

Coarse aggregate size (mm)	Description	Weight (g)	Volume of water (m^3)	Void content (%)
14	Aggregate + Mould	11509.27	0.00180	33.97
	Aggregate + Mould + Water	13306.79		
	Water	1537.52		
20	Aggregate + Mould	10956.56	0.00205	38.59
	Aggregate + Mould + Water	12998.37		
	Water	2015.81		
37	Aggregate + Mould	9973.97	0.00233	43.98
	Aggregate + Mould + Water	12300.88		
	Water	2326.91		
45	Aggregate + Mould	9240.10	0.00258	48.66
	Aggregate + Mould + Water	11814.62		
	Water	2574.52		

Table 3.8 Void content of 10 mm and 20 mm coarse aggregates

Coarse aggregate size (mm)	Description	Weight (g)	Volume of water (m^3)	Void content (%)
10	Aggregate + Mould	12614.69	0.00151	28.55
	Aggregate + Mould + Water	14125.29		
	Water	1510.60		
20	Aggregate + Mould	10996.59	0.00199	37.63
	Aggregate + Mould + Water	12987.71		
	Water	1991.12		

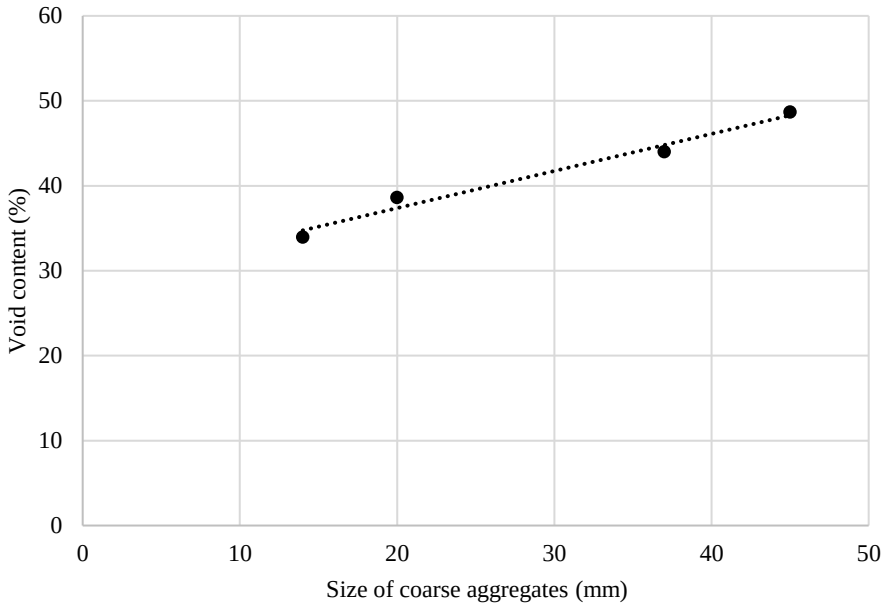

Figure 3.6 Void content of coarse aggregates

For preparation of specimens, all raw materials were weighed before mixing in the grout mixer. Moulds were cleaned, and a thin film of oil was applied uniformly. The moulds were filled with coarse aggregates of the desired size and the top surface of the moulds were levelled gently using a metal rod. Nominal compaction was applied manually with a wooden hammer to pack the coarse aggregates. To prepare the grouts, the dry ingredients, i.e. cement, supplementary cementitious materials, and sand were

mixed in the mixer for 5 minutes. SP was mixed with water and added steadily to the mix, such that there was no spilling or splashing. Mixing was performed for another 2 to 3 minutes. A trowel was used to disperse unmixed lump accumulated at the side or bottom of the mixer. Mixing was continued for another minute to ensure consistency of the grout. Fresh properties of grout were determined immediately after mixing. Grout was then added to the moulds through the desired grouting process. Gentle tapping was applied fairly consistently for all specimens to ensure efficient grouting. The specimens were then covered with plastic wraps to avoid moisture loss. The specimens were demoulded after 24 hours, cured, and tested as per guidelines and testing procedures outlined below.

Fresh properties of grout were assessed in terms of flowability and bleeding. Hardened property of grout was evaluated in terms of compressive strength. Mechanical property of PAC was evaluated in terms of compressive strength, splitting tensile strength and pull-off strength. Durability of PAC was evaluated in terms of chloride ion penetrability, excess voidage, and drying shrinkage. A flow diagram showing the tests are elaborated in Figure 3.7.

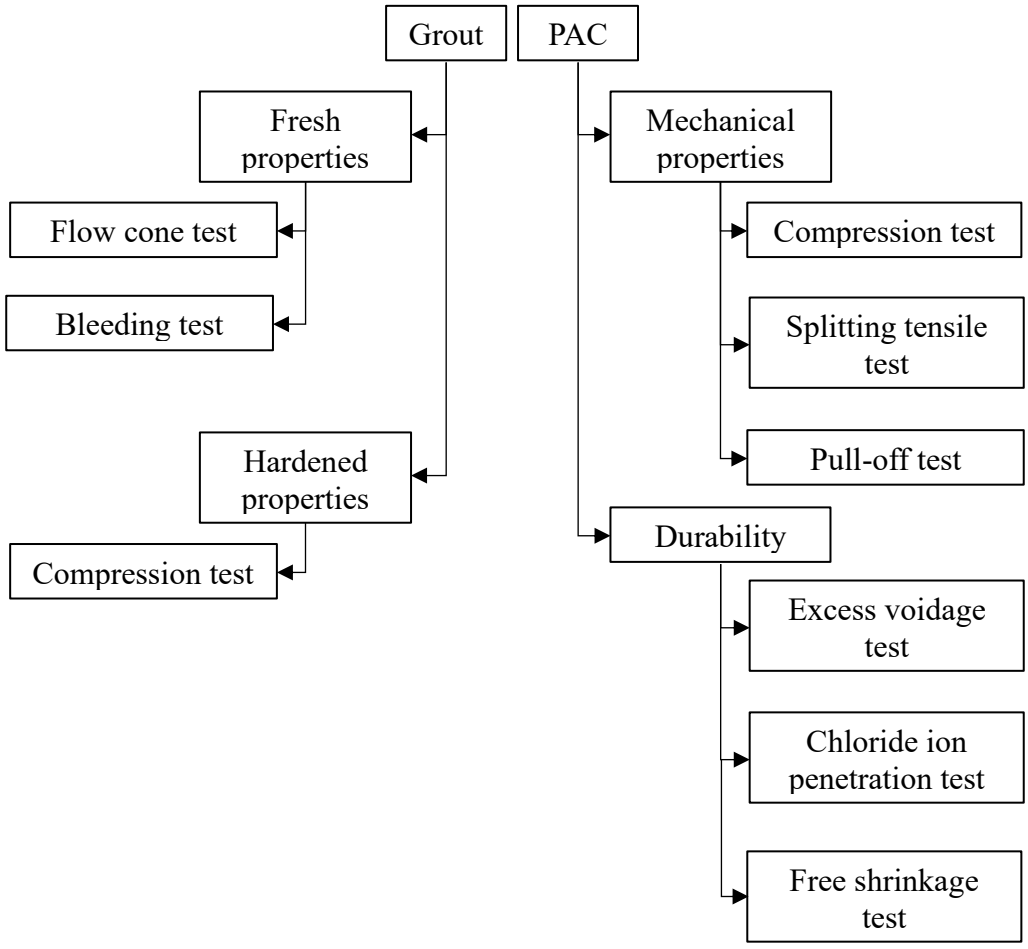

Figure 3.7 Flow chart of tests conducted

3.3.1 Testing on grout

An assessment on fresh and hardened properties of grout is essential as it influences the production of PAC. To produce quality grout, fresh properties in terms of bleeding and flowability are important. As to the latter, it primarily influences the filling ability of grout within the coarse aggregate skeleton. Hardened property of grout such as compressive strength stands as one of the factors influencing the mechanical property of PAC.

Flowability was determined by **flow cone test** as per ASTM C 939. Dimensions of flow cone and test setup of flow cone test is shown in Figure 3.8 and Figure 3.9, respectively.

Flow cone was first soaked in water for one minute to prevent absorption of moisture from grout. It was then mounted firmly on the stand and levelled. The discharge tube was closed, and 1725 ml of grout was introduced. The discharge tube was opened to allow the grout to flow. Efflux time was measured by a stopwatch, being the time for light to become visible when viewed from the top of the cone. Three readings were taken and should be within 1.8 seconds of the averaged efflux time. As a reference, water takes 8 ± 0.2 seconds to be completely discharged from the flow cone. For application on walls and structural repairs, grout with efflux time of 22 ± 2 seconds is recommended (ACI 304.1).

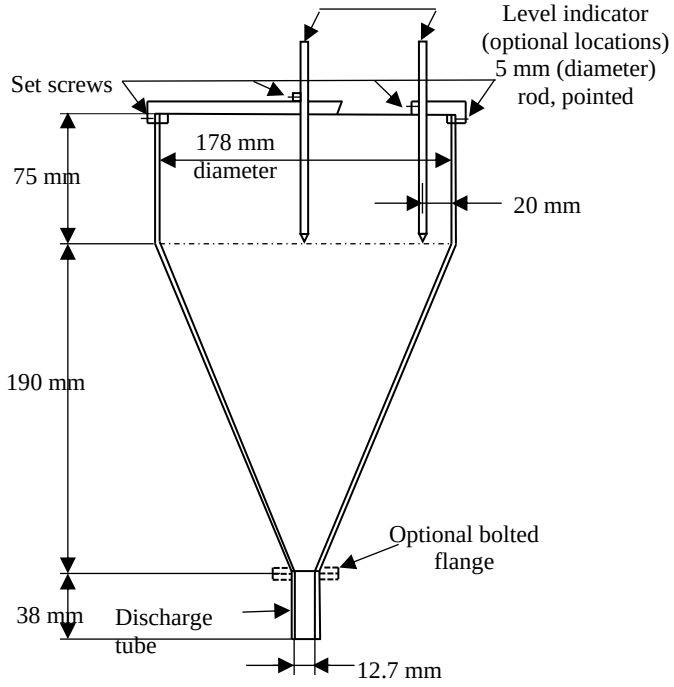

Figure 3.8 Cross-section of flow cone (ASTM C 939)

Figure 3.9 Flow cone test setup

Bleeding test was performed as per ASTM C 940. A 1000 ml graduated cylinder was filled with 800 ± 10 ml of grout within 3 minutes after mixing and it was placed on a

levelled surface. Surface of the cylinder was covered to prevent evaporation as shown in Figure 3.10. Volume of sample against time of reading was recorded. Readings of the upper surface of grout or bleed water were taken to nearest 1 ml. In the first hour, readings were taken at 15-minute intervals followed by hourly readings for 3 hours. Bleed water was transferred to a 25 ml graduated cylinder and measurements to nearest 0.5 ml was recorded. Final bleeding was then calculated as per Equation 3.3.

$$\text{Final bleeding}\ (\%) = \frac{V_w}{V_i} \times 100 \qquad \text{Equation 3.3}$$

where,

V_w = volume of decanted bleed water, ml

V_i = volume of sample at the beginning of test, ml

Figure 3.10 Bleeding of grout

Compressive strength of grout was determined as per ASTM C 942. Cube moulds of side 50 mm were coated with a thin film of oil. Grout was applied until the moulds were

half-filled. It was puddled 5 times to release any entrapped air. Finally, the moulds were completely filled with grout and puddled again. Excess grout was removed using an edged trowel. Surfaces of the moulds were covered with plastic wraps to prevent any loss of moisture. Each set comprises of 3 moulds. At least five sets were prepared for each mix to obtain compressive strength at different ages. The specimens were demoulded after 24 ± 1 hours and cured in water until the day of testing. Averaged strength of each set was calculated to nearest 0.01 MPa. Figure 3.11 shows the compression test of grout.

Figure 3.11 Grout compression test

3.3.2 Testing on hardened PAC

Hardened properties of PAC were evaluated in terms of mechanical properties, durability, and dimensional stability. Mechanical properties were assessed by compression test, split tensile test, and pull-off test. Durability of PAC was assessed by excess voidage test, chloride ion penetration test, and drying shrinkage test.

Cylinders of dimensions 1:2 (diameter: height) including 100 mm x 200 mm (diameter x height) and 150 mm x 300 mm were prepared for **compressive strength** as per ASTM C 39. The difference in size of cylinder did not affect the compressive strength of PAC. Cylindrical moulds were coated with a thin film of oil and then filled with coarse aggregates of the desired size. Top of the cylinders were levelled manually, using a trowel. Grout was applied by desired grouting process. Cylinders were covered with a plastic sheet. They were demoulded and cured in water after 24 hours.

Cylinders were taken out of the curing tank one day prior to testing, and masses of the specimens were recorded. They were then capped and air-dried for 24 hours. Capping compound was prepared using gypsum. Figure 3.12 shows the capping process. The cylinders were tested in a universal testing machine (as shown in Figure 3.13) and mode of failure was observed. Averaged properties were obtained from testing a minimum of three cylinders.

Figure 3.12 Capping of cylinders

Figure 3.13 Compression test setup

Splitting tensile strength was determined in accordance with ASTM C 496, using 100 mm x 200 mm (diameter x height) cylinders. Cylinders were produced in the same way

as that of compressive strength. Cylinders were placed underwater for curing for 28 days.

On the day of testing, cylinders were weighed. Lines were drawn on the opposite sides to ensure proper alignment during testing. They were placed in a form that consisted of a base plate and a bearing bar positioned at the top, as shown in Figure 3.14, and were tested in the universal testing machine until failure. Averaged properties were obtained from a minimum of three cylinders.

Figure 3.14 Splitting tensile test setup

Pull-off test was conducted by modifying the testing procedure to ASTM C 1583. In ASTM C 1583, firstly repair material was cast on top of the substrate, and cores were drilled through the repair material. Metal disc was then attached to the surface of the repair material. As coring could damage the bonding between repair material and substrate, PAC was cast on prefabricated gaps made using formwork to alleviate coring. This is illustrated in Figure 3.15. PAC was cast on square-shaped formwork and metal discs were replaced by metal blocks. Tensile force was applied to the metal block to determine the bond strength.

Pull-off test was conducted using a DYNA mobile pull-off tester, manufactured by "PROCEQ", as shown in Figure 3.16. It was equipped with an electronic measuring cell and a digital display. The tester was levelled by adjusting the legs, such that tensile force was applied in the perpendicular direction via the metal block attached to PAC and tested to failure. Peak values were recorded before debonding of PAC from substrate. Averaged properties were obtained from a minimum of three specimens.

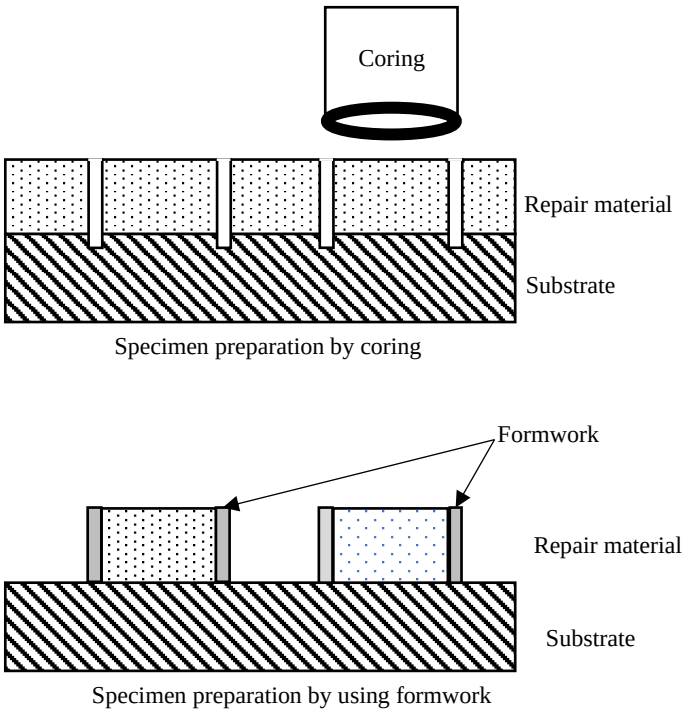

Figure 3.15 Specimen preparation for determination of bond strength by coring and using formwork

Figure 3.16 DYNA mobile pull-off tester

100 mm x 200 mm cylinders at 28 days were used to determine the water absorption of substrate (conventional concrete) as per BS 1881-122. Cylinders were placed in an oven for 72 hours and allowed to cool for 24 hours. They were immersed in water for 30 ± 5 minutes. Weight of each cylinder was recorded before and after immersion in water. Table 3.9 shows the water absorption of cylinders. Water absorption was defined as increase in mass after immersion in water. A correction factor was incorporated according to surface to volume ratio and is given by Equation 3.4. Water absorption of conventional concrete was found to be 5.55%.

$$\text{Correction factor} = \frac{\text{Volume } (\text{mm}^3)}{\text{Surface area } (mm^2) \text{ x } 12.5} \qquad \text{Equation 3.4}$$

Table 3.9 Water absorption of cylinders

Sl no.	Mass before immersion in water (M_0)	Average	Mass after 30 minutes of immersion in water (M_{30})	Average	Absorption (%)	Correction factor	Corrected absorption (%)
1	3280.9		3397.1				
2	3366.4	3316.3	3488.9	3431.3	3.47	1.6	5.55
3	3301.6		3407.8				

Excess voidage of PAC specimens was estimated as per BS EN 12504-1. Drilled cores of 100 mm diameter (as shown in Figure 3.17) were collected to estimate the excess voidage. Surfaces of cores of 125 mm x 80 mm were compared to live sized photographs with known voidage, ranging from 0% to 13%. Photographs were secured on the surface of cores, and size and number of voids on the surface of cores were assessed by two observers to avoid extremes of subjective biases. Excess voidages of 0.5% to 2.5% are considered as normal. Excess voidage above 2.5% implies inadequate compaction of concrete (BS EN 13791) and this threshold value is also applied to PAC.

Figure 3.17 Drilled cores for estimation of excess voidage

Rapid chloride ion penetration test was performed as per ASTM C 1202. Cylinders of 100 mm diameter were cut to 50 mm thick slices, using a metallographic cut-off machine, as shown in Figure 3.18. Ends of cylinders were discarded and 50 mm thick slices were cut out from the remaining part of the cylinders. The slices were coated with epoxy (peripheral area), cured, and dried. The slices were then subjected to vacuum pressure for 3 hours, followed by vacuum saturation for 1 hour and soaking for 18 hours. For testing, each slice was placed in a test cell (shown in Figure 3.19). Rubber gaskets were used to prevent leakage. Clamps were used to tighten and seal off the slices. The negative side of test cell was filled with a 3% NaCl solution, while the positive side of test cell was filled with 0.3N NaOH solution. The experimental setup is shown in Figure 3.20. A 60-volt potential was applied through lead wires and the amount of charge passing through the slices was recorded for 6 hours. Depending on the charge passed, chloride ion penetration was classified into different levels of penetrability, as shown in Table 3.10. Testing equipment for chloride ion penetration test (manufactured by Sona) can accommodate up to 6 specimens at the same time. In this study, not more than 5 specimens were tested next to each other.

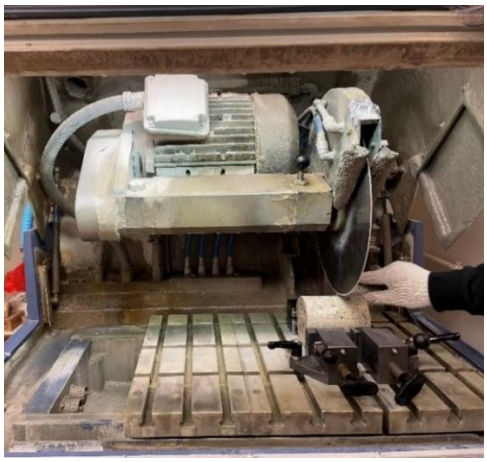

Figure 3.18 Cutting specimens into slices

Figure 3.19 PAC slice placed inside cell

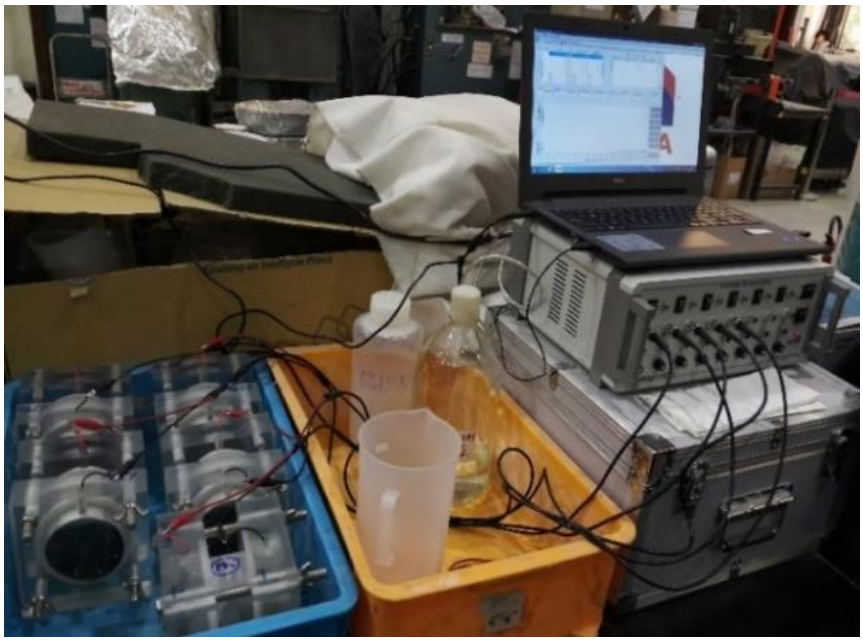

Figure 3.20 Experimental setup for chloride ion penetration test

Table 3.10 Chloride ion penetrability (ASTM C 1202)

Charge passed (C)	Chloride ion penetrability
>4000	High
2000-4000	Moderate
1000-2000	Low
100-1000	Very low
<100	Negligible

Change in length of PAC due to **drying shrinkage** was determined as per BS ISO 1920-8. Moulds were aligned and studs were attached to the moulds. A distance of 250 mm between the inner ends of each pair of studs was ensured. Coarse aggregates were introduced gently such that the studs were not dislocated or loosened. Grouting was achieved by gradually applying the grout from the top. The specimens were cautiously wrapped with plastic sheets to prevent loss of moisture and were demoulded after 24 ± 2 hours, labelled, and stored underwater for moist curing. The specimens were stored

in tap water and water was changed regularly, at least once every 7 days. pH values of water varied between 6.5 and 9.0.

The specimens were removed from water after 7 days and wiped dry with a piece of cloth. Length of specimen was recorded by a vertical length comparator (shown in Figure 3.21), by positioning the bottom gauge stud to the base anvil first. The specimens were rotated axially till the front face was parallel to the dial gauge. Three readings were taken from each specimen and were checked to ensure within 0.001 mm of the averaged reading. The specimens were then stored in humidity chambers at 25°C and 50% relative humidity. Readings were taken at regular intervals for 3 months.

Drying shrinkage is defined as measured length less the initial length and divided by the gauge length (250 mm) as shown in Equation 3.5.

$$\Delta L\ (\%) = \frac{CR - \text{initial } CR}{G} \text{ x } 100 \qquad \text{Equation 3.5}$$

where,

ΔL = Length change of specimen at any age

CR = Difference between comparator reading of specimen and reference bar at any age

G = Gauge length (mm)

Figure 3.21 Drying shrinkage test

CHAPTER 4

EFFECTS OF COARSE AGGREGATE SIZE AND GROUTING PROCESS ON PAC

4.1 Introduction

PAC is formed by preplacing coarse aggregates and applying grout by grouting process. Thus, it permits larger quantity of coarse aggregates as compared with that in conventional concrete (Omidi et al., 2019). Table 4.1 shows grouting process applied by various authors on different sizes of coarse aggregates. It is observed that smaller-sized coarse aggregates are generally accompanied by pumping process. In fact, pumping process has been successfully applied to many large-scale projects. (ACI 304.1; ACI E706). However, use of PAC in small-scale projects and repair remain somewhat restricted. This could be ascribed to the involvement of sophisticated pumping equipment which generally upscales the resources required for its operation and maintenance. This has caused the underutilization of PAC (Abdelgader and Gorski, 2002; Nowek et al., 2007).

As an alternative, gravity process is user-friendly and does not require sophisticated pumping equipment. To achieve efficient filling of voids in between the coarse aggregates by gravity process, grout with high flowability is desired and larger-sized coarse aggregates are preferred.

In this chapter, PAC produced by gravity process and pumping process was compared against size of coarse aggregates ranging from 14 mm to 45 mm. Properties including compressive strength, excess voidage, and resistance to chloride ion penetration were

evaluated. Performance of PAC was further compared with that of conventional concrete produced using same size of coarse aggregates.

Table 4.1 Literature on grouting process and coarse aggregate size of PAC

Reference	Coarse aggregate size	Grouting process
Omidi et al. (2019)	27-32 mm and 15-21 mm	Gravity followed by vibration
Du et al. (2017)	5-10 mm (Lightweight aggregates)	Pumping
Coo and Pheeraphan (2016)	19-25 mm	Pumping
Lee et al. (2016)	22.4-63 mm	Gravity
Mohammadhosseini et al. (2016)	20-38 mm	Pumping and gravity
Coo and Pheeraphan (2015)	4.75-9.5, 9.5-19, and 19-25 mm	Pumping
Abdelgader et al. (2013)	20 and 37.4 mm combined	Gravity
Morohashi et al. (2013)	5-20mm (Recycled aggregates)	Gravity followed by vibration
Neville (2011)	10-38 mm	Pumping
Marke and Marke (2010)	47, 50, and 55 mm	Gravity followed by vibration
Abdelgader et al. (2010)	9.5-37.5 mm	Pumping
Vieira et al. (2010)	19-150 mm	Gravity
Abdelgader and Elgalhud (2008)	38 mm	Pumping
Nowek et al. (2007)	16-31.5 mm	Gravity
Warner (2005)	9.5-37.5 mm	Pumping
Abdelgader (1996)	16-100 mm	Gravity
Abdul Awal (1988)	Maximum size: 38 mm	Pumping
Davis (1960)	Minimum size: 12-16 mm	Pumping

4.2 Preliminary investigation

It was conducted to determine an optimum mix proportion of grout. Bleeding tests were carried out as per ASTM C 940. Grout consistency was determined by flow cone test, measured in terms of efflux time to ASTM C 939. Grout compression tests were performed to ASTM C 942 at 7 days and 28 days.

4.2.1 Grout mix proportions

Properties of grouts play a vital role on the mechanical properties of PAC. To ensure filling up of voids in the preplaced aggregates by grout, it is essential for grout to have suitable flowability. For traditional cement-sand grout, S/B ratio usually varies from 0.5 to 2.0 (Coo and Pheeraphan, 2015; Lv et al. 2020), with S/B=1 being commonly used (ACI 304.1). In this study, PAC was intended to be produced using smaller-sized coarse aggregates via gravity process, lower ratios of S/B were applied to achieve smaller efflux time. Two sand to binder ratios ("S/B") were considered (namely 0.50 and 1.00) after a series of trial and error. Particle size distribution of sand is shown in Figure 3.2. To obtain higher strength, water to binder ratio ("W/B") was reduced and varied between 0.33, 0.37, and 0.42. Reducing W/B ratio to below 0.33 was not considered as the SP dosage was limited to 1.5% by mass of binder. SP dosage was kept constant at 0.50% by weight of binder. Mix proportions of the grouts are shown in Table 4.2. As to the mix IDs, S/B and W/B ratios are represented by Sxx and Wyy respectively, with xx and yy being the representative ratio.

Table 4.2 Grout mix design

Mix no.	Mix ID	S/B	W/B	SP by weight of B
1	S0.5W0.33	0.50	0.33	0.50%
2	S0.5W0.37	0.50	0.37	0.50%
3	S0.5W0.42	0.50	0.42	0.50%
4	S1.0W0.33	1.00	0.33	0.50%
5	S1.0W0.37	1.00	0.37	0.50%
6	S1.0W0.42	1.00	0.42	0.50%

4.2.2 Grout properties

Bleedings of all grout mixes were measured to ASTM C 940 and were well within the permissible limits, i.e. bleeding less than 2% after 120 minutes. Table 4.3 shows the efflux time of grout. As shown in Figure 4.1, efflux time decreases with increasing W/B ratio, for both S/B=0.50 and S/B=1.00. When S/B=1.00, efflux time was larger, indicating a decrease in flowability. Decrease in flowability with increasing sand content could be ascribed to angular and rough surface of sand which trapped free cement-water paste between interlocking particles, thereby increasing the viscosity of the grout (Coo and Pheeraphan, 2015). When grout is under shear stress, shear rate within sand remains zero (as sand particles do not deform). Regarding the paste of grout, shear rate of grout containing sand is higher than that of without sand (Hu, 2005). High shear rate results in higher stress and higher resistance to the flow of grout. In another words, efflux time of grout increases with increasing sand content. Efflux time of mix ID S1.0W0.37 and mix ID S1.0W0.42 was not measurable due to inconsistency of flow (flow of grout discontinued through the flow cone) and excessive segregation, respectively. The latter could be ascribed to high sand content and insufficient matrix to bond and contain sand, thus causing sand to settle. Grout with an efflux time of 22 ± 2 seconds is generally considered satisfactory for works such as walls and structural repair (ACI 304.1). Based on the above, mix ID S0.5W0.37 was found to have suitable

efflux time of 21.26 seconds, close to the recommendation by ACI 304.1. Mix ID S0.5W0.42 displayed the lowest efflux time of just 12 seconds, indicating high flowability.

Table 4.4 and Figure 4.2 show 7 days and 28 days compressive strength of grout. As shown in Figure 4.2, at the same S/B ratio, both 7 days and 28 days compressive strengths decrease with increasing W/B ratio. Mix ID S0.5W0.33 and mix ID S1.0W0.33 exhibit comparable compressive strength at the same W/B ratio and increasing S/B ratio does not have a significant effect on compressive strength of the grout. For W/B=0.37, compressive strength of grout decreases with increasing S/B ratio. This can be attributed to the fair amount of reduction in the volume of binder. Compressive strength of mix ID S1.0W0.42 could not be measured due to excessive segregation.

Overall, even though mix ID S0.5W0.42 displays smaller efflux time than that of mix ID S0.5W0.37, 28 days compressive strength of mix ID S0.5W0.42 was 38% lower than that of mix ID S0.5W0.37. Mix ID S0.5W0.33 and S1.0W0.33 displays higher compressive strength than that of mix ID S0.5W0.37. However, mix ID S0.5W0.37 displayed an efflux time that was significantly smaller than that of mix ID S0.5W0.33 and S1.0W0.33. As both flowability and compressive strength are vital properties of grout, where flowability influences the penetrability of grout through the coarse aggregate skeleton and compressive strength of grout influences the mechanical properties of PAC. Mix ID S0.5W0.37, with suitable efflux time and satisfactory compressive strength, is considered to be the optimum mix and is also applied in the subsequent study.

Table 4.3 Efflux time of grout

Mix ID	(sec)			
	1	2	3	Average
S0.5W0.33	32.65	33.45	34.16	33.42
S0.5W0.37	22.06	20.63	21.09	21.26
S0.5W0.42	11.20	12.65	12.57	12.14
S1.0W0.33	91.36	94.33	84.85	90.18
S1.0W0.37	Not consistent			
S1.0W0.42	Excessive segregation			

Table 4.4 7 days and 28 days compressive strength of grout

Mix ID	7 days (MPa)				28 days (MPa)			
	1	2	3	Average	1	2	3	28 days
S0.5W0.33	60.32	61.59	57.19	59.70	86.36	89.56	89.70	88.54
S0.5W0.37	52.06	51.96	51.92	51.98	84.89	83.28	86.98	85.05
S0.5W0.42	45.65	46.32	50.95	47.64	57.95	54.62	56.03	56.20
S1.0W0.33	62.96	58.06	57.36	59.46	87.32	86.23	86.01	86.52
S1.0W0.37	20.32	26.93	26.40	24.55	38.26	35.95	37.15	37.12
S1.0W0.42	Excessive segregation							

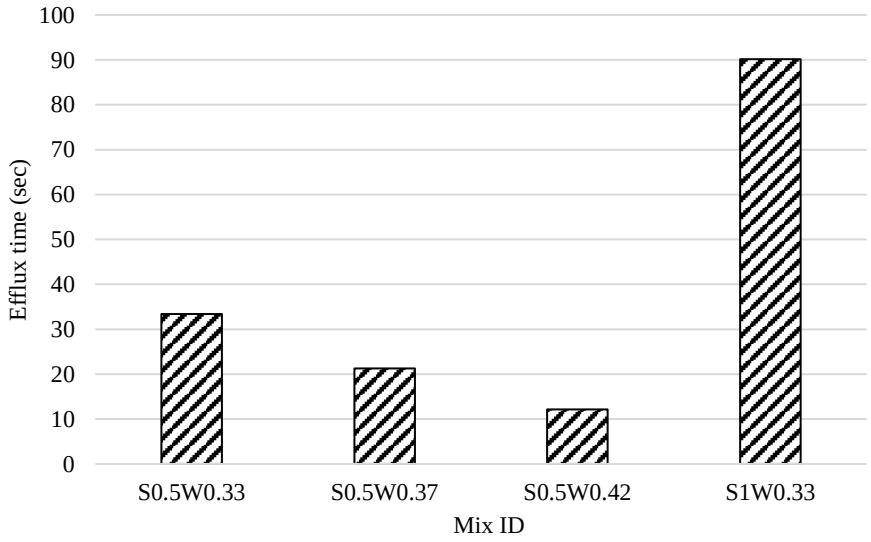

Figure 4.1 Efflux time of grout

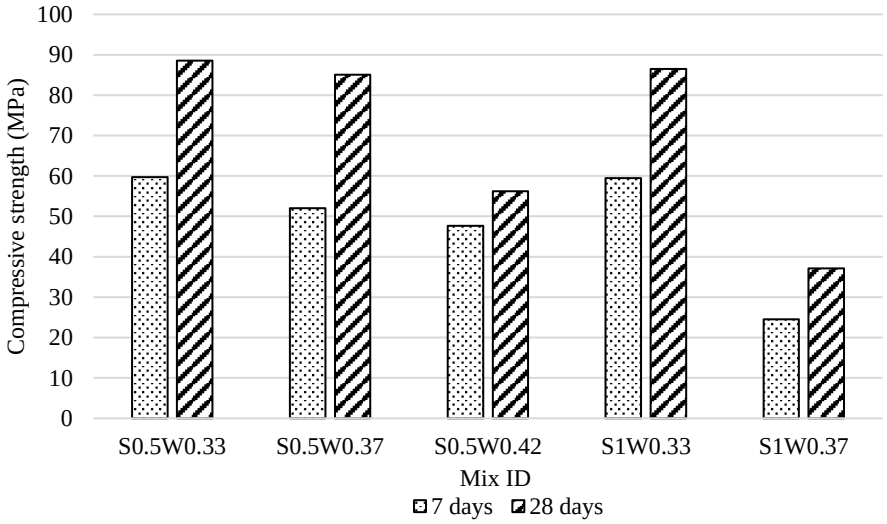

Figure 4.2 Compressive strength of grout

4.3 Specimens and tests

Mix proportion of PAC produced using different sizes of coarse aggregate is shown in Table 4.5. To monitor the flow of grout, PAC specimens were prepared using acrylic moulds. ASTM C 31 recommends the size of cylinders to be at least 3 times to that of the nominal maximum size of the coarse aggregates used. As the maximum size of coarse aggregates used was 45 mm, 150 mm diameter cylinders were used. Hollow acrylic cylinders of 150 mm internal diameter were cut to 300 mm length and split into two halves parallel to its length for easy demoulding. The cylindrical moulds were secured by metal strips. Acrylic square plate was used to form the base of the cylinder. They were glued together using silicon glue. To produce PAC by gravity process, grout was applied from the top and allowed to penetrate by the action of gravity. To produce PAC by pumping process, grout was pumped from the base under pressure. Flow of grout was regulated and controlled manually by valves. Figure 4.3 shows the setup of (a) cylindrical moulds, (b) cylindrical moulds with coarse aggregates, and (c) grouting via pumping process. A high-pressure portable grout pump with flow rate of up to

8L/min was used to perform the pumping process. Compression test was performed at 28 days as per ASTM C 39.

To estimate excess voidage and to perform chloride ion penetration test, 100 mm diameter cylinders were cored from 150 mm diameter cylindrical specimens. 150 mm diameter cylindrical specimens were first secured in concrete slabs of 300 mm thickness and later coring was performed. Excess voidage was estimated as per BS EN 12504-1. 100 mm diameter cylinders were cut into slices of 50 mm thickness for performing chloride ion penetration test to ASTM C 1202.

Table 4.5 : Mix proportion of PAC with different sizes of coarse aggregates

Coarse aggregate size (mm)	Cement (kg/m^3)	Sand (kg/m^3)	Water (kg/m^3)	SP (kg/m^3)	Coarse aggregate (kg/m^3)
14	388	194	146	1.94	1849
20	431	215	162	2.16	1684
37	502	251	188	2.51	1569
45	555	277	208	2.77	1438

(a)

(b)

(c)

Figure 4.3 Experimental procedure

4.4 Effect coarse aggregate sizes on grouting process

Four different sizes of coarse aggregates, i.e. 14 mm, 20 mm, 37 mm, and 45 mm were considered. Table 3.3 shows grading of coarse aggregates. A suitable grout proportion

with S/B=0.50 and W/B=0.37, as determined in the preliminary investigation, was applied to produce PAC via gravity process and pumping process. Compressive strength, excess voidage, and resistance to chloride ion penetration against coarse aggregate size and grouting process were evaluated. Conventional concrete was produced using traditional mixing method to draw a comparison to PAC.

4.4.1 Excess voidage

Excess voidage is referred to as pockets of entrapped air in hardened concrete. In this study, 100 mm diameter cores were collected from PAC specimens for estimation of excess voidage to BS EN 12504-1. The results are summarized in Table 4.6. Figure 4.4 is the pictorial representation of excess voidage of PAC, X mm, G/P, Y%, where X is coarse aggregate size, G/P is gravity process/pumping process, and Y is excess voidage.

Table 4.6 Excess voidage versus 28 days compressive strength of PAC and conventional concrete

Grouting process	Coarse aggregate size	Excess voidage	28 days compressive strength (MPa)			
			1	2	3	Average
Gravity process	14 mm	3.0%	28.96	31.35	31.43	30.58
	20 mm	1.5%	43.52	43.12	40.74	42.46
	37 mm	1.5%	34.65	32.96	33.40	33.67
	45 mm	1.5%	32.21	31.65	32.74	32.20
Pumping process	14 mm	1.5%	37.96	38.08	35.08	37.04
	20 mm	0.5%	44.09	43.65	43.00	43.58
	37 mm	0.5%	35.26	35.02	34.60	34.96
	45 mm	0.5%	35.85	33.45	34.65	34.65
Conventional concrete	20 mm	-	37.32	36.56	36.10	36.66

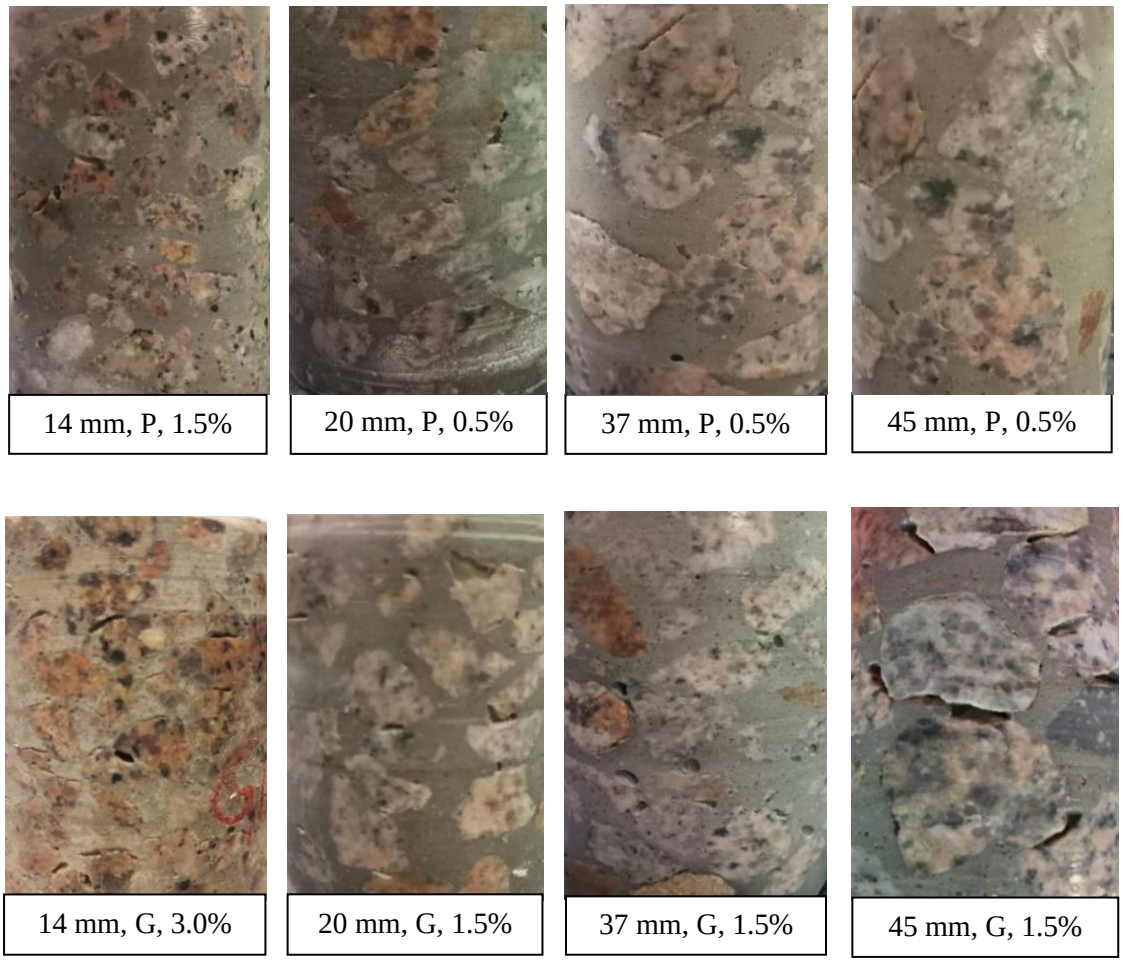

Figure 4.4 Excess voidage in PAC

Excess voidage between 0.5% and 2.5% is generally considered to be normal whereas excess voidage exceeding 2.5% implies inadequate compaction (BS EN 13791). For PAC produced using 20 mm, 37 mm, and 45 mm coarse aggregates, excess voidage was 1.5% and 0.5% for gravity process and pumping process, respectively. When coarse aggregate size was reduced to 14 mm, excess voidage increased to 3.0% for gravity process and 1.5% for pumping process. PAC produced using coarse aggregates of 20 mm and above had larger void content, enabling efficient penetrability of grout, thereby resulting in acceptable excess voidage. However, with the reduction in coarse aggregate size to 14 mm, passage for grout to penetrate through narrowed down,

impeding the flow of grout, thereby increasing the excess voidage. Pumping process resulted in a lower excess voidage as grouting under pressure assists in filling up the voids between the coarse aggregates efficiently.

4.4.2 Compressive strength

Compressive strength of PAC produced by both gravity process and pumping process is given in Table 4.6. Figure 4.5 is the graphical representation of compressive strength. Compressive strength increases with decreasing coarse aggregate size and reaches peak value at 20 mm coarse aggregate size. Based on the above, the optimum coarse aggregate size is suggested to be 20 mm. Similar observations were made by Alexander and Wardlaw (1960), on conventional concrete, where the optimum size of coarse aggregates was suggested to be 19 mm as further decrease in the size of coarse aggregates did not increase the compressive strength.

Walker and Bloem (1960) and Bloem and Gaynor (1963) concluded that increasing coarse aggregate size reduces the compressive strength of conventional concrete. Failure in concrete typically occurs at the matrix-coarse aggregate interface. The stresses developed at the interface causing failure can be reduced by increasing surface area of the coarse aggregates, which can be achieved by reducing the coarse aggregate size (Cordon and Gillespie, 1963; Rashid and Mansur, 2009). Use of small-size coarse aggregates is favourable for improving the structure of interfacial transition zone (Guo, et al., 2020). ACI 363 suggests minimizing the maximum size of coarse aggregates to produce concrete with compressive strength greater than 41 MPa.

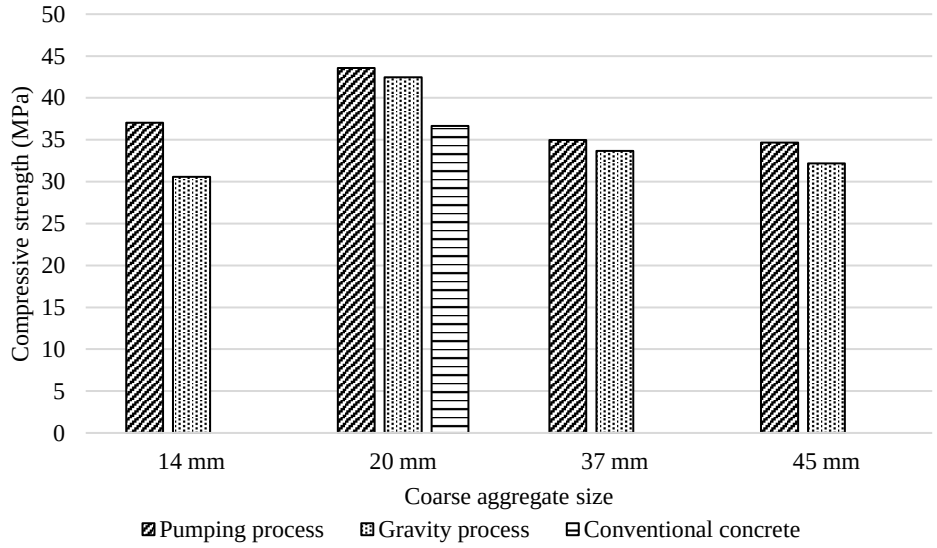

Figure 4.5 Compressive strength of PAC and conventional concrete

For PAC with coarse aggregate size at 20 mm and above, the difference in compressive strength of PAC produced by gravity process and pumping process is insignificant. As the void content (space in between coarse aggregates occupied by grout) between the coarse aggregates increases, cross-section of the passages through which the grout passes also increase, enabling efficient penetration of grout. Vice versa, reducing the coarse aggregate size to 14 mm results in a decrease in compressive strength. This is due to reduced void content thereby impeding the flow of grout.

PAC produced using 14 mm coarse aggregates via gravity process exhibited highest excess voidage (pockets of entrapped air in hardened concrete) of 3% and displayed 17% lower compressive strength than that of pumping process. Strength of concrete is greatly reduced by the presence of excess voidage. For instance, excess voidage of 5% and 2% in concrete may reduce the strength of concrete by 30% and 10%, respectively (Neville, 1958). In pumping process, as the grout is injected under pressure, air trapped between the coarse aggregates is forced out and thus the voids can be efficiently filled

up by grout. This ensures better performance in terms of both excess voidage and strength, especially when smaller size coarse aggregates are used. Based on the above, gravity process is limited to coarse aggregate size of 20 mm or above. Reduction in coarse aggregate size below 20 mm compromises the compressive strength of PAC and pumping process is a better alternative.

4.4.3 Chloride ion penetration

Chloride ion penetration test was conducted at 28 days. Table 4.7 shows chloride ion penetration of PAC. For 45 mm coarse aggregates, high chloride ion penetrability was recorded. This was attributed to a higher percentage of grout area per cross-sectional area, providing larger cross-section for chloride ions to pass through. Figure 4.6 shows indicative pictorial representation traced from the cross-sectional surfaces of PAC specimens. For coarse aggregate sizes ranging from 37 mm to 14 mm, chloride ion penetrability was moderate. PAC with 20 mm coarse aggregates exhibited the lowest chloride ion penetrability.

Chloride ion penetrability increases with further reduction in size of coarse aggregates from 20 mm to 14 mm. Excess voidage of PAC produced using 14 mm coarse aggregates was 1% and 1.5% greater than that of PAC produced using 20 mm or larger coarse aggregates for gravity process and pumping process, respectively; resulting in an increase in air pockets entrapped in between the coarse aggregates and thus, increasing penetrability. PAC produced via pumping process displayed a better resistance to chloride ion penetration compared to that of gravity process. This could be related to the reduced excess voidage in PAC produced by injecting grout under pressure in pumping process.

Table 4.7 Chloride ion penetration of PAC and conventional concrete

Grouting process	Coarse aggregate size	Charge passed (C)				Chloride ion penetrability
		1	2	3	Average	
Gravity process	14 mm	3992.45	3864.16	3883.02	3913.21	Moderate
	20 mm	3256.23	3323.10	3930.93	3503.42	Moderate
	37 mm	3269.23	3712.12	4104.16	3695.17	Moderate
	45 mm	4462.65	4523.55	4849.53	4611.91	High
Pumping process	14 mm	3556.21	3621.45	3332.60	3503.42	Moderate
	20 mm	3236.54	3452.30	3315.17	3334.67	Moderate
	37 mm	3324.12	3521.65	3484.97	3443.58	Moderate
	45 mm	4568.23	4236.12	4244.54	4349.63	High
Conventional concrete	20 mm	5523.55	5006.12	5078.43	5202.70	High

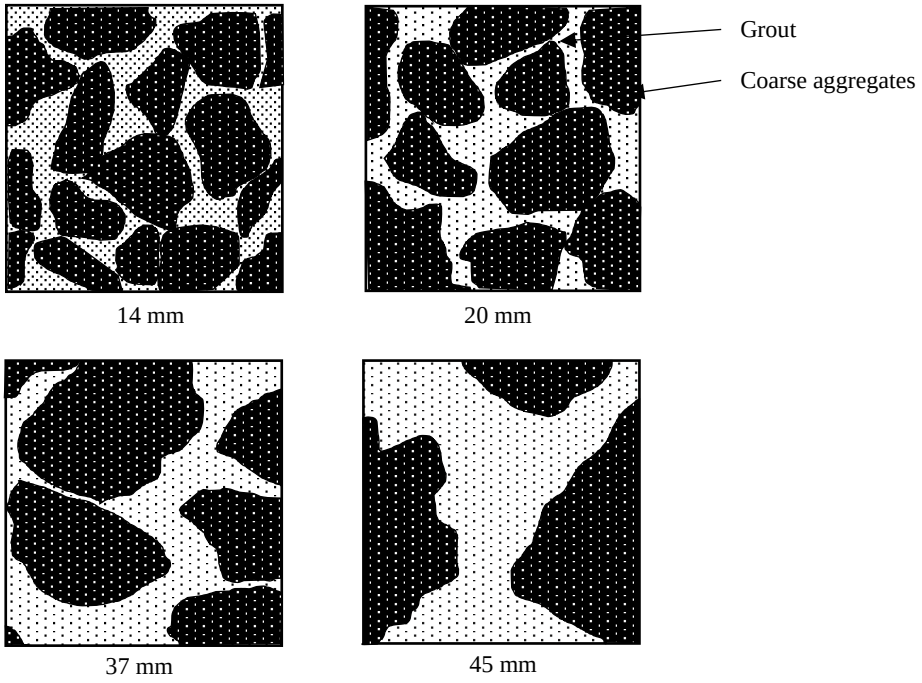

Figure 4.6 Cross-section of PAC for different coarse aggregate sizes

4.5 Comparison between PAC and conventional concrete

Conventional concrete was produced by conventional mixing techniques while maintaining the same quantity of coarse aggregates + fine aggregates. Table 4.8 compares the mix proportion of both conventional concrete and PAC produced using 20 mm coarse aggregates. Conventional concrete specimens were compacted on a vibration table.

As shown in Figure 4.5 and Table 4.7, PAC at same coarse aggregate size displays 15% higher compressive strength and higher resistance to chloride ion penetration than that of conventional concrete. The former could be attributed to the point-to-point contact of coarse aggregates in PAC, leading to a more efficient stress transfer between coarse aggregates and grout. The latter could be the result of lesser cross-sectional area of cement-sand paste in PAC due to high coarse aggregate content, thereby reducing the passages for chloride ion penetration.

75 mm x 75 mm x 285 mm prisms were produced to determine drying shrinkage as per ASTM C 157. As shown in Figure 4.7, using 20 mm coarse aggregates, PAC displays better dimensional stability with drying shrinkage less than half of that produced by conventional concrete. This could be attributed to coarse aggregate-to-coarse aggregate contact (Abdelgader and Elgalhud, 2008) and higher coarse aggregate content in PAC. Response of PAC to drying shrinkage agree with those observed by Emmons (1993).

Table 4.8 Mix proportion of PAC and conventional concrete

Concrete	Cement (Kg)	Water (Kg)	Fine aggregates (Kg)	Coarse aggregates (Kg)	SP by wt. of B
PAC	431	165	215	1685	0.5 %
Conventional	413	162	742	1154	0.5 %

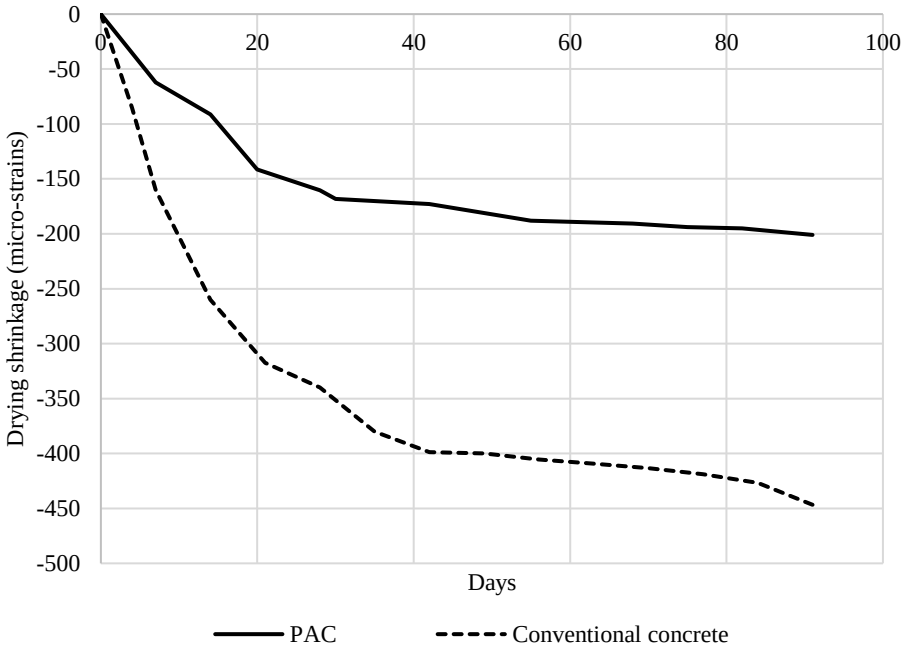

Figure 4.7 Drying shrinkage of PAC and conventional concrete

4.6 Summary

A preliminary investigation was conducted to determine suitable mix proportion for grout. S/B and W/B ratios were compared against efflux time and compressive strength of grout. High S/B ratio resulted in excessive segregation. Reduction in W/B ratio enhanced the strength of grout, reducing the flowability. An optimized grout mix with suitable efflux time of 21.26 seconds and compressive strength of 85.05 MPa was applied to produce PAC using different sizes of coarse aggregates i.e. 14 mm, 20 mm, 37 mm, and 45 mm; employing both gravity process and pumping process.

PAC was examined for excess voidage, compressive strength, and chloride ion penetration. Compressive strength and resistance to chloride ion penetration improved with decreasing coarse aggregate size with the peak value at 20 mm coarse aggregate size for both gravity process and pumping process. PAC produced using 14 mm coarse aggregates displayed higher excess voidage leading to lower compressive strength and

higher chloride ion penetration. Gravity process was used successfully for production of PAC with coarse aggregate size of 20 mm or higher, displaying compatible performance to that of pumping process. For further reduction in the size of coarse aggregates, pumping process is recommended as it ensures better penetrability of grout through coarse aggregates.

Using 20 mm coarse aggregates and traditional grout formed by cement-sand composite, PAC displayed higher strength and comparable resistance to chloride ion penetration compared to that of conventional concrete. PAC displayed better dimensional stability with drying shrinkage less than half of that produced by conventional concrete.

CHAPTER 5

INFLUENCE OF GROUT PROPERTIES TO PAC

5.1 Introduction

In this chapter, effects of mix proportions of grout and their properties on the mechanical properties, durability, and dimensional stability of PAC are evaluated. To develop a user-friendly approach, grouting was performed by gravity process. Supplementary cementitious materials namely GGBS and SF were incorporated to improve the properties of PAC. Moreover, given that production of cement alone contributes to the third-largest anthropogenic emission of CO_2 (Tuyan et al., 2020), successful utilization of industrial by-products like GGBS and SF to form PAC is pursued to reduce the carbon footprint, with economic and environmental benefits.

As flowability of grout is a major factor in producing quality PAC, effects of grout constituent materials and their proportions on the flowability of grout were investigated. According to ACI 304.1, an efflux time of 22 ± 2 seconds is recommended on application to form walls and structural repairs. Further, our previous studies (Chapter 4) suggest that size of coarse aggregates has a significant effect on the required efflux time and that the grouting process also influences the required efflux time.

In this chapter, study on the impact of flowability on hardened properties of PAC was considered. Supplementary cementitious materials, i.e. GGBS and SF were used as partial replacement of cement to enhance properties of PAC. Mix proportions of grout were optimized to produce PAC with superior properties. Steel fibers were incorporated to enhance the tensile strength and dimensional stability of PAC.

5.2 Experimental program

5.2.1 Specimens and tests

Grouts were subjected to bleeding tests as per ASTM C 940 to ensure bleeding within the permissible limits, i.e. bleeding less than 2% after 120 minutes. Grout consistency (flowability) was determined by flow cone test in terms of efflux time to ASTM C 939. Grout compression tests at 7 days, 28 days, and 56 days were performed using 50 mm x 50 mm cubes to ASTM C 942.

Mechanical properties of PAC were determined based on compressive strength and splitting tensile strength. Durability and dimensional stability of PAC were evaluated by chloride ion penetration test and drying shrinkage test, respectively. Cylindrical specimens of 100 mm x 200 mm (diameter x height) were prepared to determine 28 days and 56 days compressive strength as per ASTM C 39. Splitting tensile strength was determined by using 100 mm x 200 mm cylinders as per ASTM C 496 at 28 days. 50 mm thick slices were cut to size from 100 mm diameter cylinders for chloride ion penetration test to ASTM C 1202 at 28 days. Drying shrinkage test was performed as per BS ISO 1920-8 using 75 mm x 75 mm x 285 mm prisms over 90 days.

5.2.2 Mix proportion of grout

Based on the preliminary investigation (Chapter 4), S/B=0.50 and W/B=0.37 were applied to form grouts with and without adding GGBS and SF. Cement was partially replaced by GGBS and SF at 0 to 40% and 0 to 10% by weight of binder, respectively. Properties of grout, i.e. efflux time and compressive strength, were used to optimize the ratios for GGBS and SF. To ascertain GGBS/B and SF/B ratios, samples were prepared through trial and error. For grout with partial replacement of cement by GGBS above 40%, compressive strength of grout decreased significantly (by more than 30%). Hence,

GGBS was limited to 40%. For grout with partial replacement of cement by SF above 10%, flowability was reduced. With 10% SF as partial replacement of cement, it was difficult to achieve efflux time less than 20 seconds. Hence, SF/B ratio was not increased further. Mix proportions of grout constituting different combinations of GGBS and/or SF were considered.

Four sets of mix proportions were prepared. For Set 1, flowability of grout was evaluated at constant SP dosage of 0.5 %, whereas for Set 2, efflux time was regulated to less than 20 seconds by modifying the SP dosage. Set 3 was a modification of Set 2 with S/B ratio reduced to 0.00. With the reduction in S/B ratio, SP demand reduced significantly, enabling Set 4 at 0.33 W/B ratio. The grout mix proportions are shown in Table 5.1. As to the mix IDs, GRTn represents the n^{th} set of grouts. The first two digits after the hyphen depict the binder proportion of GGBS, and the last two digits represent the binder proportion of SF.

Table 5.1 Mix proportion of grout incorporating GGBS and SF

Set no.	Mix ID	GGBS/B	SF/B	S/B	W/B	Dry materials in percentage (%)			
						C	GGBS	SF	S
Set 1	GRT1-0000	0.00	0.00	0.50	0.37	50.00	0.00	0.00	50.00
	GRT1-4000	0.40	0.00	0.50	0.37	30.00	20.00	0.00	50.00
	GRT1-0010	0.00	0.10	0.50	0.37	45.00	0.00	5.00	50.00
	GRT1-2005	0.20	0.05	0.50	0.37	37.50	10.00	2.50	50.00
	GRT1-3505	0.35	0.05	0.50	0.37	30.00	17.50	2.50	50.00
	GRT1-3010	0.30	0.10	0.50	0.37	30.00	15.00	5.00	50.00
	GRT1-4010	0.40	0.10	0.50	0.37	25.00	20.00	5.00	50.00
Set 2	GRT2-0000	0.00	0.00	0.50	0.37	50.00	0.00	0.00	50.00
	GRT2-4000	0.40	0.00	0.50	0.37	30.00	20.00	0.00	50.00
	GRT2-0010	0.00	0.10	0.50	0.37	45.00	0.00	5.00	50.00
	GRT2-2005	0.20	0.05	0.50	0.37	37.50	10.00	2.50	50.00
	GRT2-4010	0.40	0.10	0.50	0.37	25.00	20.00	5.00	50.00
Set 3	GRT3-0000	0.00	0.00	0.00	0.37	100.00	0.00	0.00	0.00
	GRT3-4000	0.40	0.00	0.00	0.37	60.00	40.00	0.00	0.00
	GRT3-0010	0.00	0.10	0.00	0.37	90.00	0.00	10.00	0.00
	GRT3-2005	0.20	0.05	0.00	0.37	75.00	20.00	5.00	0.00
	GRT3-4010	0.40	0.10	0.00	0.37	50.00	40.00	10.00	0.00
Set 4	GRT4-0000	0.00	0.00	0.00	0.33	100.00	0.00	0.00	0.00
	GRT4-4000	0.40	0.00	0.00	0.33	60.00	40.00	0.00	0.00
	GRT4-0010	0.00	0.10	0.00	0.33	90.00	0.00	10.00	0.00
	GRT4-2005	0.20	0.05	0.00	0.33	75.00	20.00	5.00	0.00
	GRT4-4010	0.40	0.10	0.00	0.33	50.00	40.00	10.00	0.00

5.3 Grout properties

Grout consistency was determined by flow cone test and the results are shown in Table 5.2. For Set 1, efflux time decreased with the incorporation of GGBS and increased greatly with the incorporation of SF. A decrease in efflux time by 22% was observed between mix ID GRT1-0000 and GRT1-4000, while an increase in efflux time by 81% was observed between mix ID GRT1-0000 and GRT1-0010. The former could be attributed to the lubricating effect of GGBS while the latter could be ascribed to the fine

particle size of SF. Babalola et al. (2020) indicated that GGBS acts like a lubricant in concrete attributing to its spherical and glass texture. According to Johari et al. (2011), GGBS improves workability by better particle dispersion. Smooth and dense surface characteristics of GGBS particles also absorb less water during mixing. Mixes incorporating both GGBS and SF displayed efflux time within suitable range. Mix ID GRT1-4010, incorporating both GGBS and SF displayed an efflux time similar to that of mix ID GTR1-0000, which was devoid of any GGBS or SF.

For Set 2, Set 3, and Set 4, flowability of grout varied in a similar fashion. However, as the efflux time was controlled within a constant range to less than 20 seconds in these three sets, SP dosage was adjusted to maintain the required efflux time. Compared to Set 2, the flowability of grout was significantly improved in Set 3. This was attributed to the absence of sand. Based on the significant reduction in SP demand in Set 3, as indicated in Table 5.2, W/B ratio in Set 4 was further reduced.

Compressive strength of grout is shown in Table 5.3. The 28 days compressive strength of grout increased with increasing SF content, which could be attributed to the increase in the pozzolanic reaction between SiO_2 in SF and $Ca(OH)_2$ from the hydration products. GGBS reduced the compressive strength of grout at 28 days. This could be attributed to the reduction in cement content due to high replacement ratios of GGBS.

Figures 5.1 to 5.4 show the variation in compressive strengths of grout against its age for Sets 1 to 4, respectively. Mixes incorporating SF exhibited significant strength development at 28 days, with insignificant strength development from 28 days to 56 days. On the other hand, mixes incorporating GGBS displayed slower strength development at 28 days, with significant strength development after 28 days. This could

be attributed to latent-hydraulic reaction and longer period required for the formation of calcium hydroxide in concrete incorporating GGBS (Oner and Akyuz, 2007).

Based on the above, GGBS reduces the 28 days compressive strength but enhances the flowability of grout whereas SF improves the 28 days compressive strength but reduces the flowability of grout. By combining GGBS and SF, they compromise against each other producing grouts with acceptable compressive strength and suitable flowability. This indicates that industrial by-products like GGBS and SF can be optimized to achieve acceptable flowability and strength.

Grout mixes with equivalent GGBS and SF replacements in Set 1 and Set 2 displayed comparable compressive strengths despite differed in flowability. Mixes without sand (Set 3) displayed a higher compressive strength than mixes with sand (Set 1 and Set 2). However, with the removal of sand, binder content in grout increases. This subsequently increases the cost of producing PAC along with increase in carbon footprint. In Set 4, the compressive strength of the grout increased ascribing to the reduction in W/B ratio.

Table 5.2 Efflux time of grout incorporating GGBS and SF

Mix ID	SP @ B (%)	Efflux time (sec)			
		1	2	3	Average
GRT1-0000	0.50	20.56	19.12	20.86	20.18
GRT1-4000	0.50	16.02	15.88	14.84	15.58
GRT1-0010	0.50	35.95	37.12	36.91	36.66
GRT1-2005	0.50	23.55	23.25	23.88	23.56
GRT1-3505	0.50	21.32	22.15	23.49	22.32
GRT1-3010	0.50	28.06	27.00	30.53	28.53
GRT1-4010	0.50	23.01	23.10	20.04	22.05
GRT2-0000	0.58	19.17	19.06	19.22	19.15
GRT2-4000	0.42	17.56	18.06	16.43	17.35
GRT2-0010	1.50	20.22	20.65	19.88	20.25
GRT2-2005	1.00	18.95	18.56	18.23	18.58
GRT2-4010	0.82	19.01	19.33	18.69	19.01
GRT3-0000	0.50	17.23	17.52	16.91	17.22
GRT3-4000	0.30	16.95	15.95	15.19	16.03
GRT3-0010	0.80	19.67	20.06	17.84	19.19
GRT3-2005	0.62	19.06	19.03	18.84	18.98
GRT3-4010	0.50	17.85	18.65	18.61	18.37
GRT4-0000	1.00	19.23	19.55	18.88	19.22
GRT4-4000	0.60	16.55	15.95	15.59	16.03
GRT4-0010	1.50	19.00	19.65	19.22	19.29
GRT4-2005	1.00	18.33	18.77	17.43	18.18
GRT4-4010	1.24	21.09	19.85	20.17	20.37

Table 5.3 Compressive strength of grout incorporating GGBS and SF

Mix ID	7 days				28 days				56 days			
	1	2	3	Average	1	2	3	Average	1	2	3	Average
GRT1-0000	68.33	65.23	67.45	67.00	83.95	86.01	83.41	84.46	85.62	86.09	84.25	85.32
GRT1-4000	61.52	57.22	61.14	59.96	63.55	65.89	63.28	64.24	79.26	79.09	77.45	78.60
GRT1-0010	70.15	69.22	65.59	68.32	87.02	86.09	87.54	86.88	90.36	90.01	86.66	89.01
GRT1-2005	63.32	61.05	62.68	62.35	70.12	70.03	67.19	69.11	76.25	76.52	73.19	75.32
GRT1-3505	65.96	61.20	62.83	63.33	69.02	68.95	66.36	68.11	71.96	73.33	72.09	72.46
GRT1-3010	63.25	65.95	68.14	65.78	80.95	83.25	84.38	82.86	86.03	83.96	86.39	85.46
GRT1-4010	64.85	63.95	67.97	65.59	79.01	80.09	77.48	78.86	89.36	88.09	86.70	88.05
GRT2-0000	58.23	61.74	60.99	60.32	81.44	80.95	78.00	80.13	83.12	82.92	84.97	83.67
GRT2-4000	55.26	59.25	61.35	58.62	61.33	64.85	62.42	62.87	75.62	76.56	74.17	75.45
GRT2-0010	72.36	66.89	71.71	70.32	87.29	85.78	85.47	86.18	88.96	86.95	89.14	88.35
GRT2-2005	65.26	62.89	63.10	63.75	71.32	71.09	67.68	70.03	76.95	77.81	76.69	77.15
GRT2-4010	68.62	65.82	68.12	67.52	75.93	77.08	77.75	76.92	86.85	85.93	84.89	85.89
GRT3-0000	75.05	70.01	66.56	70.54	85.96	82.98	83.06	84.00	87.95	89.12	89.18	88.75
GRT3-4000	63.33	60.74	62.62	62.23	66.66	67.95	66.51	67.04	81.09	82.36	82.40	81.95
GRT3-0010	71.29	70.09	69.70	70.36	89.09	89.02	87.25	88.45	90.09	90.11	86.95	89.05
GRT3-2005	65.23	64.89	70.43	66.85	78.03	76.99	77.97	77.66	85.63	85.22	82.11	84.32
GRT3-4010	69.69	67.98	67.98	68.55	80.96	78.95	79.59	79.83	88.03	87.12	87.35	87.50
GRT4-0000	75.26	71.33	70.52	72.37	86.85	88.06	86.24	87.05	90.34	89.95	87.46	89.25
GRT4-4000	62.15	65.89	65.16	64.40	66.85	69.85	69.85	68.85	80.44	76.22	78.39	78.35
GRT4-0010	75.99	72.33	74.88	74.40	94.25	93.89	90.86	93.00	96.31	95.82	93.56	95.23
GRT4-2005	70.95	68.95	67.76	69.22	80.15	81.22	81.54	80.97	85.03	85.91	82.62	84.52
GRT4-4010	70.23	73.60	72.86	72.23	81.36	79.32	79.95	80.21	87.03	88.21	90.65	88.63

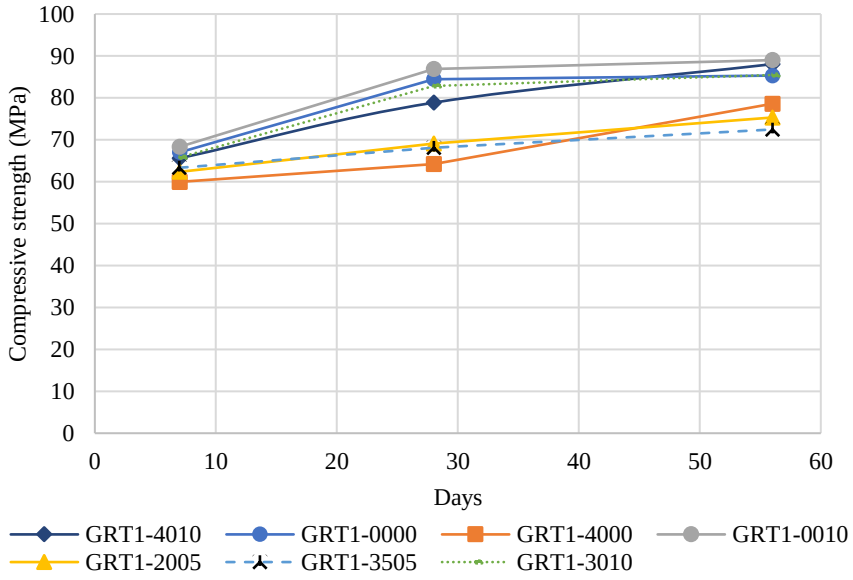

Figure 5.1 Compressive strength of grout for Set 1

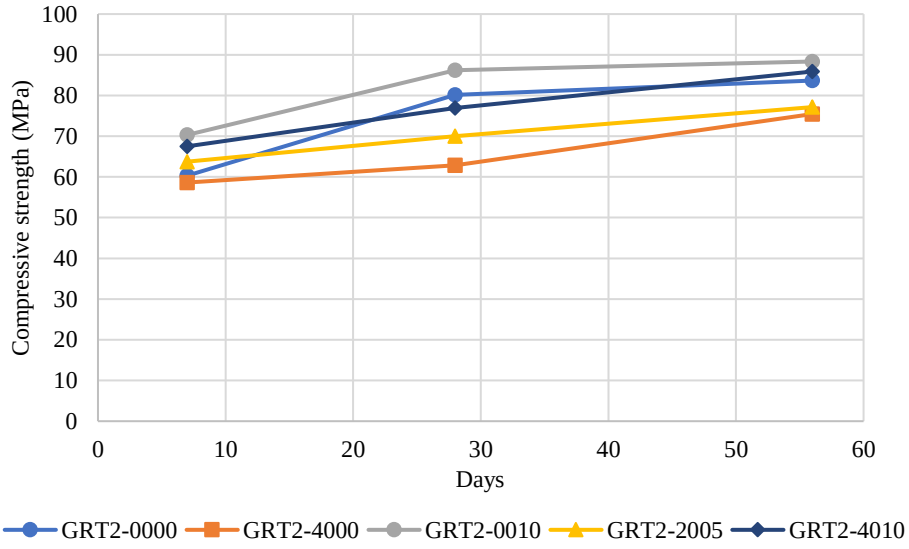

Figure 5.2 Compressive strength of grout for Set 2

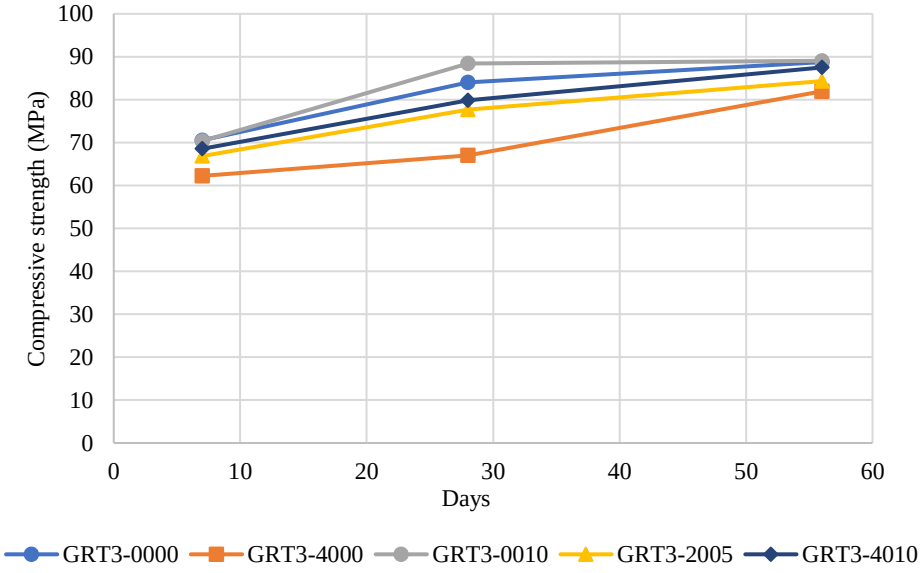

Figure 5.3 Compressive strength of grout for Set 3

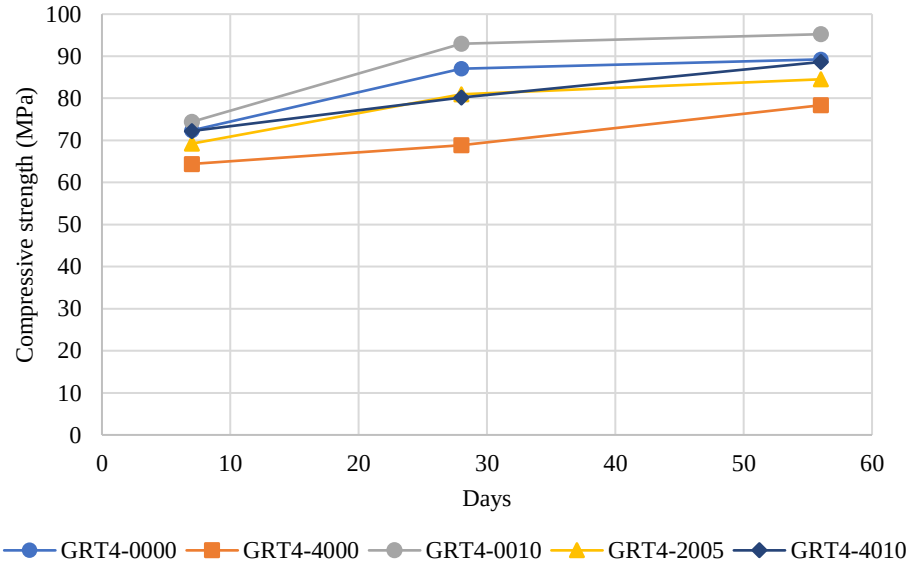

Figure 5.4 Compressive strength of grout for Set 4

5.4 PAC properties

PAC was produced by gravity process. Moulds were first filled with coarse aggregates and grout was applied from top to fill up the voids in between the coarse aggregates. Coarse aggregate size of 20 mm was used (to be optimum as discussed in Chapter 4).

To produce PAC employing grout mix proportion of Set 1, manual compaction was applied on the sides of the moulds using a wooden hammer. As mentioned above, with removal of sand, flowability of grout increases even with reduced W/B ratio in Set 4. ACI 304.1 recommends minimum size of coarse aggregates to be at least 4 times larger than that of maximum size of fine aggregates used in grout. Elimination of sand together with improved flowability of grout enabled reduction in coarse aggregate size. Therefore, additional set of PAC was produced by applying grout mix proportions of Set 4 to10 mm coarse aggregates. Coarse aggregate gradation is shown in Figure 3.3. Mix proportions of PAC incorporating GGBS and SF are given in Table 5.4.

To compare with PAC, conventional concrete was prepared by conventional method of casting. The amount of binder, aggregates (fine aggregates + coarse aggregates), and water in PAC (Set 1) and conventional concrete was kept nearly the same. The main difference was the coarse aggregates to fine aggregates ratio, with a higher proportion of coarse aggregates in PAC (Davis, 1960; Abdul Awal, 1988). Mix proportion of conventional concrete is shown in Table 5.5 (in binder ratios) and Table 5.6 (in kg/m^3). As to the mix IDs, COC represents conventional concrete, followed by the proportion of GGBS and SF.

Table 5.4 Mix proportion of PAC incorporating GGBS and SF

Mix ID	Cement (kg/m^3)	GGBS (kg/m^3)	SF (kg/m^3)	Sand (kg/m^3)	Water (kg/m^3)	SP (kg/m^3)	Coarse aggregate (kg/m^3)
PAC1-0000	429	0	0	215	159	2.15	1746
PAC1-4000	254	169	0	211	156	2.11	1746
PAC1-0010	381	0	42	212	157	2.12	1746
PAC1-2005	317	85	21	212	157	2.12	1746
PAC1-3505	252	147	21	210	156	2.10	1746
PAC1-3010	251	126	42	209	155	2.09	1746
PAC1-4010	209	167	42	209	154	2.09	1746
PAC2-0000	429	0	0	215	159	2.49	1746
PAC2-4000	254	169	0	211	156	1.78	1746
PAC2-0010	381	0	42	212	157	6.35	1746
PAC2-2005	317	85	21	212	157	4.23	1746
PAC2-4010	209	167	42	209	154	3.42	1746
PAC3-0000	547	0	0	0	202	2.73	1746
PAC3-4000	322	215	0	0	199	1.61	1746
PAC3-0010	484	0	54	0	199	4.30	1746
PAC3-2005	403	107	27	0	199	3.33	1746
PAC3-4010	264	211	53	0	195	2.64	1746
PAC4-0000-20	581	0	0	0	192	5.81	1746
PAC4-4000-20	341	228	0	0	188	3.41	1746
PAC4-0010-20	513	0	57	0	188	8.56	1746
PAC4-2005-20	427	114	28	0	188	5.70	1746
PAC4-4010-20	280	224	56	0	184	6.93	1746
PAC4-0000-10	440	0	0	0	145	4.40	2001
PAC4-4000-10	259	173	0	0	142	2.59	2001
PAC4-0010-10	389	0	43	0	143	6.49	2001
PAC4-2005-10	324	86	22	0	142	4.32	2001
PAC4-4010-10	212	170	42	0	140	5.25	2001

Table 5.5 Mix proportion of conventional concrete

Mix ID	GGBS/B	SF/B	S/B	CA/B	W/B	SP @ B (%)
COC-0000	0.00	0.00	1.60	3.00	0.37	0.50
COC-4000	0.40	0.00	1.60	3.00	0.37	0.50
COC-0010	0.00	0.10	1.60	3.00	0.37	0.50
COC-3505	0.35	0.05	1.60	3.00	0.37	0.50
COC-3010	0.30	0.10	1.60	3.00	0.37	0.50

@ B= by mass of binder

Table 5.6 Mix proportion of conventional concrete in kg/m^3

Mix ID	Cement (kg/m^3)	GGBS (kg/m^3)	SF (kg/m^3)	Sand (kg/m^3)	Coarse aggregate (kg/m^3)	Water (kg/m^3)	SP (kg/m^3)
COC-0000	423	0	0	677	1270	157	2.12
COC-4000	253	168	0	673	1263	156	2.10
COC-0010	379	0	42	674	1263	156	2.11
COC-3505	252	147	21	672	1260	155	2.10
COC-3010	252	126	42	671	1258	155	2.10

5.4.1 Compressive strength

The 28 days and 56 days compressive strengths of PAC are shown in Table 5.7. As for the mix IDs, PAC is followed by the set number of the grout employed. The first two digits after the hyphen represent the binder proportion of GGBS and the last two digits represent the binder proportion of SF. For PAC produced employing Set 4 grout mix proportions, coarse aggregate size follows the binder proportions.

Except for mix ID PAC1-0010, SF enhances the compressive strength of PAC at 28 days. SF eliminates weak links between paste and aggregates at the interfacial transition zone by forming a homogenous and dense microstructure at the interfacial region, thereby strengthening the binder-aggregate bond (Khan and Siddique, 2011). The

reduction in compressive strength in mix ID PAC1-0010 could be attributed to decrease in flowability of grout by the fine particle size of SF and this caused inefficient filling of voids in PAC, leaving behind honeycombs. Figure 5.5 shows presence of honeycombs in the interior and exterior surface of mix ID PAC1-0010 in comparison to mix ID PAC1-0000.

GGBS reduces the compressive strength of PAC at 28 days. PAC with 40% GGBS exhibited the lowest compressive strength in each set. The reduction in compressive strength could be ascribed to slow reactivity of GGBS and high dilution levels due to high replacement of cement by GGBS (Johari et al., 2011). PAC incorporating GGBS exhibited improved strength at optimized SF. Mix ID PAC1-3010, constituting 30% GGBS and 10% SF displayed the highest compressive strength at 28 days. This could be attributed to the combined effect of improved strength due to the presence of SF and enhanced flowability due to the presence of GGBS. However, with further increase in GGBS content, compressive strength of PAC decreases, as evidenced by mix ID PAC1-4010 compared to mix ID PAC1-3010. This could be attributed to decrease in cement content due to increase in GGBS content in the binder. Nevertheless, PAC incorporating 40% GGBS and 10% SF exhibited comparable compressive strength to that of PAC without any GGBS or SF. This suggests that GGBS and SF can be successfully used to replace up to half of the cement in binder without compromising the compressive strength. Although GGBS does not improve the 28 days compressive strength of PAC, strength development continues at 56 days attributing to its latent-hydraulic reaction. The long-term strength development of PAC containing GGBS was higher than that of PAC containing SF only or containing neither of them.

Table 5.7 Compressive strength of PAC incorporating GGBS and SF

Mix ID	28 days (MPa)				Alpha (α)	56 days (MPa)			
	1	2	3	Average		1	2	3	Average
PAC1-0000	42.93	42.06	43.35	42.78	0.51	45.36	42.66	44.52	44.18
PAC1-4000	27.33	29.36	29.04	28.58	0.44	33.69	32.96	31.33	32.66
PAC1-0010	40.03	39.86	37.83	39.24	0.45	41.33	39.86	39.32	40.17
PAC1-2005	32.65	33.89	32.58	33.04	0.48	38.23	36.75	36.65	37.21
PAC1-3505	29.85	30.96	32.04	30.95	0.45	34.62	34.95	36.21	35.26
PAC1-3010	56.32	54.86	53.88	55.02	0.66	60.36	60.11	56.98	59.15
PAC1-4010	39.45	40.34	40.60	40.13	0.51	47.62	47.88	46.46	47.32
PAC2-0000	43.85	44.75	40.43	43.01	0.54	45.02	45.09	44.83	44.98
PAC2-4000	29.98	15.39	33.86	31.92	0.51	39.36	38.05	36.74	38.05
PAC2-0010	48.12	48.63	47.31	48.02	0.56	52.63	50.97	47.48	50.36
PAC2-2005	35.44	34.15	35.74	35.11	0.50	39.20	38.61	39.07	38.96
PAC2-4010	43.63	42.23	42.00	42.62	0.55	49.36	49.66	45.94	48.32
PAC3-0000	35.03	33.33	36.34	34.90	0.42	35.21	37.09	36.15	36.15
PAC3-4000	29.33	30.15	30.90	30.13	0.45	38.00	38.96	36.59	37.85
PAC3-0010	40.36	41.2	38.16	39.91	0.45	44.74	43.69	42.52	43.65
PAC3-2005	32.16	34.65	34.86	33.89	0.44	39.03	39.09	38.61	38.91
PAC3-4010	34.33	33.95	34.35	34.21	0.43	40.55	38.05	41.88	40.16
PAC4-0000-20	37.35	38.66	36.04	37.35	0.43	41.96	42.11	39.59	41.22
PAC4-4000-20	32.63	34.51	33.39	33.51	0.49	41.21	39.05	42.68	40.98
PAC4-0010-20	42.36	40.33	43.10	41.93	0.45	44.09	42.84	42.82	43.25
PAC4-2005-20	34.69	36.21	36.50	35.80	0.44	39.65	40.03	42.00	40.56
PAC4-4010-20	36.02	35.96	38.97	36.98	0.46	42.20	41.66	44.42	42.76
PAC4-0000-10	44.36	45.06	45.46	44.96	0.52	46.12	47.10	47.54	46.92
PAC4-4000-10	35.23	35.19	32.90	34.44	0.50	44.03	41.01	42.88	42.64
PAC4-0010-10	51.39	51.45	47.85	50.23	0.54	54.66	52.22	52.60	53.16
PAC4-2005-10	41.85	42.33	39.87	41.35	0.51	46.05	46.23	46.80	46.36
PAC4-4010-10	22.65	42.63	43.59	43.11	0.54	47.95	49.33	50.95	49.41

Alpha (α) = PAC compressive strength/grout compressive strength

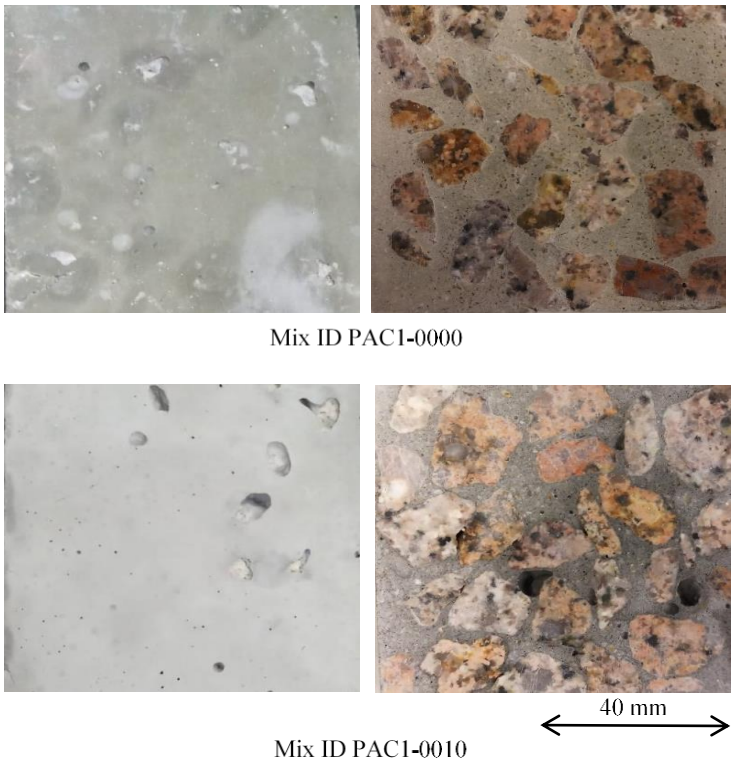

Figure 5.5 Interior and exterior surface of PAC1-0000 and PAC1-0010

Table 5.8 shows compressive strength of conventional concrete. Comparing mix ID PAC1-0000 and COC-0000, compressive strength of PAC was higher than that of conventional concrete. This could be attributed to efficient stress transfer through the aggregate skeleton and better mechanical interlocking between the coarse aggregates in PAC. Common to all conventional concrete, compressive strength increased with partial replacement of cement by GGBS and/or SF. Comparing mix ID PAC1-0010 and COC-0010, conventional concrete displayed about 40% higher compressive strength than that of PAC. The reduction in compressive strength of PAC due to reduced flowability (as discussed above) was overcome by enhancing the flowability of grout with incorporation of GGBS, as evidenced by mix ID PAC1-3010 which displayed 15% higher compressive strength than that of mix ID COC-3010.

Table 5.8 Compressive strength of conventional concrete incorporating GGBS and SF

Mix ID	28 days				56 days			
	1	2	3	Average	1	2	3	Average
COC-0000	42.26	38.22	37.10	39.20	43.01	42.59	43.52	43.04
COC-4000	44.14	46.49	42.71	44.45	44.50	48.44	42.92	45.29
COC-0010	56.30	54.59	54.67	55.19	57.47	56.69	54.15	56.10
COC-3505	38.42	38.74	44.57	40.58	43.87	45.24	42.94	44.02
COC-3010	49.17	47.31	47.02	47.83	53.14	52.17	53.76	53.02

Comparing Set 1 and Set 2, except for mix ID PAC1-0010 and PAC2-0010, PAC with equivalent grout mix proportion displayed comparable compressive strength attributing to suitable efflux time. The reduction in compressive strength by 18% between mix ID PAC2-0010 and PAC1-0010 was ascribed to the increase in efflux time from 20.25 seconds to 36.66 seconds (given in Table 5.2), leading to inefficient penetrability of the grout. This indicates the necessity to ensure grout with suitable flowability in addition to strength. Hence, it is essential for the efflux time to be regulated within a suitable range when specifying a mix proportion for grout.

With exclusion of sand in Set 3, compressive strength of PAC decreased. This is in contrast to the compressive strength of grout (shown in Table 5.3) which increased with exclusion of sand. This indicates that sand plays a unique role in the strength development of PAC. Although exclusion of sand improved flowability and compressive strength of grout, the compatibility of grout with coarse aggregate skeleton, together forming a composite, was inadequate. This could be explained by the packing theory of intermittent grading (Furnas, 1931) by considering mix ID PAC2-0000 and PAC3-0000 as a 3-component (containing cement, sand, and coarse aggregates) and 2-component (containing cement and coarse aggregates) system. The solution of intermittent grading was given graphically, and the results obtained were

plotted to curves for maximum possible voids. The type of curve for maximum packing density was determined by voids in the bed of uniformly packed material and the ratio of the size limits of the system. Since the efflux time of grouts for both mixes were regulated to less than 20 seconds, penetrability of grout through the coarse aggregates was similar. Void content of coarse aggregates was 38% as shown in Table 3.8. The ratio of smallest to largest particle size was 0.000875, where the smallest and the largest size were the size of cement (0.0175 mm) and coarse aggregates (20 mm), respectively. Figure 5.6 indicates that possible minimum void of concrete for 3-component system is lower than that of 2-component system. This suggests that denser structure is produced in the presence of sand, resulting in higher compressive strength.

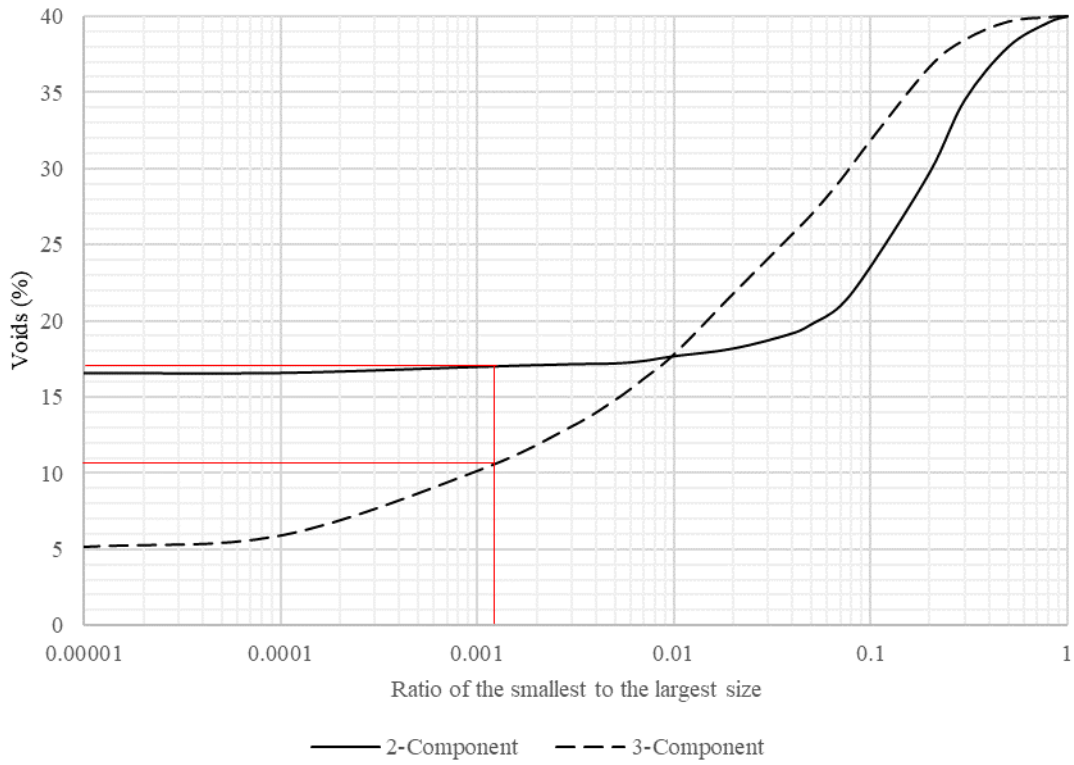

Figure 5.6 Computed possible minimum voids in bed of two and three component sizes if internal voids in bed of uniformly sized material are 40 per cent (Furnas, 1931)

Generally, W/B ratio as low as 0.33 reduces the flowability of grout significantly, inducing voids in between the preplaced coarse aggregates. However, increase in flowability of grout with removal of sand enabled a reduction in W/B ratio in Set 4 to as low as 0.33, without compromising the flowability of the grout. With reduction in W/B ratio, compressive strength of PAC increases. Reduction in coarse aggregate size from 20 mm to 10 mm exhibited significant increase in compressive strength, attributing to higher mechanical interlocking in between the coarse aggregates and larger bonding area in between coarse aggregates and grout. Further, as shown in Table 3.8, with reduction in coarse aggregate size from 20 mm to 10 mm, void content of coarse aggregates decreases by 9%, indicating a lower volume of grout required to produce PAC. Although removal of sand in Set 3 reduces compressive strength and increases the binder content, this was compensated by reduction in coarse aggregate size in Set 4. This is evidenced by mix ID PAC4-0000-10, having the same proportion cement as that of mix ID PAC2-0000 while displaying higher compressive strength.

Equation 5.1 defines compatibility factor Alpha ("α") (given in Table 5.7). It expresses the compatibility of grout with skeleton of coarse aggregates, in forming PAC. α determines the efficiency of grout in imparting the mechanical properties to PAC. Grouts with high compressive strength and high α indicates high PAC compressive strength.

$$\alpha = \frac{\text{PAC compressive strength at 28 days}}{\text{Grout compressive strength at 28 days}} \qquad \text{Equation 5.1}$$

Comparing Set 1 and Set 2, PAC with efflux time within less than 20 seconds (Set 2) displayed smaller variation on α. α for Set 3 was lower than that of Set 2, signifying the influence of sand on compressive strength of PAC. For instance, while mix ID GRT3-

0010 displayed a higher grout compressive strength than that of mix ID GRT2-0010, it produced a smaller α and PAC compressive strength was 18% lower. Although increase in binder content improves the compressive strength of grout, it does not necessarily increase the compressive strength of PAC. The above is in agreement with Abdelgader (1996).

5.4.2 Splitting tensile strength

Table 5.9 shows the splitting tensile strength of PAC at 28 days. GGBS decreased the splitting tensile strength of PAC. This can be attributed to high replacement ratio of cement by GGBS. Except for mix ID PAC1-0010, PAC incorporating SF displayed an increase in splitting tensile strength ascribing to a high pozzolanic reaction in the presence of SF. This exception could be related to high efflux time of grout, resulting in inefficient penetrability of the grout through the coarse aggregate skeleton. This reflects the significance of regulating efflux time of grouts to suitable range, i.e. less than 20 seconds in this case. PAC with 40% GGBS and 10% SF displayed comparable splitting tensile strength to that of the PAC without any GGBS or SF, attributing to the combined effect of improved strength and enhanced flowability due to SF and GGBS, respectively. This indicates that GGBS and SF can be applied to produce PAC without compromising the splitting tensile strength.

Abdelgader and Elgalhud (2008) suggested that variation in S/B ratio did not have a significant impact on the splitting tensile strength of PAC at high W/B ratio (0.4 to 0.6). This was attributed to a weak grout matrix due to excessive free water that leads to bleeding, resulting in formation of capillary voids in the interface and underneath the coarse aggregates (Coo and Pheeraphan, 2015). However, the effect of variation of sand in splitting tensile strength was observed to be distinct at low W/B ratios (Coo and

Pheeraphan, 2015). In Set 3, with reduction in S/B ratio to 0.00, splitting tensile strength of PAC decreases. This could be ascribed to the high energy required to overcome the resistance in crack propagation and crack growth due to larger and angular shapes of sand particles. The reduction in splitting tensile strength was compensated to a certain extend by reducing the W/B ratio to 0.33 in Set 4. With reduction in coarse aggregate size to 10 mm, splitting tensile strength of PAC was further improved. This was ascribed to larger contact areas between grout and coarse aggregates due to reduction in void content with decreasing coarse aggregate size. This increases the interfacial bonding and mechanical interlocking in between the coarse aggregates, thus improving the frictional properties.

Figure 5.7 shows the relationship between splitting tensile strength and compressive strength of PAC at 28 days. Most of the splitting tensile strength values are in close proximity to the equation used for predicting the splitting tensile strength of conventional concrete, given by ACI 318, as shown in Equation 5.2. This implies that relationship between splitting tensile strength and compressive strength in PAC follows a similar fashion as that of conventional concrete and that the equation given by ACI 318 for conventional concrete can be used to predict the splitting tensile strength of PAC.

$$f_{spt} = 0.56(f_c)^{0.5} \qquad \text{Equation 5.2}$$

where,

f_{spt} = Splitting tensile strength

f_c = Compressive strength

Table 5.9 Splitting tensile strength of PAC incorporating GGBS and SF

Mix ID	1	2	3	Average
PAC1-0000	3.75	3.66	3.87	3.76
PAC1-4000	2.84	3.16	2.94	2.98
PAC1-0010	3.62	3.56	3.56	3.58
PAC1-2005	3.20	3.26	3.17	3.21
PAC1-3505	3.50	3.52	3.45	3.49
PAC1-3010	3.76	3.77	3.72	3.75
PAC1-4010	3.83	4.01	3.89	3.91
PAC2-0000	3.89	3.85	3.90	3.88
PAC2-4000	3.20	3.16	3.15	3.17
PAC2-0010	4.21	4.03	4.21	4.15
PAC2-2005	3.55	3.62	3.36	3.51
PAC2-4010	4.02	4.12	4.01	4.05
PAC3-0000	2.96	3.21	3.16	3.11
PAC3-4000	2.79	2.63	2.83	2.75
PAC3-0010	3.42	3.41	3.43	3.42
PAC3-2005	3.06	3.05	3.04	3.05
PAC3-4010	3.06	3.10	3.08	3.08
PAC4-0000-20	3.23	3.20	3.20	3.21
PAC4-4000-20	3.00	3.04	3.02	3.02
PAC4-0010-20	3.80	3.81	3.76	3.79
PAC4-2005-20	3.20	3.16	3.21	3.19
PAC4-4010-20	3.09	3.14	3.09	3.11
PAC4-0000-10	3.56	3.60	3.57	3.58
PAC4-4000-10	3.30	3.32	3.25	3.29
PAC4-0010-10	4.23	4.01	4.07	4.10
PAC4-2005-10	3.46	3.43	3.60	3.50
PAC4-4010-10	3.66	3.70	3.69	3.68

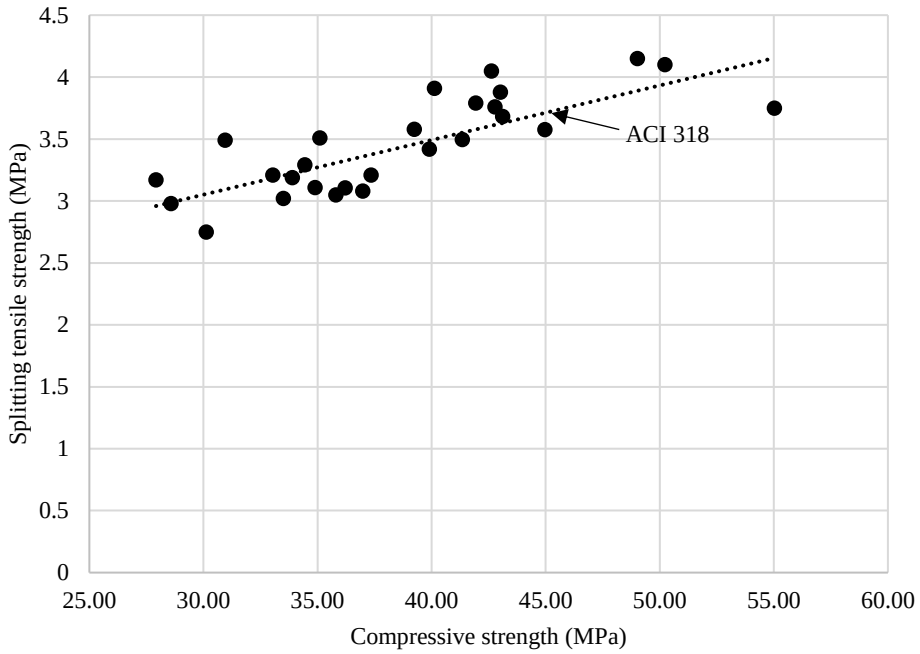

Figure 5.7 Splitting tensile strength versus compressive strength of PAC

5.4.3 Chloride ion penetration

Charge passed through PAC during chloride ion penetration is shown in Table 5.10. PAC containing both GGBS and SF at their highest levels displayed very low to low chloride ion penetrability. This could be attributed to high replacement of cement by GGBS and SF. The results are consistent with that of Cheng (2005) and Poon et al. (2006) for conventional concrete. GGBS in concrete improves the pore structure by introducing extra C-S-H gel in the paste forming a denser microstructure thereby reducing porosity (Cheng, 2005). SF in concrete acts as micro-fillers and densifies the mix, reducing chloride ion penetration (Poon et al., 2006). It further enhances the microstructure of concrete by accelerating the hydration rate and improving the packing density.

Table 5.10 Chloride ion penetration of PAC incorporating GGBS and SF

Mix ID	Charge passed (C)				Penetrability
	1	2	3	Average	
PAC1-0000	3445.23	3623.10	3438.12	3502.15	Moderate
PAC1-4000	2736.21	2598.32	2738.47	2691.00	Moderate
PAC1-0010	1689.23	1795.55	1855.22	1780.00	Low
PAC1-2005	1345.52	1121.06	1137.41	1201.33	Low
PAC1-3505	1535.00	1642.30	2162.70	1780.00	Low
PAC1-3010	1652.00	1554.00	1117.00	1441.00	Low
PAC1-4010	552.00	496.21	667.19	571.80	Very low
PAC2-0000	2903.10	3152.54	2969.11	3008.25	Moderate
PAC2-4000	2466.45	2795.85	2240.70	2501.00	Moderate
PAC2-0010	695.22	765.12	687.66	716.00	Very low
PAC2-2005	1285.00	4265.78	1093.00	1189.00	Low
PAC2-4010	569.12	582.32	717.92	623.12	Very low
PAC3-0000	4895.52	4425.85	4652.42	4657.93	High
PAC3-4000	3018.16	3226.45	2685.61	2976.74	Moderate
PAC3-0010	1356.85	1163.52	1195.46	1238.61	Low
PAC3-2005	2195.45	2226.45	2055.04	2158.98	Moderate
PAC3-4010	1201.00	1356.20	1623.09	1393.43	Low
PAC4-0000-20	3568.20	4001.25	3317.34	3628.93	Moderate
PAC4-4000-20	2315.85	2019.45	2059.53	2131.61	Moderate
PAC4-0010-20	1354.56	1596.45	1269.75	1406.92	Low
PAC4-2005-20	1666.95	1795.20	1568.07	1676.74	Low
PAC4-4010-20	1562.64	1165.00	1152.65	1293.43	Low
PAC4-0000-10	2265.45	2465.85	1836.60	2189.30	Moderate
PAC4-4000-10	1568.52	1733.65	1366.58	1556.25	Very low
PAC4-0010-10	951.20	856.10	911.39	906.23	Low
PAC4-2005-10	1659.21	1659.00	343.29	1220.50	Low
PAC4-4010-10	562.10	616.21	563.25	580.52	Very low

Chloride ion penetration was also performed for conventional concrete at 28 days to ASTM C 1202. The results are shown in Table 5.11. Similar to PAC, chloride ion penetration of conventional concrete reduced significantly with incorporation of GGBS and SF. Chloride ion penetration of conventional concrete incorporating GGBS (mix ID COC-4000) was reduced to nearly half of that produced by the control mix (mix ID

COC-0000). With incorporation of SF, chloride ion penetration was further reduced. Conventional concrete incorporating 10% SF (mix ID COC-0010 and mix ID COC 3010) displayed very low chloride ion penetrability.

Comparing conventional concrete and PAC, except for 10% SF (mix ID COC-0010 and mix ID PAC1-0010), PAC displayed higher resistance to chloride ion penetration than conventional concrete. Reduction in chloride ion penetration in PAC could be attributed to reduced passages for chloride ions to penetrate through due to a lesser area of binder per cross-section in PAC than that of conventional concrete. The exception in case of mix ID PAC1-0010 could be the result of tiny honeycombs formed due to the inefficient filling up of voids by the grout, as illustrated in Figure 5.5, which subsequently increased the permeability of PAC.

Table 5.11 Chloride ion penetration of conventional concrete

Mix ID	Charge passed (C)				Penetrability
	1	2	3	Average	
COC-0000	5454.95	6127.69	5528.51	5703.72	High
COC-4000	2417.65	2632.28	2824.98	2624.97	Moderate
COC-0010	932.86	856.44	769.84	853.05	Very Low
COC-3505	1553.41	1590.01	1511.71	1551.71	Low
COC-3010	750.81	823.38	4863.20*	787.09	Very Low
*Result not considered due to leakage of solution from the test setup					

PAC employing grout mixes from Set 2 displayed a higher resistance to chloride ion penetration than that of Set 1, especially for 10% SF (mix ID PAC2-0010 and PAC1-0010), indicating that suitable flowability of grout produces PAC with improved resistance to chloride ion penetration. High flowability of grout results in efficient filling of voids between the coarse aggregates, reducing honeycombs and excess voidage, thereby reducing the permeability in PAC.

Comparing Set 2 and Set 3, mix ID PAC2-0010 and PAC2-4010 displayed very low chloride ion penetrability, whereas mix ID PAC3-0010 and PAC3-4010 displayed low chloride ion penetrability, indicating that mixes incorporating sand exhibit greater resistance to chloride ion penetration. This was further evidenced by mix ID PAC3-0000 (cement water grout), which measured the highest coulombs of charge passed. This could be attributed to an increase in water and binder content per cross-sectioned area with the removal of sand. Mix ID PAC3-4010, constituting the same cement content as that of mix ID PAC1-0000 and PAC2-0000 displayed a higher resistance to chloride ion penetration. This indicates that replacing sand with binder comprising GGBS and SF enhances the durability of PAC. The reduction in resistance to chloride ion penetration due to removal of sand was compensated to a certain extent by reducing the W/B ratio in Set 4. This was evidenced by comparing mix ID PAC3-0000 and PAC4-0000-20 and comparing PAC3-2005 and PAC4-2005-20, that chloride ion penetrability improved from high to moderate and moderate to low, respectively.

Reduction in coarse aggregate size from 20 mm to 10 mm displayed significant increase in resistance to chloride ion penetration. Reduction in coarse aggregate size lowers the void content between coarse aggregates and reduces the amount of grout per surface area of PAC. This reduces the passage for chloride ions to pass through, and subsequently reduces the chloride ion penetration. Due to lower restraining effects, possibility of microcracking in the interfacial transitional zone for concrete produced using smaller-sized coarse aggregates reduces (Bisschop and Van Mier, 2002). This could be another reason for PAC produced using smaller-sized coarse aggregates to achieve lower chloride ion penetration. Mix ID PAC1-4010 and PAC4-4010-10, at same binder content, exhibit comparable resistance to chloride ion penetration. This

indicates that reasonable durability can be maintained by PAC produced using grout without sand and employing smaller-sized coarse aggregates.

5.4.4 Drying shrinkage

Figures 5.8 to 5.12 show the drying shrinkage of PAC employing grouts from Sets 1 to 4 using 20 mm coarse aggregates, and Set 4 using 10 mm coarse aggregates, respectively. By adding GGBS and SF, drying shrinkage of PAC increased. Finer pore structure of GGBS in the mix lowers the relative humidity and increases the degree of self-desiccation in the cement paste (Lura, 2003). Incorporation of GGBS results in denser mix with fine capillary pores. This increases capillary pore water pressure that leads to higher shrinkage strains (Saluja et al., 2019). SF exhibited higher drying shrinkage than that of GGBS and more than twice as much drying shrinkage than that of PAC without any GGBS or SF. Increase in drying shrinkage due to incorporation of SF could be attributed to the introduction of high pozzolanic reaction and pore size refinement mechanism of SF (Rao, 2001). With incorporation of SF, high amount of C-S-H is formed. Presence of high amount of C-S-H holds high amount of gel water. As drying shrinkage occurs due to expulsion of gel water from concrete, high amount of gel water released by concrete incorporating SF results in higher drying shrinkage (Varghese et al., 2017).

Figure 5.13 shows drying shrinkage of conventional concrete. Similar to PAC, both GGBS and SF increased the drying shrinkage of conventional concrete. Comparing PAC and conventional concrete at 30 days, incorporation of 40% GGBS (mix ID PAC1-4000 and mix ID COC-4000) increased the drying shrinkage by 37% and 32% for PAC and conventional concrete, respectively. Inclusion of 10% SF (mix ID PAC1-0010 and mix ID COC-0010) increased the drying shrinkage by 63% and 48% for PAC

and conventional concrete, respectively. Even though drying shrinkage due to inclusion of GGBS and SF was higher in PAC, the overall drying shrinkage of PAC was significantly lower than that of conventional concrete. At 90 days, comparable drying shrinkage was exhibited by mix ID PAC1-3505, PAC1-3010, and COC-0000, indicating that drying shrinkage exhibited by PAC incorporating GGBS and SF was comparable to that of conventional concrete without any GGBS or SF.

Figure 5.14 shows the drying shrinkage of selected PAC and conventional concrete mixes at 30, 60, and 90 days. Mix ID COC-3010 displayed an increase in drying shrinkage by more than 200 microstrain from 30 days to 60 days, followed by mix ID COC-0010 and COC-4000 with an increase at about 100 microstrain. On the other hand, PAC displayed the minimum increase in drying shrinkage of about 25 microstrain for mix ID PAC1-0000 from 30 days to 60 days. For the other mixes, the increase in drying shrinkage from 30 days to 60 days in PAC was significantly lower than that of conventional concrete. This could be attributed to higher coarse aggregate content and initial point-to-point contact between the coarse aggregates in PAC (Neville, 2011).

For Set 1 and Set 2, PAC displayed comparable drying shrinkage for mixes with equivalent mix proportions, indicating that drying shrinkage was unaffected by the flowability of the grout. Drying shrinkage of PAC increased with the removal of sand in Set 3. At 30 days, an increase in drying shrinkage by 48%, 35%, 20%, 8%, and 14% was observed between mix ID PAC2-0000 and PAC3-0000, PAC2-4000 and PAC3-4000, PAC2-0010 and PAC3-0010, PAC2-2005 and PAC3-2005, and PAC2-4010 and PAC3-4010, respectively. The increase in drying shrinkage was attributed to the increase in binder and water content in Set 3, due to exclusion of sand. With increase in binder and water content, shrinkage increases as water and binder represent the

shrinkage phase, whereas sand remains inert. Hence, with reduction in W/B ratio in Set 4, the drying shrinkage of PAC decreased to a certain extent. Reduction in water content in a mix reduces the evaporable water, which reduces the potential of concrete to shrink. Therefore, mixes with lower W/B ratio consequences in lower drying shrinkage (Soroka, 1993).

Drying shrinkage of PAC decreased with the reduction in coarse aggregate size. This could be attributed to decrease in void content with decreasing coarse aggregate size. Decrease in void content of coarse aggregates reduces the grout content and subsequently the drying shrinkage. Unlike grout paste, the coarse aggregates are not subjected to shrinkage because of its low permeability, restricting the overall deformations. Neville (2002) indicated that with a higher aggregate/cement ratio, lower shrinkage strain could be achieved as the fraction of composite material prone to shrinkage decreases.

According to Emmons (1993), 500 microstrain at 30 days was considered as the acceptable limit for shrinkage. Fu et al. (2016) proposed a shrinkage limit of 450 microstrain at 28 days to ensure satisfactory resistance to cracking. Overall, although the drying shrinkage of PAC increased with the incorporation of GGBS and/or SF, or exclusion of sand; it was well within the acceptable limit. This suggests that strength and durability of PAC and can be improved by compromising shrinkage within an acceptable level.

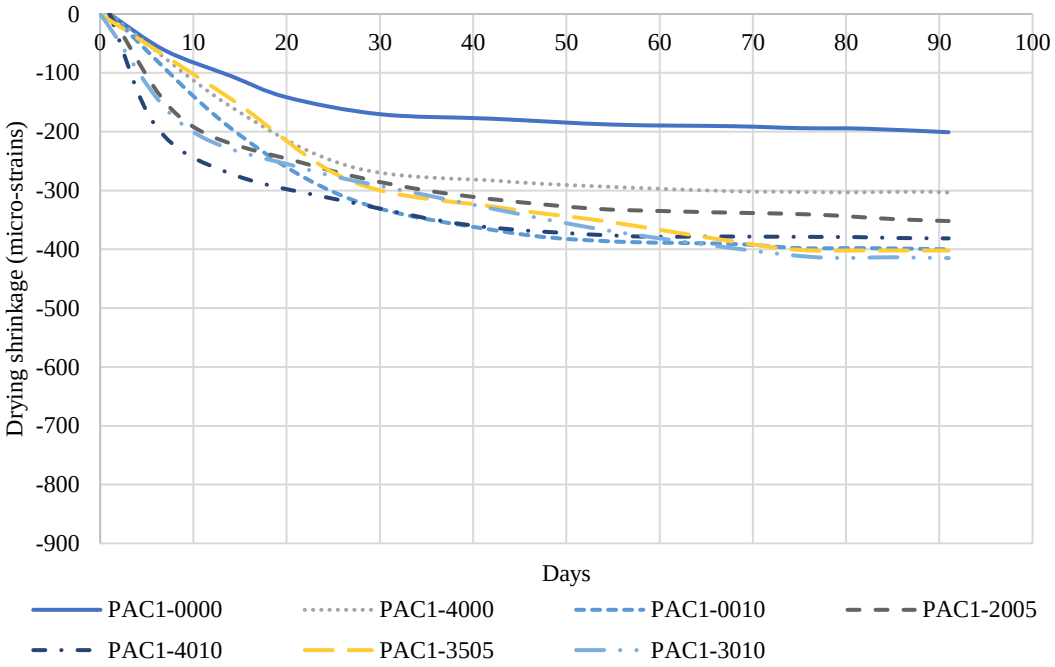

Figure 5.8 Drying shrinkage of PAC produced employing Set 1 grout

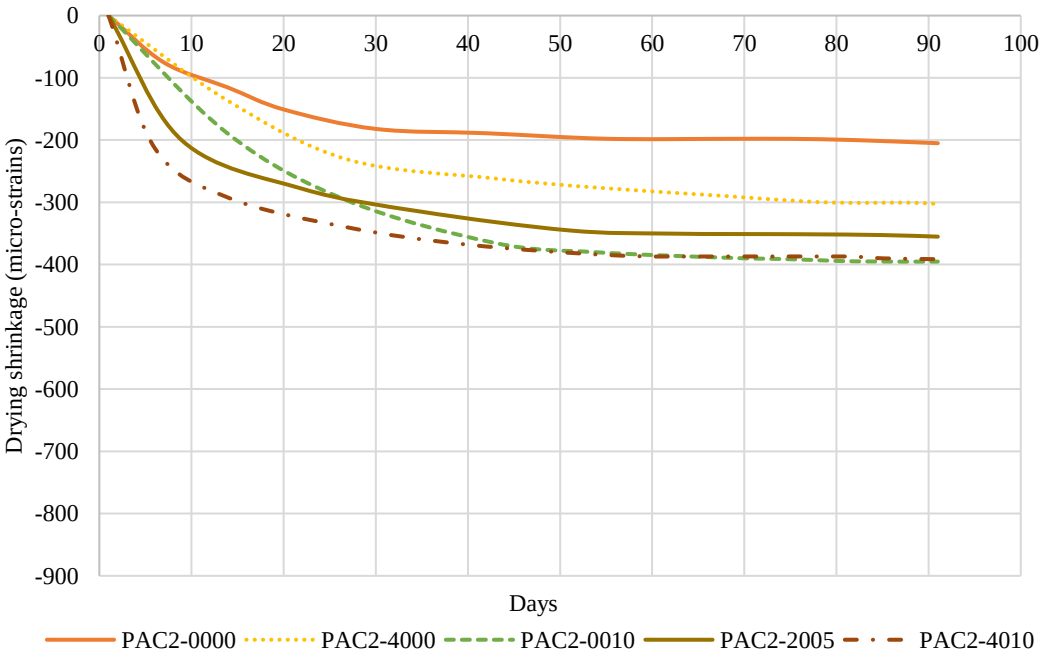

Figure 5.9 Drying shrinkage of PAC produced employing Set 2 grout

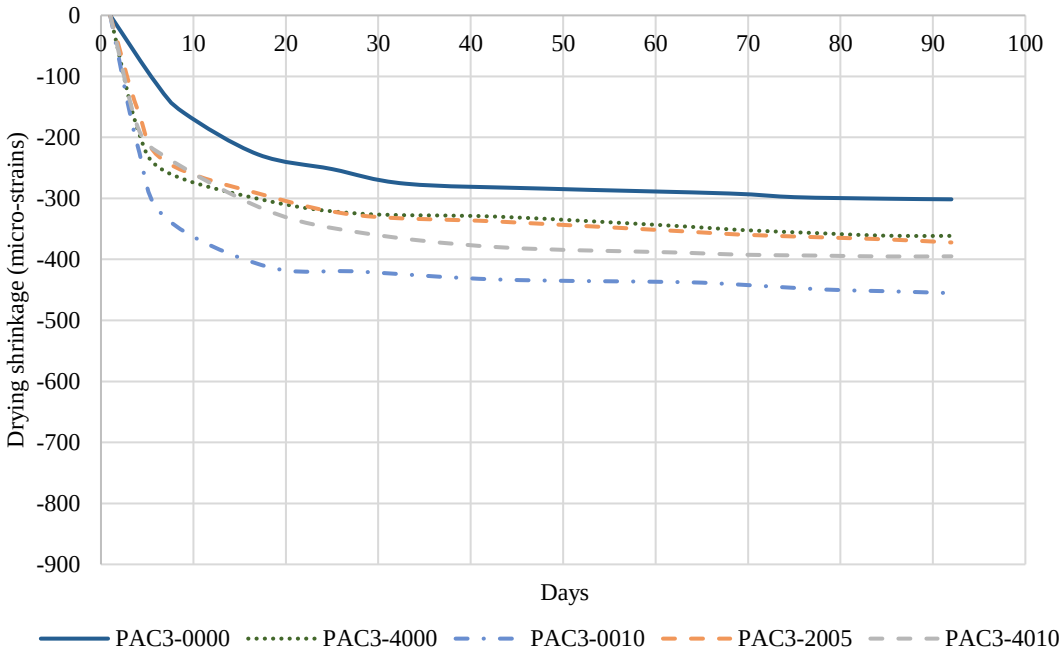

Figure 5.10 Drying shrinkage of PAC produced employing Set 3 grout

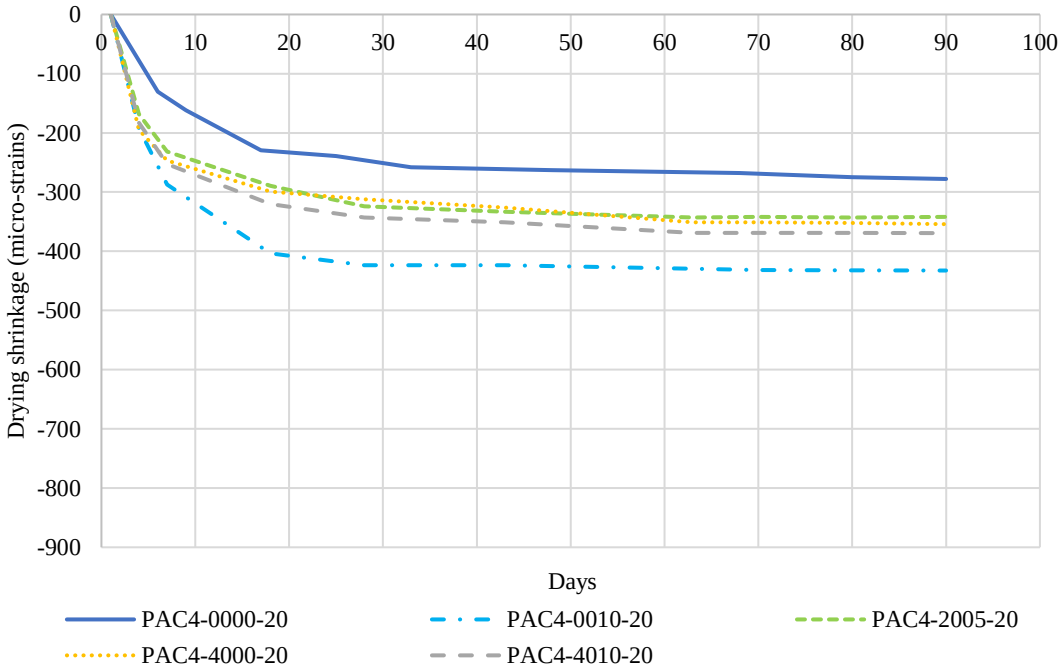

Figure 5.11 Drying shrinkage of PAC produced employing Set 4 grout using 20 mm coarse aggregates

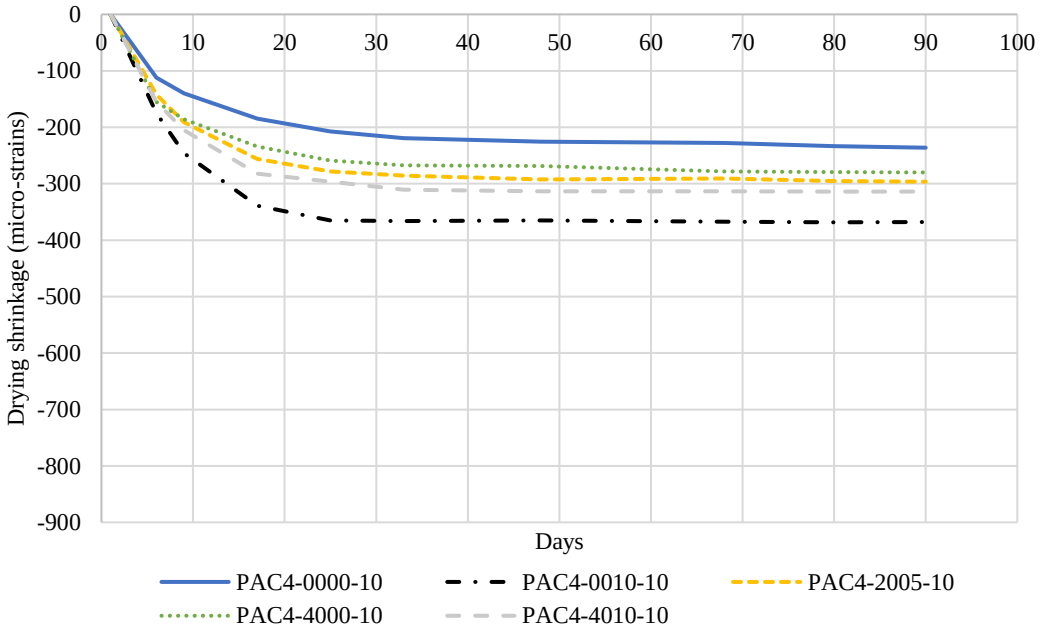

Figure 5.12 Drying shrinkage of PAC produced employing Set 4 grout using 10 mm coarse aggregates

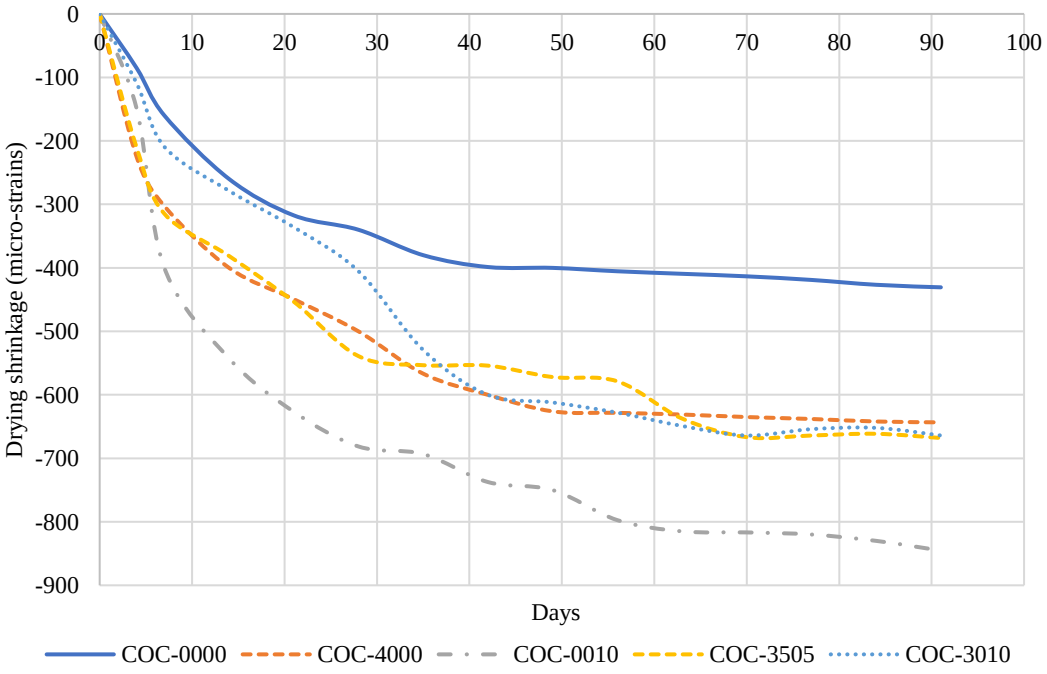

Figure 5.13 Drying shrinkage of conventional concrete

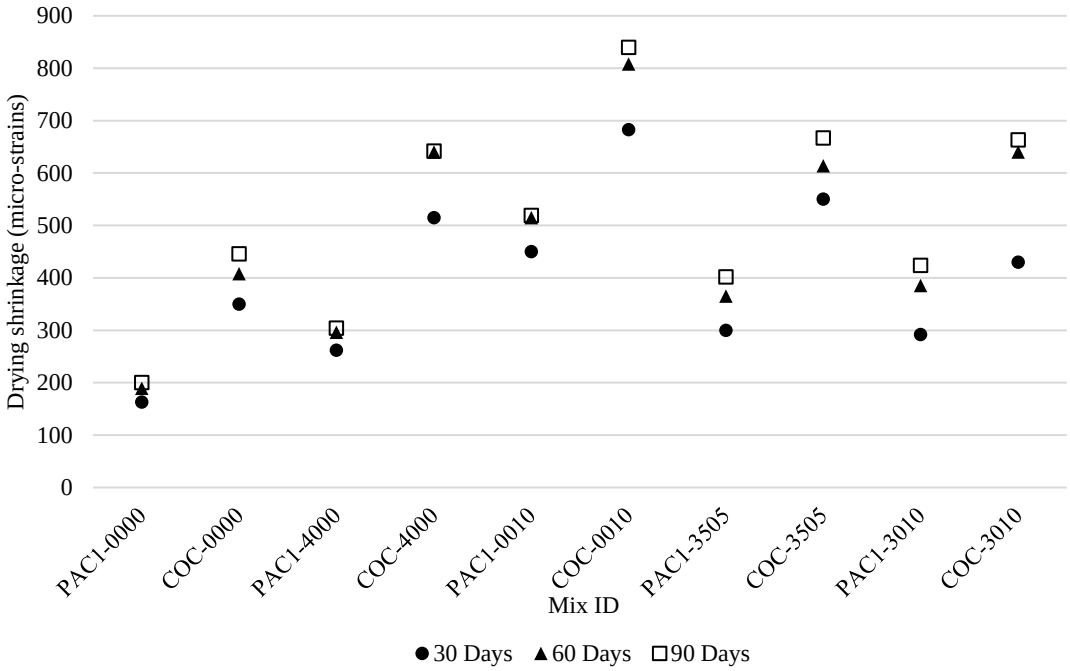

Figure 5.14 Drying shrinkage of PAC produced employing Set 1 grout and conventional concrete at 30, 60, and 90 days

5.5 Incorporation of steel fibers in PAC

In conventional concrete, while the incorporation of fibers improves splitting tensile strength, flexural strength (Gao et al.,1997) and ductility, it adversely affects its workability (Barr and El-Baden, 2003). This restricts the dosage of fibers applied to concrete. However, in PAC as the fibers can be preplaced along with coarse aggregates, complications associated with workability can be minimized to a larger extent. To the best understanding of author, steel fibers have not been prevalently incorporated in PAC. Steel fibers may enhance the mechanical properties and dimensional stability of PAC and pave way for future investigations.

As fibers will be mixed and preplaced with coarse aggregates, nylon fibers or natural fibers have a tendency to stick to the surface of coarse aggregates during mixing. High stiffness of steel fibers compared to synthetic or natural fibers makes it suitable for application to PAC. During mixing, length of steel fibers plays an important role in its

even distribution throughout the coarse aggregate skeleton. Long steel fibers (fibers with high aspect ratio) crumbles into balls and break during mixing with coarse aggregates. Steel fibers of 13 mm length (properties of steel fibers are shown in Table 3.6.) were found to be appropriate and selected for this study. Coarse aggregate size of 10 mm was selected. Steel fibers were mixed with the coarse aggregates. They were dispersed evenly and mixed vigorously using a trowel. With 10 mm coarse aggregates, the fibers remain trapped in between the coarse aggregates without falling to bottom after grouting. Grout with S/B=0.00, SF/B=0.10, and W/B=0.33 (identified by mix ID PAC4-0010-10) was selected to be blended with steel fibers to produce PAC.

Based on trial and error, the dosage of steel fibers was limited to 1% of the total volume of PAC. Further increase in the dosage of steel fibers resulted in the steel fibers to be crumbled into balls. Coarse aggregates blended with steel fibers were preplaced in the moulds and grout was applied via gravity process. For better penetrability of the grout, compaction was applied manually using a wooden hammer on the sides of the moulds.

5.5.1 Compressive strength and splitting tensile strength

Table 5.12 and Table 5.13 show the 28 days compressive strength and splitting tensile strength of PAC incorporating steel fibers, respectively. As for the mix IDs, dosage of steel fiber is represented inside the brackets. With the incorporation of steel fibers in PAC, both compressive strength and splitting tensile strength of PAC increased with increasing fiber content. Compressive strength increased by more than 30% and 60% with the incorporation of steel fibers by 0.5% and 1%, respectively. Splitting tensile strength increased enormously by more than 60% and 80% with inclusion of fibers by 0.5% and 1%, respectively. This could be ascribed to the even distribution and

intersecting fibers throughout PAC which suppresses the formation of cracks, thus enhancing the strength.

Table 5.12 Compressive strength of PAC incorporating steel fibers

Mix ID	Steel fiber	Compressive strength (MPa)			
		1	2	3	Average
PAC4-0010-10(0.0)	0.00	51.39	51.45	47.85	50.23
PAC4-0010-10(0.5)	0.50	61.79	69.53	66.27	65.86
PAC4-0010-10(1.0)	1.00	87.38	82.54	84.84	84.92

Table 5.13 Splitting tensile strength of PAC incorporating steel fibers

Mix ID	Steel fiber	Splitting tensile strength (MPa)			
		1	2	3	Average
PAC4-0010-10(0.0)	0.00	4.23	4.01	4.07	4.10
PAC4-0010-10(0.5)	0.50	6.78	6.71	6.74	6.74
PAC4-0010-10(1.0)	1.00	8.39	6.53	7.30	7.41

5.5.2 Drying shrinkage

Figure 5.15 shows drying shrinkage of fiber reinforced PAC. Drying shrinkage of PAC decreased with increasing fiber content. Reduction in drying shrinkage was significant at early age, attributing to the bridging effect of steel fibers (Yousefieh et al., 2017). Reduction in drying shrinkage with increasing fiber content from 0% to 0.5% was significantly higher than that of 0.5% to 1%, indicating the possibility of the diminishing influence of steel fibers beyond a certain level.

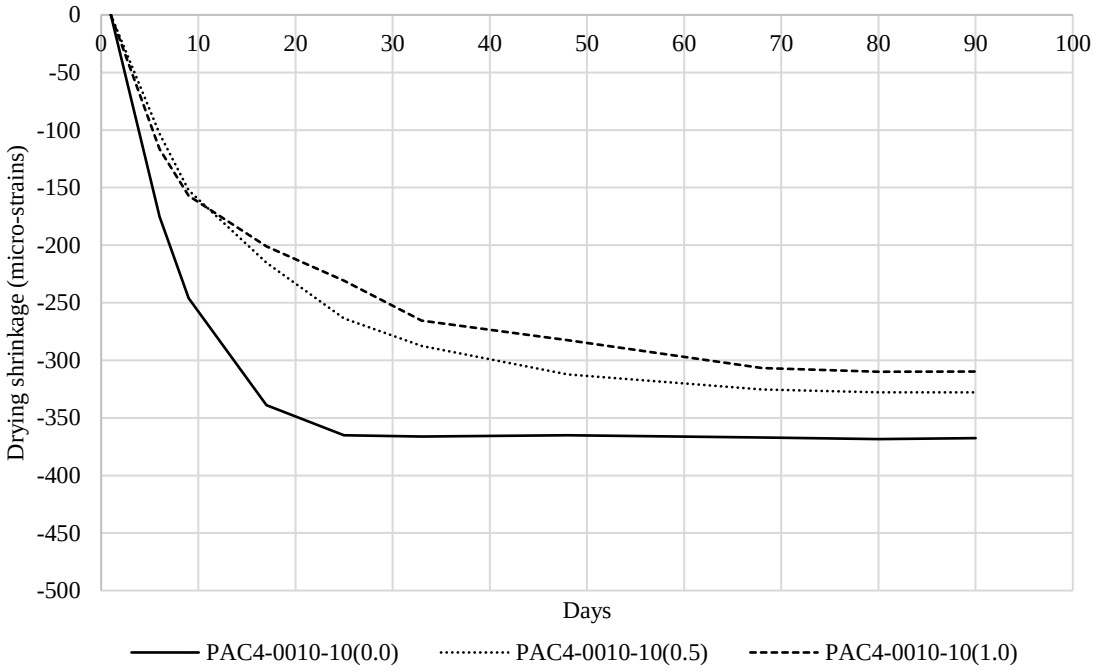

Figure 5.15 Drying shrinkage of PAC incorporating steel fibers

5.6 Summary

Grouts were produced with GGBS and/or SF in different proportions with varying SP dosage, S/B ratio, and W/B ratio. Grout was evaluated for flowability and compressive strength. PAC was produced employing different sizes of coarse aggregates and assessed for mechanical properties, durability, and dimensional stability. A comparison between PAC and conventional concrete was also carried out. Further, PAC was reinforced with steel fibers to enhance its mechanical properties and durability.

Partial replacement of cement by GGBS enhanced flowability with reduction in compressive strength of grout, whereas partial replacement of cement by SF improved compressive strength with reduction in flowability of grout. Removal of sand from the grout improved flowability and compressive strength of grout. It significantly reduced the SP demand in grout, based on which, W/B ratio was reduced. Recommended lowest

W/B ratio in the presence of sand is 0.37. However, with the removal of sand, W/B ratio can be reduced to 0.33.

Grout with high compressive strength generally produces PAC with superior mechanical properties. This is subjected to efficient filling of voids between the preplaced coarse aggregates by grout with high flowability. Therefore, grout with efflux time controlled within a suitable range is important to produce quality PAC.

Grout with GGBS/B=0.40, SF/B=0.10, S/B=0.00, and W/B=0.33 (mix ID GRT4-4010) at controlled efflux time of less than 20 seconds was observed to be the optimum mix proportion for PAC, produced using 10 mm coarse aggregates via gravity process. PAC so formed exhibits improved mechanical properties along with superior durability and high dimensional stability, making it suitable for small scale construction and repair.

PAC exhibits comparable compressive strength to that of conventional concrete with higher resistance to chloride ion penetration and smaller drying shrinkage. Drying shrinkage displayed by PAC incorporating 40% GGBS and 10% SF was comparable to that of conventional concrete without any GGBS or SF.

Properties of PAC improves with incorporation of steel fibers. Compressive strength and splitting tensile strength of PAC significantly increases with incorporation of steel fiber at the dosage of 1% by total volume of PAC. Drying shrinkage of PAC was reduced with increasing steel fiber content.

CHAPTER 6

BOND STRENGTH OF PAC

6.1 Introduction

Repair of concrete has become an important part in the construction industry. Some of the major factors influencing the compatibility of substrate and repair material are durability, dimensional stability, and bond compatibility of repair material. Durability and dimensional stability have been discussed elaborately in Chapters 2. Bond compatibility is defined as development of a satisfactory level of bonding between the substrate and repair material and is the most important aspect of an efficient repair system (Oluokun and Haghayeghi, 1998; Ali and Ambalavanan, 1999). A repair system can be divided into three different components, i.e. substrate, repair material, and interfacial transition zone between substrate and repair material. In particular, the interfacial transition zone is the weakest component in a repair system (Li et al., 2001).

Failure of bond between substrate and repair material is affected by preparation of substrate, application procedure, compaction, curing, workmanship, and properties of substrate and repair material (Silfwerbrand and Beushausen, 2005; Tayeh et al, 2013). Preparation of substrate includes cleaning and roughening the substrate surface before application of repair material (Espeche and Leon, 2011; Omar et al., 2013). Improving the surface roughness of substrate promotes mechanical interlocking and adhesion between substrate and repair material (Momayez et al., 2005; Courard et al., 2014).

Application of repair material depends on accessibility and method of repair. For instance, patch repair can be conducted by trowel method or by cast-in-place method. In trowel method, repair material is applied directly using a trowel. It is best when

applied horizontally. Whereas, in cast-in-place method, repair material is placed by constructing a formwork around the repair area and is suitable for vertical application.

Composition of repair material may significantly influence the interfacial transition zone (Yuan and Marosszeky, 1991). Use of supplementary cementitious materials such as SF or fly ash as partial replacement of cement enhances bond strength by changing the microstructure of the interfacial transition zone, attributing to its micro filler effect (Cohen et al., 1994; Kuroda et al., 2000; Li, 2003). Partial replacement of cement by SF at 7% was found to improve the bond strength between substrate and repair material (Momayez et al., 2005).

Although improvements on rehabilitation and repair have been going-on for decades, the rate of failure to achieve a successful repair system remains high and warrants further investigation (Tayeh et al, 2013). In this study, bond strength between conventional concrete (substrate) and PAC (repair material) was evaluated by pull-off test. PAC was produced employing 10 mm and 20 mm coarse aggregates. SF was used as partial replacement of cement. To draw a comparison with PAC, bond strength between substrate and conventional concrete was investigated.

6.2 Experimental program

6.2.1 Specimens and tests

To determine the mechanical properties, compression test and splitting tensile test of conventional concrete and PAC were performed using 100 mm x 200 mm (diameter x length) cylinders as per ASTM C 39 and ASTM C 496, respectively. To determine the bond strength, pull-off test was conducted as per ASTM C 1583 at 28 days from the day of the casting of PAC/conventional concrete on the substrate. To prevent damaging

the interfacial transition zone during coring, test procedure of ASTM C 1583 was modified to fit the testing conditions as discussed in Chapter 3.

6.2.2 Casting of substrates

Substrate was cast by conventional concrete in the form of slabs of size 300 mm x 300 mm x 50 mm, as shown in Figure 6.1. Mix proportion and properties of conventional concrete are shown in Table 6.1. While casting the substrate, conventional concrete was poured into the moulds and compacted on vibration table. After casting, substrate was wrapped with plastic sheets for 24 hours to prevent loss of moisture. Afterwards, curing was conducted by ponding, i.e. by adding water into the moulds, for 28 days. The substrate was then exposed to the atmosphere for another 60 days, allowing it to mature over time. When applying PAC/conventional concrete as repair material, the substrate was not subjected to prewetting or presoaking.

Table 6.1 Mix proportion and properties of conventional concrete substrate

Substrate	Mix proportion				Property	
	W/B	S/B	CA/B	SF/B	Slump (cm)	Compressive strength (MPa)
	0.40	2.00	3.00	0.00	50	51.63

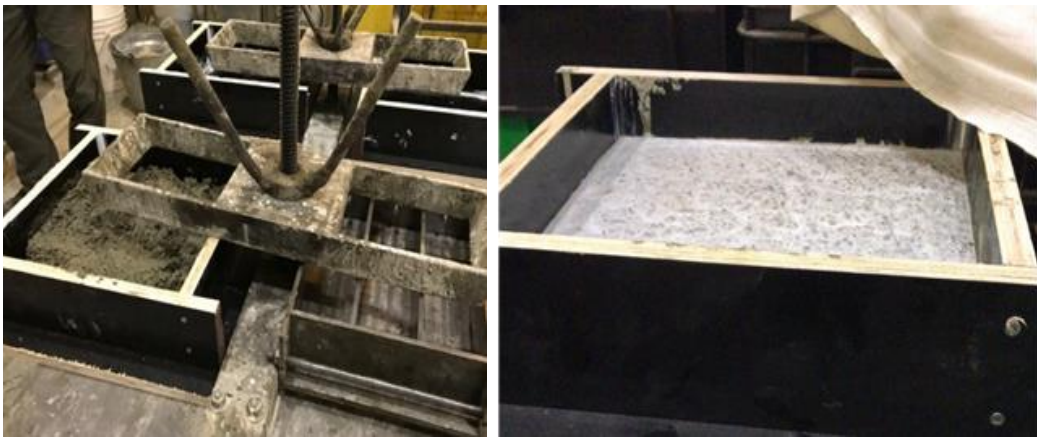

Figure 6.1 Casting of substrates

6.2.3 Preparation of repair material

Repair materials of nominal size 50 mm x 50 mm x 50 mm each were cast on the substrate (as shown in Figure 6.2) and were separated with sufficient space for the installation of pull-off testing machine. The repair material was cast using polystyrene formwork, as shown in Figure 6.3. Dimensions of the repair material were measured before testing to ensure all samples within 10% of the specified dimensions.

As shown in Figure 6.4, both PAC and conventional concrete were cast horizontally on the substrate as repair material. PAC was cast using either 20 mm or 10 mm coarse aggregates. Gradation of coarse aggregates is shown in Figure 3.3. SF was added as partial replacement for cement to form grout. For PAC, W/B was 0.33. For efficient penetrability of grout through coarse aggregates, ACI 304.1 recommends maximum size of fine aggregates to be at least four times smaller than that of smallest size of coarse aggregates. As the smallest size of coarse aggregate in 10 mm coarse aggregate grading was 5 mm, sand was eliminated, i.e. S/B=0.00. To maintain suitable flowability of grout, efflux time of grout was controlled to less than 20 seconds by adjusting the SP dosage. For casting, coarse aggregates of desired size were preplaced into the formwork, followed by application of grout via gravity process.

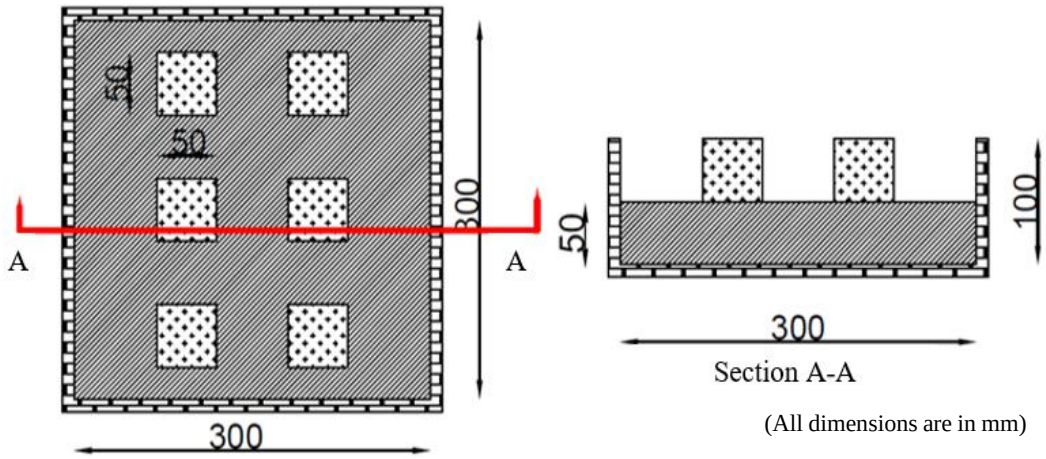

Figure 6.2 Top and section view of substrate and repair material

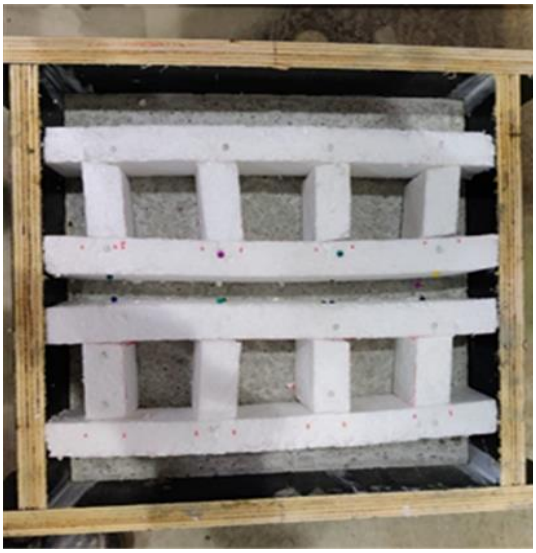

Figure 6.3 Preparation of moulds for placement of repair material

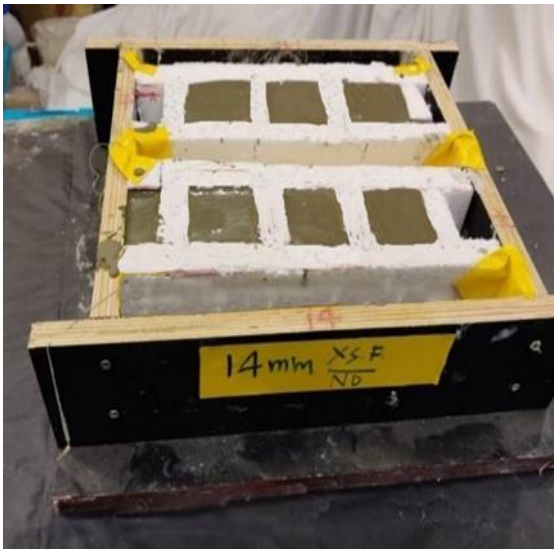

Figure 6.4 Casting of repair material

Conventional concrete was prepared using conventional method and compaction was achieved using a metal rod. After casting, the specimens were covered with plastic wraps. After 24 hours, the specimens were cured by ponding. Mix proportion of repair materials is shown in Table 6.2 (in binder proportion) and Table 6.3 (in kg/m^3). As for

the mix IDs, COC and PAC represent conventional concrete and PAC respectively, followed by proportion of SF and size of coarse aggregates.

Table 6.2 Mix proportion of repair material in binder ratios

Mix ID	Concrete type	Mix proportion					
		W/B	S/B	CA/B	SF/B	SP @ B (%)	CA size (mm)
COC0010	Conventional concrete	0.42	2.00	2.70	0.00	0.00	10.00
PAC0020	PAC	0.33	0.00	-	0.00	1.00	20.00
PAC1020	PAC	0.33	0.00	-	0.10	1.50	20.00
PAC0010	PAC	0.33	0.00	-	0.00	1.00	10.00
PAC1010	PAC	0.33	0.00	-	0.10	1.50	10.00

Table 6.3 Mix proportion of repair material in kg/m^3

Mix ID	Cement (kg/m^3)	SF (kg/m^3)	Sand (kg/m^3)	Water (kg/m^3)	SP (kg/m^3)	Coarse aggregate (kg/m^3)
COC0010	401	0	803	169	2.01	1083
PAC0020	581	0	0	192	5.81	1684
PAC1020	513	57	0	188	5.70	1684
PAC0010	440	0	0	145	6.60	1929
PAC1010	389	43	0	143	6.49	1929

After 28 days of casting the repair material, test blocks were attached to the top surface of repair material (as shown in Figure 6.5) using epoxy. After epoxy had gained sufficient strength, the tester was placed on top of each specimen, as shown in Figure 6.6. Figure 6.7 shows the experimental setup for the pull-off test.

Figure 6.5 Metal block attached to repair material

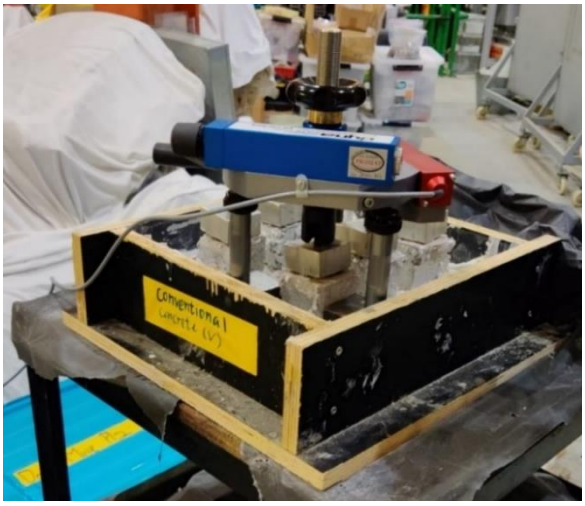

Figure 6.6 Placement of tester over specimens

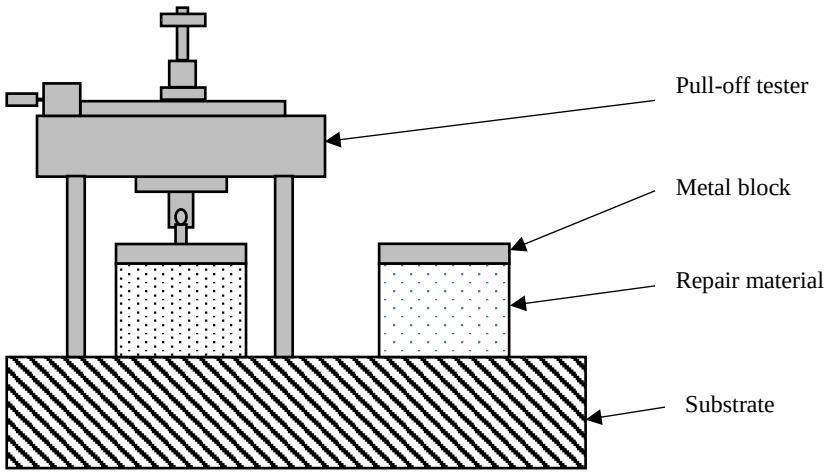

Figure 6.7 Experimental setup of pull-off test

6.3 Results and discussions

6.3.1 Compressive strength

As shown in Table 6.4, compressive strength of PAC produced using 10 mm coarse aggregates was comparable to that of conventional concrete. PAC produced using 20 mm coarse aggregates displayed lower compressive strength. With reduction in coarse aggregate size from 20 mm to 10 mm and incorporation of SF, PAC with mix ID

PAC1010 displayed higher compressive strength than that of conventional concrete. This could be attributed to the greater mechanical interlocking due to decrease in void content with reduction in coarse aggregate size, and increase in the pozzolanic reaction due to incorporation of SF.

Table 6.4 Compressive and splitting tensile strength of repair material

Mix ID	Compressive strength (MPa)				Splitting tensile strength (MPa)			
	1	2	3	Average	1	2	3	Average
COC0010	41.95	46.52	-	44.24	3.53	3.59	-	3.56
PAC0020	37.35	38.66	36.04	37.35	3.23	3.20	3.20	3.21
PAC1020	42.36	40.33	43.10	41.93	3.80	3.81	3.76	3.79
PAC0010	44.36	45.06	45.46	44.96	3.56	3.60	3.57	3.58
PAC1010	51.39	51.45	47.85	50.23	4.23	4.01	4.07	4.10

6.3.2 Splitting tensile strength

Cylinders ruptured into equal halves breaking through the coarse aggregates, indicating a strong interfacial transition zone. As shown in Table 6.4, splitting tensile strength of PAC, except for mix ID PAC0020, was higher than that of conventional concrete. With the decrease in coarse aggregate size, splitting tensile strength increased. This was attributed to larger coarse aggregate-grout bonding area and higher mechanical interlocking in between coarse aggregates due to reduction in void content with decreasing coarse aggregate size. Incorporation of SF as partial replacement of cement further enhances the splitting tensile strength of PAC ascribing to a high pozzolanic reaction in the presence of SF. Mix ID PAC1010 displayed the highest splitting tensile strength.

6.3.3 Bond strength

Bond strength at interfacial transition zone is assessed by conducting pull-off test. It is a destructive technique, used for surface zone assessment. This concept was first developed at Queens University, Belfast in the 1970s. Test configurations and procedures were further developed in several other countries such as Denmark, the United States of America, and the United Kingdom. Due to its popularity, testing equipment is now commercially available. It measures the strength at interfacial transition zone for assessing bonding (Bungey and Madandoust, 1992). Pull-off testing apparatus is quick and straightforward to use.

Figure 6.8 shows the modes of failure of repair system. In general, there are four possible modes of failure, i.e. failure at substrate, failure at substrate/repair material interface, failure at repair material, and failure at metal block/repair material interface. Failure at substrate/repair material interface is the most preferred mode of failure. In this case, it provides good estimate of the bond strength between substrate and repair material. For the other three modes of failure, bond strength between substrate and repair must not be lesser than the maximum value of pull-off strength obtained.

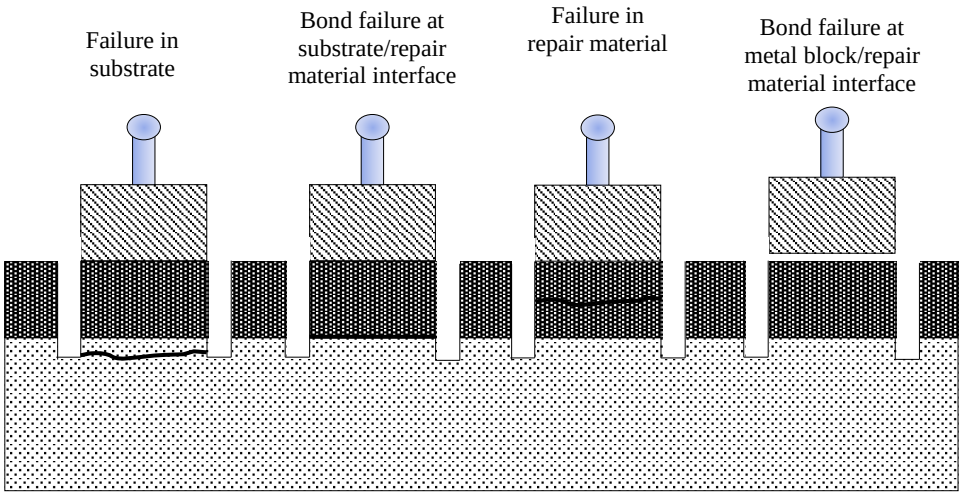

Figure 6.8 Schematic diagram of failure modes (ASTM C 1583, 2004)

Table 6.5 and Table 6.6 show pull-off strength of all specimens and modes of failure, respectively. Bond strengths of specimens with modes of failure not at repair/substrate interface are underlined in Table 6.4. Figure 6.9 represents pull-off strength graphically. For specimens with mode of failure at metal block/repair interface, pull-off strength was considered to be greater than that of obtained strength. Some of the specimens displayed unexpectedly high pull-off strength values and this resulted in machine overloading. These specimens were rejected.

Table 6.5 Pull-off strength of repair material and substrate

Mix ID	Pull-off strength (MPa)				
	1	2	3	4	Average
COC0010	1.50	1.63	1.80	1.94	1.72
PAC0020	>0.46	0.51	0.80	-	0.65
PAC1020	0.87	1.08	1.12	-	1.02
PAC0010	0.24	0.31	0.45	-	0.33
PAC1010	0.22	>0.51	>0.52	-	0.52

Table 6.6 Modes of failure during pull-off test

Mix ID	Mode of failure			
	1	2	3	4
COC0010	Repair/substrate interface	Repair/substrate interface	Repair/substrate interface	Repair/substrate interface
PAC0020	Metal block/repair interface	Repair/substrate interface	Repair/substrate interface	-
PAC1020	Repair/substrate interface	Repair/substrate interface	Repair/substrate interface	-
PAC0010	Repair/substrate interface	Repair/substrate interface	Repair/substrate interface	-
PAC1010	Repair/substrate interface	Metal block/repair interface	Metal block/repair interface	-

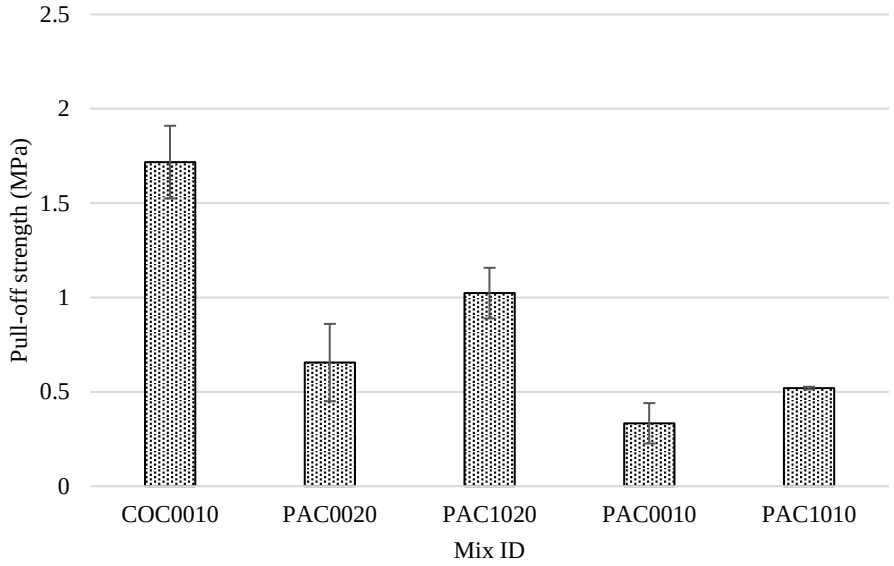

Figure 6.9 Pull-off strength between substrate and repair material

6.3.3.1 PAC versus conventional concrete

Conventional concrete displayed higher pull-off strength than PAC. This was attributed to the nature of production of PAC and conventional concrete. In PAC, as coarse aggregates are preplaced, lesser binder paste is in direct contact with the substrate after grouting, resulting in insufficient bonding between substrate and PAC. In conventional concrete, as all the constituent materials are mixed together to form a homogenous composite, binder paste is in direct contact with the entire substrate area, resulting in higher bond strength. This is illustrated in Figure 6.10.

Compaction applied during casting of conventional concrete could be another reason for improved bonding, as compaction of repair material is one of the important factors influencing the quality of bond between substrate and repair (Silfwerbrand and Beushausen, 2005). Possibilities of voids between coarse aggregates in some PAC specimens due to inefficient penetrability of grout (shown in Figure 6.11) may result in low pull-off strength values, especially for PAC produced using smaller-size coarse

aggregates. However, sample in Figure 6.11 was an extreme case. Test result was discarded and not used in the analysis.

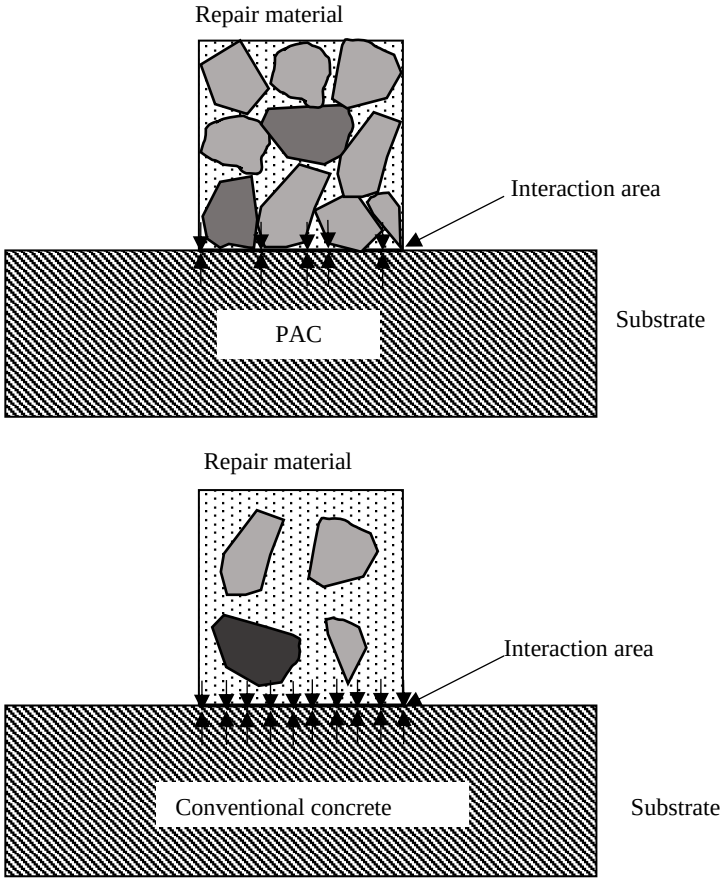

Figure 6.10 Binder paste-substrate interaction

Figure 6.11 Inefficient penetrability of grout in PAC

6.3.3.2 Effects of coarse aggregate size

Unlike compressive strength and splitting tensile strength, pull-off strength of PAC decreases with reduction in coarse aggregate size. With reduction in coarse aggregate size from 20 mm to 10 mm, void content between the coarse aggregates decreases from 38% to 29% (given in Table 3.8). With the reduction in grout content, grout per surface area in substrate/repair material interface reduces, thereby decreasing the bond strength of PAC produced using smaller-sized coarse aggregates. This is in contrast with conventional concrete, where the bond strength decreases with increasing coarse aggregate size (Cheng et al., 2019).

6.3.3.3 Effect of SF

Similar to compressive strength and splitting tensile strength, pull-off strength increases with incorporation of SF. Increase in pull-off strength was observed for both PACs produced using 10 mm and 20 mm coarse aggregates. For PAC produced using 20 mm coarse aggregates, pull-off strength increased by 27%. The results are consistent with that of Momayez et al. (2005) for conventional concrete, where bond strength increased by as much as 22% with incorporation of 7% SF. Increase in pull-off strength due to incorporation of SF could be attributed to change in microstructure of interfacial transition zone due to micro filler effect of SF (Cohen et al, 1994; Kuroda et al, 2000).

6.4 Summary

Pull-off test was conducted to determine the bond strength of repair material made of conventional concrete or PAC and applied to conventional concrete substrate. For PAC as repair material, two sizes of coarse aggregates were considered, i.e. 10 mm and 20 mm. Further, SF was used to partially replace cement at 10% by weight of binder.

In terms of repair material, conventional concrete displayed higher pull-off strength than PAC. As coarse aggregates were preplaced in PAC, lesser binder paste was in direct contact with the substrate at the substrate/repair material interface, resulting in reduced bonding. Unlike compressive strength and splitting tensile strength, with increasing size of coarse aggregates in PAC, pull-off strength increased. This was attributed to increase in void content in between coarse aggregates with increasing coarse aggregate size. This increases the bonding area in the substrate/repair material interface, thus enhanced the bond strength. Incorporation of SF further increased the pull-off strength of PAC.

Overall, although PAC displayed superior mechanical properties, it had low bond attributed to lesser binder paste in direct contact with the substrate. To achieve better bond properties using PAC, larger-size coarse aggregates is recommended (20 mm in this case), and grout is to be supplemented with SF. The expected bond strength for structural repair and non-structural repair are 1.5 MPa and 0.8 MPa, respectively (BS EN 1504-3). Conventional concrete was observed to be suitable for application to both structural and non-structural repair. However, PAC with 20 mm coarse aggregates and grout supplemented with SF satisfied the requirement for non-structural repair.

CHAPTER 7

AN EMPIRICAL MODEL FOR PAC

7.1 Introduction

Many codes of practice and standards provide the basis on mix design of concrete with desired properties (ACI 211.1; BS 8500; IS 10262). They offer recommendations to produce concrete to specified strength and workability, avoiding excessive trial mixes and reducing wastage of resources.

As the casting technique of PAC is unique to that of conventional concrete, mix design of conventional concrete is not suitable for PAC. For instance, reduction in W/B ratio generally results in higher compressive strength in conventional concrete; whereas in PAC, reduction in W/B ratio affects the flowability of grout, which subsequently affects the penetrability of grout through the coarse aggregate skeleton and reduces compressive strength.

This study aims to develop an empirical relationship between the compressive strength of PAC and its constituent components. Mix proportions against 28 days compressive strengths of PAC obtained from the study and other studies and are analysed to develop an empirical relationship. A binder factor Beta ("β") was introduced to account for the change in compressive strength of PAC due to incorporation of GGBS and/or SF. The analysis was conducted by performing statistical analysis.

7.2 Review

Mix proportion of PAC constituting cement-sand grout, compiled from available literatures was used to develop an empirical relationship to predict the compressive strength of PAC. S/B and W/B ratios being the basic constituents of grout and size of

coarse aggregates being the primary factor among other coarse aggregate parameters (shape, texture, and type), influencing penetrability of grout and compressive strength of PAC, was considered. Table 7.1 shows mix proportion of grout and coarse aggregate size in the study and used by others to produce PAC. As coarse aggregate size of 20 mm was found to be optimum size of coarse aggregates to produce PAC using traditional cement-sand grout (Chapter 4), coarse aggregate size was expressed as ratio between maximum nominal size of coarse aggregates ("CA") and 20 mm. Cube compressive strength was converted into cylinder compressive strength by multiplying a factor of 0.8 (BS EN 12504-1). Mix proportions not recommended by the other authors or with constituting supplementary cementitious materials were not considered. For mix proportions considered in Table 7.1, penetrability of grout through the preplaced aggregates was assumed to be satisfactory. Some of the mix proportions by Abdelgader and Elgalhud (2008), displaying high efflux time (around 80 to 180 seconds) were not considered. As such high efflux time may impede the penetrability of grout through preplaced coarse aggregates and compromise with the strength of PAC. Study conducted by Abdelgader et al. (2010) was not considered. PAC in this case was designed for underwater application.

Table 7.1 Mix proportions and compressive strength of PAC

References	Sl. No.	CA (mm)	CA/20	W/B	S/B	PAC compressive strength (MPa)	PAC cylinder strength (MPa)	Predicted PAC cylinder strength (MPa)
Lv et al., 2020*	1	9.50	0.48	0.30	1.00	72.00	57.60	46.38
	2	9.50	0.48	0.30	1.50	66.00	52.80	47.56
	3	9.50	0.48	0.30	2.00	57.50	46.00	48.74
	4	9.50	0.48	0.35	1.00	67.50	54.00	43.42
	5	9.50	0.48	0.35	1.50	61.00	48.80	44.59
	6	9.50	0.48	0.35	2.00	52.50	42.00	45.77
	7	9.50	0.48	0.40	1.00	58.00	46.40	40.45
	8	9.50	0.48	0.40	1.50	55.00	44.00	41.62
	9	9.50	0.48	0.40	2.00	45.00	36.00	42.80
	10	9.50	0.48	0.45	1.00	47.50	38.00	37.48
	11	9.50	0.48	0.45	1.50	44.00	35.20	38.66
Cheng et al., 2019*	12	20.00	1.00	0.42	1.00	39.60	31.68	36.62
	13	20.00	1.00	0.42	1.00	43.90	35.12	36.62
	14	20.00	1.00	0.48	1.30	36.20	28.96	33.76
	15	20.00	1.00	0.54	1.60	33.50	26.80	30.91
	16	20.00	1.00	0.42	1.10	48.00	38.40	36.85
	17	20.00	1.00	0.48	1.30	40.00	32.00	33.76
	18	20.00	1.00	0.54	1.60	35.00	28.00	30.91
Das and Lam, 2019 (Chapter 4)	19	45.00	2.25	0.37	0.50	32.20	32.20	32.12
	20	37.00	1.85	0.37	0.50	33.67	33.67	34.13
	21	20.00	1.00	0.37	0.50	42.46	42.46	38.41
	22	45.00	2.25	0.37	0.50	34.65	34.65	32.12
	23	37.00	1.85	0.37	0.50	34.96	34.96	34.13
	24	20.00	1.00	0.37	0.50	43.58	43.58	38.41
Abdelgader et al., 2018*	25	50.00	2.50	0.45	1.50	30.82	24.66	28.47
	26	50.00	2.50	0.50	1.50	27.82	22.26	25.50
	27	50.00	2.50	0.55	1.50	23.72	18.98	22.53
	28	50.00	2.50	0.45	1.00	30.65	24.52	27.29
	29	50.00	2.50	0.50	1.00	27.10	21.68	24.32
	30	50.00	2.50	0.55	1.00	23.55	18.84	21.35
	31	50.00	2.50	0.45	0.80	30.78	24.62	26.82
	32	50.00	2.50	0.50	0.80	27.23	21.78	23.85
	33	50.00	2.50	0.55	0.80	23.68	18.94	20.88
Nehdi et al., 2017	34	40.00	2.00	0.45	1.00	31.50	31.50	29.80

Mohammadhosseini et al., 2016	35	20.00	1.90	0.50	1.50	33.00	33.00	33.05
	36	20.00	1.90	0.50	1.50	32.00	32.00	33.05
Najjar et al., 2016	37	40.00	2.00	0.44	1.00	31.50	31.50	30.40
Coo and Pheeraphan, 2015*	38	9.50	0.48	0.33	0.00	50.92	40.74	42.25
	39	9.50	0.48	0.33	1.00	57.63	46.10	44.60
	40	25.00	1.25	0.33	0.00	40.37	32.30	38.35
	41	19.00	0.95	0.33	0.50	55.63	44.50	41.04
Saud et al., 2014	42	50.00	2.50	0.45	1.00	32.00	32.00	27.29
	43	50.00	2.50	0.50	1.00	30.00	30.00	24.32
	44	50.00	2.50	0.55	1.00	25.00	25.00	21.35
	45	50.00	2.50	0.65	1.00	17.50	17.50	15.41
Abdelgader et al, 2013*	46	37.40	1.87	0.55	1.00	26.23	20.98	24.52
	47	37.40	1.87	0.65	1.00	16.89	13.51	18.58
	48	37.40	1.87	0.75	1.00	17.56	14.05	12.65
	49	37.40	1.87	0.80	1.00	14.89	11.91	9.68
	50	37.40	1.87	0.65	1.25	20.89	16.71	19.17
	51	37.40	1.87	0.75	1.25	19.78	15.82	13.24
	52	37.40	1.87	0.80	1.25	13.78	11.02	10.27
	53	37.40	1.87	0.65	1.50	24.00	19.20	19.76
	54	37.40	1.87	0.75	1.50	19.78	15.82	13.83
	55	37.40	1.87	0.80	1.50	12.44	9.95	10.86
	56	37.40	1.87	0.65	2.00	24.67	19.74	20.94
	57	37.40	1.87	0.75	2.00	16.89	13.51	15.00
	58	37.40	1.87	0.80	2.00	18.00	14.40	12.03
Abdelgader and Elgalhud, 2008	59	25.00	1.25	0.80	0.50	13.69	13.69	11.62
	60	25.00	1.25	0.80	1.00	15.07	15.07	12.80
	61	25.00	1.25	0.80	1.50	16.01	16.01	13.98
	62	25.00	1.25	0.80	0.50	14.39	14.39	11.62
	63	25.00	1.25	0.80	1.00	15.79	15.79	12.80
	64	25.00	1.25	0.80	1.50	16.31	16.31	13.98
Abdelgader, 1999*	65	63.00	3.15	0.45	1.50	30.36	24.29	25.20
	66	63.00	3.15	0.50	1.50	26.60	21.28	22.23
	67	63.00	3.15	0.55	1.50	22.84	18.27	19.26
	68	63.00	3.15	0.45	1.00	30.34	24.27	24.02
	69	63.00	3.15	0.50	1.00	26.58	21.26	21.05
	70	63.00	3.15	0.55	1.00	22.82	18.26	18.08
	71	63.00	3.15	0.45	0.80	30.33	24.26	23.55
	72	63.00	3.15	0.50	0.80	26.57	21.26	20.58
	73	63.00	3.15	0.55	0.80	22.80	18.24	17.61
	74	63.00	3.15	0.45	1.50	30.82	24.66	25.20

	75	63.00	3.15	0.50	1.50	27.27	21.82	22.23
	76	63.00	3.15	0.55	1.50	23.72	18.98	19.26
	77	63.00	3.15	0.45	1.00	30.65	24.52	24.02
	78	63.00	3.15	0.50	1.00	27.10	21.68	21.05
	79	63.00	3.15	0.55	1.00	23.55	18.84	18.08
	80	63.00	3.15	0.45	0.80	30.78	24.62	23.55
	81	63.00	3.15	0.50	0.80	27.23	21.78	20.58
	82	63.00	3.15	0.55	0.80	23.68	18.94	17.61
	83	63.00	3.15	0.45	1.50	31.05	24.84	25.20
	84	63.00	3.15	0.50	1.50	27.28	21.82	22.23
	85	63.00	3.15	0.55	1.50	23.52	18.82	19.26
	86	63.00	3.15	0.45	1.00	31.14	24.91	24.02
	87	63.00	3.15	0.50	1.00	27.37	21.90	21.05
	88	63.00	3.15	0.55	1.00	23.60	18.88	18.08
	89	63.00	3.15	0.45	0.80	31.20	24.96	23.55
	90	63.00	3.15	0.50	0.80	27.44	21.95	20.58
	91	63.00	3.15	0.55	0.80	23.67	18.94	17.61
Abdul Awal, 1988	92	38.00	1.90	0.52	1.50	28.90	28.90	27.33
	93	38.00	1.90	0.50	1.50	29.00	29.00	28.52

***** Indicates that cube strengths were converted to cylinder strengths

Linear regression was used to analyse the data and determine the effect of the above-mentioned factors on the compressive strength of PAC. Figure 7.1 shows Pareto chart for compressive strength of PAC. It provides the standardized effects of factors which are represented by bars in descending order. Length of each bar represents significance of factor. As shown, W/B had the highest significance on the compressive strength of PAC, followed by CA. S/B had the shortest bar length, indicating that it had a lower significance on compressive strength of PAC, compared to W/B and CA. Equation 7.1 shows the empirical relationship between compressive strength of PAC, CA, W/B, and S/B. It suggests that with the increase in CA and W/B ratio, compressive strength of PAC decreases. However, with increase in S/B ratio, compressive strength of PAC increases slightly.

Table 7.2 shows model summary of Equation 7.1. Sigma (σ) is standard deviation of distance between data values and fitted values. It is measured in units of the response (MPa in this case) and represents how far the actual values fall from the fitted values. R^2 is percentage of variation, explained by the equation. It is 1 minus ratio of error sum of squares to total sum of squares. Higher the value of R^2, better the equation fits the data. Adjusted R^2 indicates the significance of considered factors (CA, W/B, and S/B). It is 1 minus ratio of mean square error to mean square total. Lower the difference between R^2 and adjusted R^2, greater is the significance of the factors. Predicted R^2 determines how well the equation predicts the data. Equations with larger predicted R^2 values indicate better predictive ability. Based on the model summary, regression equation developed was considered to have a satisfactory degree of fit. Figure 7.2 compares predicted compressive strength against actual compressive strength. The data values lie within ± 15% confidence lines (shown by dotted lines in the figure), indicating a reasonably good prediction.

Subsequent to formulating Equation 7.1, PAC mixes (mix ID PAC1 and mix ID PAC 2) were produced to verify the equation. Coarse aggregate size, grout mix proportion and properties of grout are shown in Table 7.3. Table 7.4 shows experimental compressive and predicted compressive strength of PAC. Experimental compressive strength of PAC was close to the predicted compressive strength, implying reliable prediction by Equation 7.1.

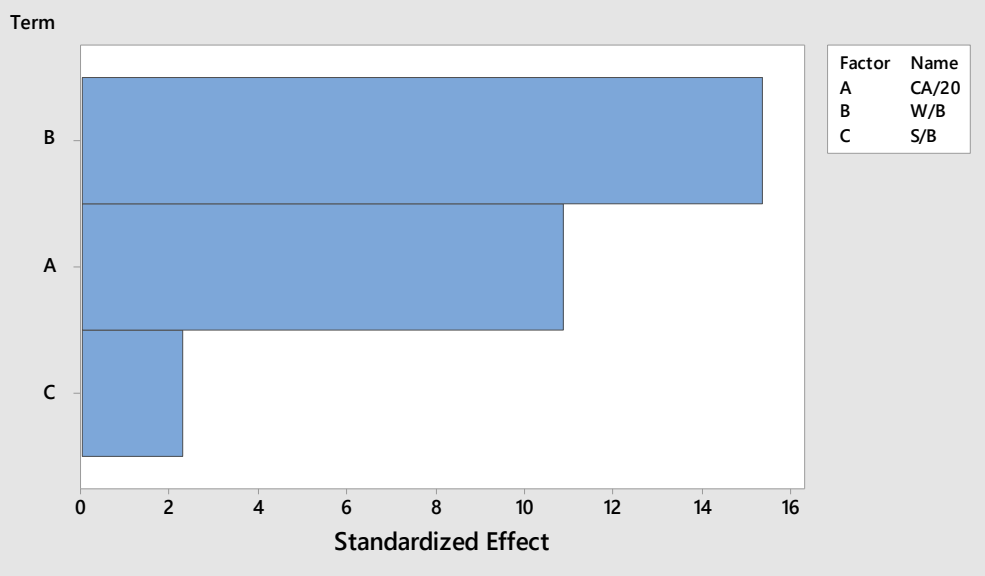

Figure 7.1 Pareto chart of standardized effects on compressive strength of PAC

$$f_c' = 64.23 - 5.03\left(\frac{CA}{20}\right) - 59.37\left(\frac{W}{B}\right) + 2.35\left(\frac{S}{B}\right) \quad \text{Equation 7.1}$$

Table 7.2 Model summary for Equation 7.1

σ	R^2	Adjusted R^2	Predicted R^2
3.836	87.12%	86.66%	85.27%

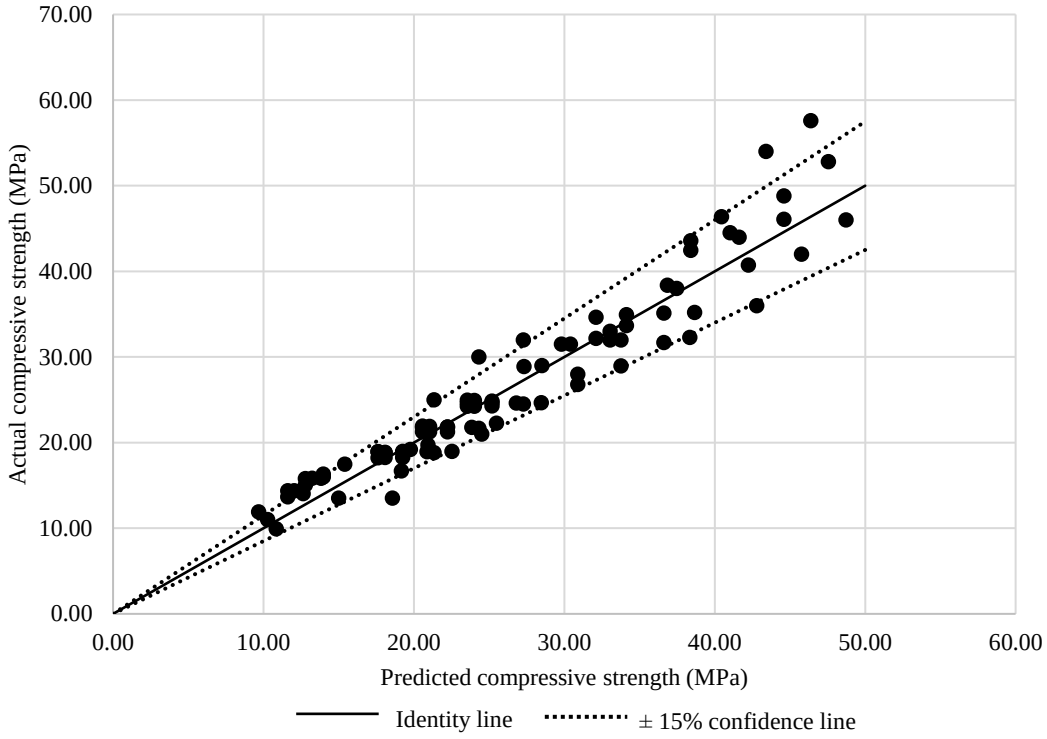

Figure 7.2 Predicted compressive strength versus actual compressive strength

Table 7.3 Coarse aggregate size, grout mix proportion and properties of grout

Mix ID	CA size (mm)	W/B	S/B	GGBS/B	SF/B	SP @ B	Efflux time (sec)	Compressive strength (MPa)			
								1	2	3	Average
PAC1	45.00	0.50	0.50	0.00	0.00	0.00	16.05	50.36	51.46	54.63	52.15
PAC2	10.00	0.40	0.00	0.00	0.00	0.20	19.16	82.69	79.56	79.13	80.46
PAC3	45.00	0.38	0.50	0.20	0.08	0.60	19.33	76.06	74.25	73.34	74.55
PAC4	20.00	0.55	0.30	0.35	0.00	0.00	14.76	57.92	60.33	57.61	58.62
PAC5	10.00	0.35	0.00	0.00	0.10	1.20	20.29	91.78	88.65	92.21	90.88
PAC6	20.00	0.45	0.20	0.15	0.02	0.00	17.02	72.59	73.96	72.57	73.04

Table 7.4 Experimental and predicted compressive strength of PAC

Mix ID	Experimental compressive strength (MPa)				Predicted compressive strength (MPa)	Percentage error (%)
	1	2	3	Average		
PAC1	23.24	24.15	23.29	23.56	24.40	4.87
PAC2	41.72	42.11	44.48	42.77	37.97	9.73
PAC3	30.51	31.45	30.68	30.88	31.26	1.07
PAC4	22.10	21.60	22.15	21.95	22.96	7.74
PAC5	47.66	47.90	49.43	48.33	45.11	5.54
PAC6	35.01	34.94	34.07	33.34	31.40	4.17

7.3 Incorporation of GGBS and/or SF

To incorporate the influence of GGBS and/or SF into the above empirical relationship, experimental investigation was conducted. Grout was produced by partially replacing cement by GGBS and SF at different proportions, based on design of experiment. A 2-level, full factorial design with center points was considered to determine various grout proportions and to develop a binder factor Beta ("β"). β was introduced into the empirical relationship to account for the change in compressive strength due to incorporation of GGBS and/or SF.

7.3.1 Specimens and tests

Grouts were subjected to bleeding tests as per ASTM C 940 and bleeding of all grout mixes were within the permissible limits, i.e. bleeding less than 2% after 120 minutes. Grout consistency was determined by flow cone test to ASTM C 939. Grout compression test at 28 days was performed as per ASTM C 942 using cubes with 50 mm sides. Compressive strength of PAC was performed using 100 mm x 200 mm (diameter x length) cylinders as per ASTM C 39 at 28 days.

7.3.2 Design of the experiment

The parameters in the experiment were considered by applying a 2-level full factorial design (2^k), where 2 is the level of each factor, and superscript k is the number of factors to be studied (Montgomery, 2017). Two factors were selected, namely GGBS/B and SF/B. Center points were included, forming a face-centered central composite design, as shown in Figure 7.3. To estimate the experimental errors, center point was replicated twice. To remove all sources of extraneous variation, mixes were prepared in random order (Coo and Pheeraphan, 2015). Levels for high, midpoint, and low values were +1, 0, and -1, respectively. Interaction between the factors was not considered. Linear regression analysis was used to analyse the data.

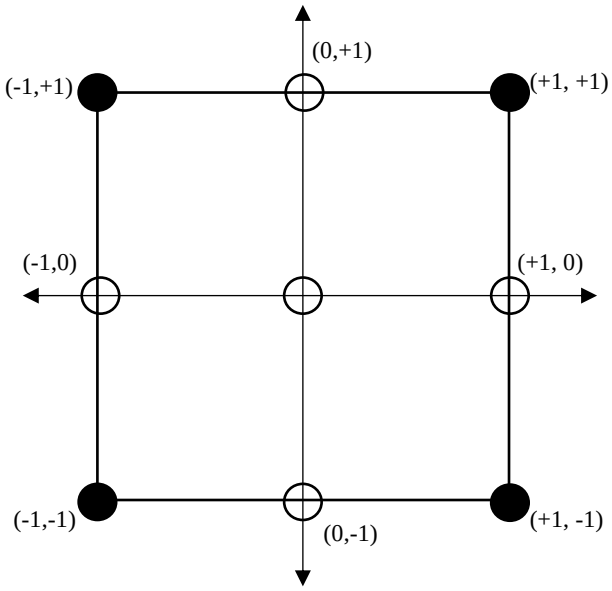

Figure 7.3 Face-centered central composite design

7.3.3 Grout mix design

Based on the trial mixes, W/B ratio was assigned to the lowest possible value of 0.33. SP dosage was modified to obtain an efflux time smaller than 20 seconds. As sand can significantly reduce flowability of grout (Abdelgader, 1996; Abdelgader et al., 2013),

S/B=0.00 was included. This may isolate the effects of GGBS and SF on grout along with achieving a suitable efflux time. Hence, S/B and W/B for all mixes were set constant at 0.00 and 0.33, respectively.

Cement was partially replaced by GGBS and SF at 0% to 40% and 0% to 10% by weight of binder, respectively. Table 7.5 shows the mix proportion of grout. Lowest factor levels (-1) for both GGBS/B and SF/B were set to 0.00, representing a pure cement-water grout. Highest factor levels (+1) for GGBS/B and SF/B were set to 0.40 and 0.10, respectively. As to the mix IDs, GRT represents grout, whereas the first two digits represent the mix proportion of GGBS, the following two digits depict the mix proportion of SF.

Table 7.5 Mix proportion of grout

Sl. no.	Mix ID	Coded level		Actual material ratio	
		GGBS/B	SF/B	GGBS/B	SF/B
1	GRT0000	-1	-1	0.00	0.00
2	GRT4005	1	0	0.40	0.05
3	GRT0010	-1	1	0.00	0.10
4	GRT2010	0	1	0.20	0.10
5	GRT2005	0	0	0.20	0.05
6	GRT4010	1	1	0.40	0.10
7	GRT2005	0	0	0.20	0.05
8	GRT2000	0	-1	0.20	0.00
9	GRT0005	-1	0	0.00	0.05
10	GRT4000	1	-1	0.40	0.00
11	GRT2005	0	0	0.20	0.05

7.3.4 Grout properties

Table 7.6 and Table 7.7 shows efflux time and 28 days compressive strength of grout, respectively. Figure 7.4 and Figure 7.5 represents Pareto chart and contour plot of SP

dosage applied to obtain an efflux time smaller than 20 seconds, respectively. As shown in Figure 7.4, SF/B has a higher significance on efflux time than GGBS/B. This indicates that a small increase or decrease in SF content has larger influence on the flowability of grout than GGBS. Figure 7.5 shows that with increasing GGBS/B, SP dosage requirement to achieve efflux time smaller than 20 seconds decreases. This was attributed to the lubricating effect of GGBS, enhancing the flowability of grout. With increasing SF/B, SP dosage requirement increased, ascribing to increase in water demand by SF due to its fine particle size. At SF/B=0.10, high dosage of SP (>1.4) was required to maintain efflux within 20 seconds. The pattern of contour plot suggests that SF/B can be optimized with GGBS/B to achieve suitable flowability, without increasing SP dosage.

Figure 7.6 and Figure 7.7 shows Pareto chart and contour plot of compressive strength of grout at 28 days, respectively. GGBS/B displays higher significance on compressive strength of grout than SF/B. Contour plot shows that high compressive strength was achieved with high levels of SF/B and low levels of GGBS/B. Mixes incorporating highest level of SF/B with GGBS/B=0 displays compressive strength above 90 MPa. Whereas mixes incorporating highest level of GGBS/B with SF/B=0 displays compressive strength below 70 MPa.

Table 7.6 Efflux time of grout

Mix ID	SP @ B (%)	Efflux time (sec)			
		1	2	3	Average
GRT0000	1.00	19.23	19.55	18.88	19.22
GRT4005	0.84	19.35	19.02	19.11	19.16
GRT0010	1.50	19.00	19.15	19.42	19.19
GRT2010	1.20	20.33	20.69	21.05	20.69
GRT2005	1.00	18.73	18.97	18.97	18.89
GRT4010	1.24	21.09	19.85	20.17	20.37
GRT2005	1.00	18.33	18.77	17.43	18.18
GRT2000	0.70	20.65	21.33	21.02	21.00
GRT0005	1.15	16.23	18.22	18.14	17.53
GRT4000	0.60	16.55	15.95	15.59	16.03
GRT2005	1.00	19.06	18.36	19.49	18.97

Table 7.7 28 days grout compressive strength and binder factor β

Mix ID	28 days compressive strength (MPa)				β
	1	2	3	Average	
GRT0000	86.85	88.06	86.24	87.05	1.00
GRT4005	72.56	75.11	74.56	74.08	0.85
GRT0010	94.25	93.89	90.86	93.00	1.07
GRT2010	82.33	84.06	85.28	83.89	0.96
GRT2005	80.06	80.61	78.82	79.83	0.92
GRT4010	81.36	79.32	79.95	80.21	0.92
GRT2005	80.36	80.11	79.83	80.10	0.92
GRT2000	74.95	72.33	78.08	75.12	0.86
GRT0005	90.62	88.56	88.78	89.32	1.03
GRT4000	66.85	69.85	69.85	68.85	0.79
GRT2005	80.15	81.22	81.54	80.97	0.93

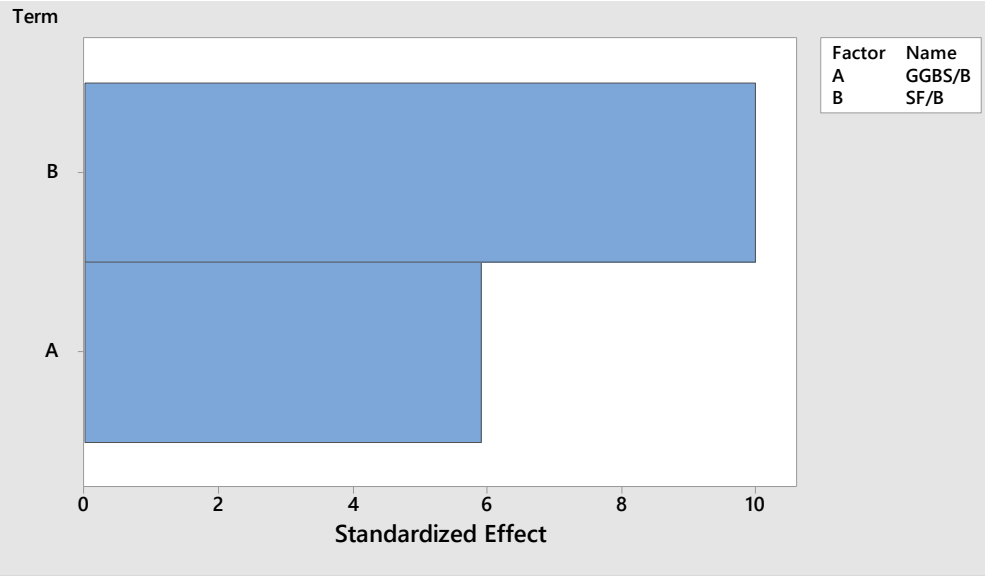

Figure 7.4 Pareto chart of standardized effects on SP dosage

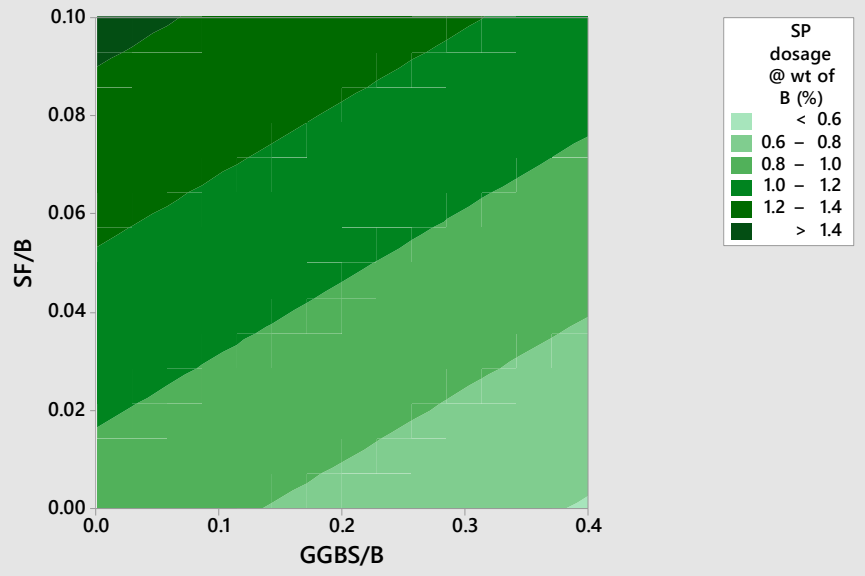

Figure 7.5 Contour plot of SP dosage versus SF/B, GGBS/B

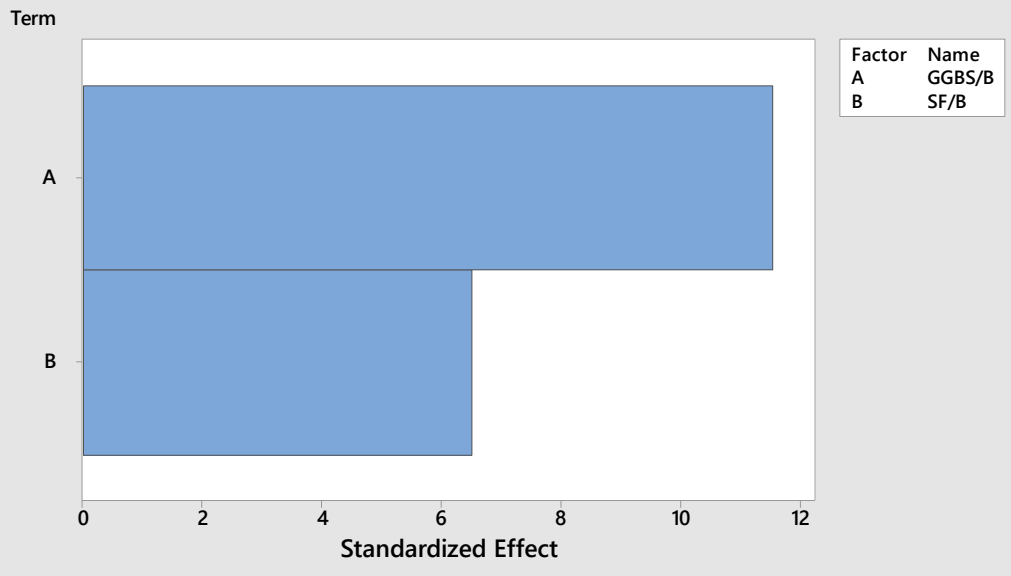

Figure 7.6 Pareto chart of standardized effects on grout compressive strength

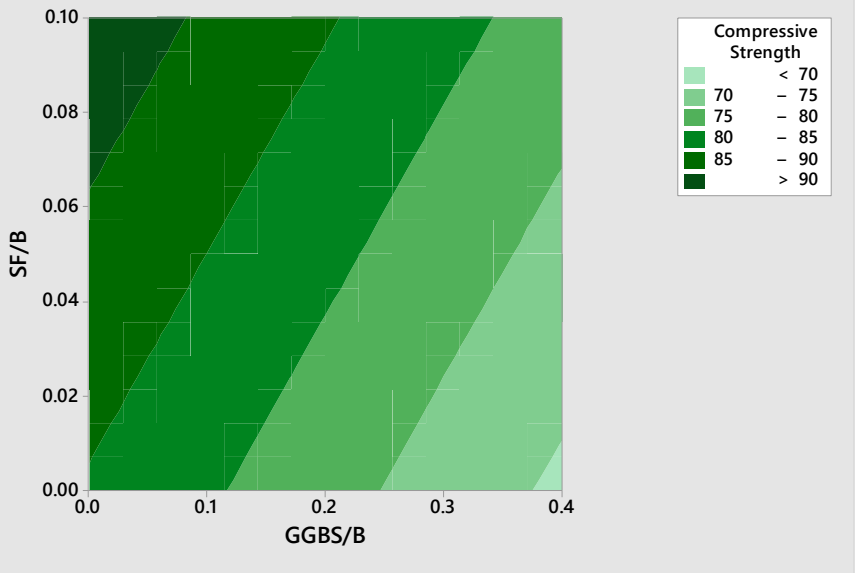

Figure 7.7 Contour plot of compressive strength versus SF/B, GGBS/B

7.4 Binder factor Beta (“β”)

Influence of GGBS and/or SF on compressive strength of PAC at 28 days is indicated by a binder factor Beta (“β”). It was derived from the experimental data. Table 7.7 shows β for grout mixes obtained experimentally. β for control grout mix (GRT-0000)

was considered as reference and was normalized to 1. β was calculated as ratio between compressive strength of grout mix to compressive strength of control grout mix. β was analysed statistically to derive a regression equation that fits the experimental data. Equation 7.2 shows empirical relationship between β, GGBS/B, and SF/B. Table 7.8 shows model summary of Equation 7.2. R^2 and adjusted R^2 values are above 90%. Figure 7.8 compares predicted values against experimental values of β. All data points lie well within ± 10% confidence lines, indicating a reasonably good prediction.

$$\beta = 1 - 0.45\left(\frac{GGBS}{B}\right) + 1.02\left(\frac{SF}{B}\right) \qquad \text{Equation 7.2}$$

Table 7.8 Model summary for Equation 7.2

σ	R^2	Adjusted R^2	Predicted R^2
0.019	95.55%	94.43%	89.30%

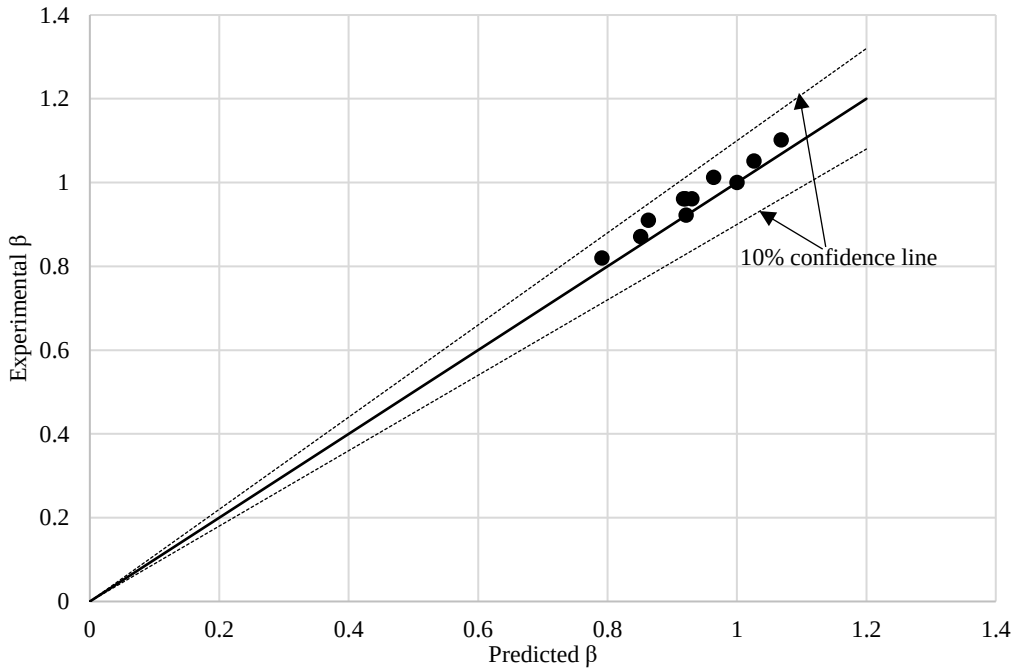

Figure 7.8 Predicted β versus experimental β

Equation 7.1 was modified to incorporate the influence of GGBS and/or SF by introducing β, as shown in Equation 7.3.

$$f'_{c(GGBS,SF)} = (f'_c)(\beta \times \gamma) \quad \text{or} \quad \gamma = \frac{f'_{c(GGBS,SF)}}{f'_c \, x \, \beta} \qquad \text{Equation 7.3}$$

A correlation coefficient "γ" was introduced to correlate compressive strength of grout and PAC, incorporating GGBS and/or SF. Figure 7.9 shows γ value for PAC from Chapter 5. Only mixes with efflux time of grout controlled within 20 seconds were considered. From Figure 7.9, correlation coefficient "γ" was close to 1.

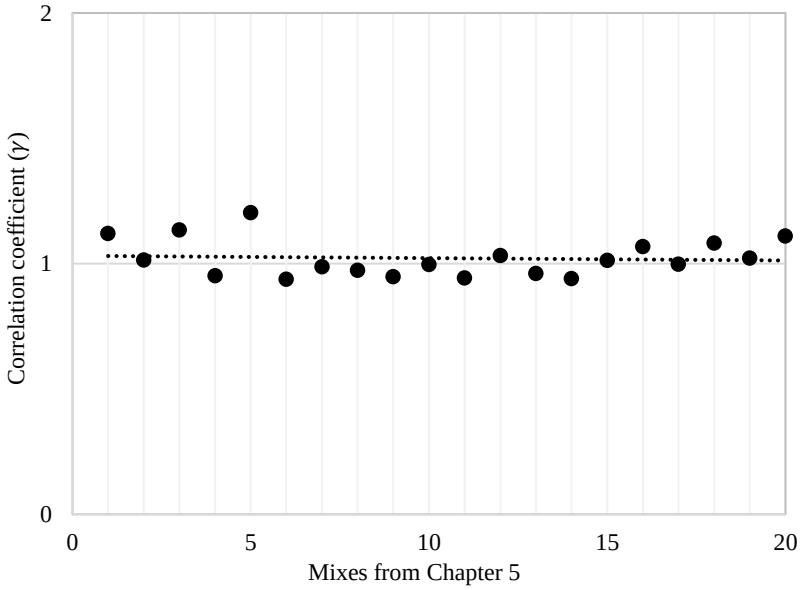

Figure 7.9 Correlation coefficient γ

Equation 7.4 predicts 28 days compressive strength of PAC using GGBS and/or SF as partial replacement of cement within the replacement range of 0 to 40% and 0 to 10%, respectively.

As γ =1, Equation 7.3 was expressed as:

$$=> f'_{c(GGBS,SF)} = (f'_c)(\beta)$$

$$=> f'_{c(GGBS,SF)} = \left\{64.23 - 5.03\left(\frac{CA}{20}\right) - 59.37\left(\frac{W}{B}\right) + 2.35\left(\frac{S}{B}\right)\right\}\left\{1 - 0.45\left(\frac{GGBS}{B}\right) + 1.02\left(\frac{SF}{B}\right)\right\} \quad \text{Equation 7.4}$$

PAC mixes (mix ID PAC3, mix ID PAC4, mix ID PAC5, and mix ID PAC6) were produced to verify the equation (shown in Table 7.4). Results show that compressive strength of PAC obtained experimentally was close to the predicted compressive strength. This indicates that Equation 7.4 provides a reasonable prediction of compressive strength of PAC at 28 days, incorporating GGBS and/or SF. The model is limited to PAC with coarse aggregate size of 9.5 mm to 63 mm, W/B ratio of 0.3 to 0.8, S/B ratio of 0 to 2, GGBS/B ratio of 0 to 0.4, and SF/B ratio of 0 to 0.1.

7.5 Summary

In this chapter, mix design of 28 days compressive strength of PAC incorporating GGBS and/or SF was predicted. Mix proportions along with 28 days compressive strengths of PAC from the study and literatures were statistically analysed to derive an empirical relationship between compressive strength of PAC, CA, W/B, and S/B. To incorporate the effects of GGBS and/or SF in the derived relation, mixes were produced by partially replacing cement with GGBS and SF at different proportions in the grout. Binder factor Beta ("β") was introduced to account for the variation in compressive strength due to incorporation of GGBS and/or SF. 28 days compressive strength of PAC incorporating GGBS and/or SF was derived by introducing β in the above-mentioned empirical relationship. Equation 7.4 predicts the 28 days compressive strength of PAC incorporating GGBS and/or SF at 0 to 40% and 0 to 10% by weight of binder,

respectively. Results predicted by empirical relationship are in good agreement with that of mixes produced for verification.

CHAPTER 8

CONCLUSIONS AND FURTHER STUDIES

8.1 Conclusions

Experimental investigations were conducted to determine the feasibility of producing PAC with easily available resources and without the use of sophisticated pumping equipment. Properties of PAC were evaluated by varying its mix proportion and coarse aggregate size for different grouting processes. Supplementary cementitious materials and fibers were incorporated to enhance the properties of PAC. Mix proportions of grouts were optimized to improve the overall novelty of this unique technique of producing concrete. Based on the study, following conclusions were drawn:

- Mix proportion of grout plays a vital role in grouting process. Generally, W/B ratio contributes towards strength and S/B ratio influences flowability. For a traditional cement-sand grout with efflux time close to 21 seconds, gravity process was successfully used to produce PAC with coarse aggregate size of 20 mm or higher, displaying compatible performance to that of pumping process. For coarse aggregate size below 20 mm, pumping process was recommended as it ensures better penetrability of grout through the coarse aggregates.
- As flowability of grout influences the properties of PAC, it is essential to regulate the flowability of grout within a suitable range by modifying the SP dosage. This ensures efficient penetrability of grout through the preplaced coarse aggregates.
- On one hand, SF reduces flowability and GGBS increases flowability of grout. On the other hand, SF increases compressive strength and GGBS reduces compressive strength of grout. By combining GGBS and SF, they compromise

against each other producing grouts with acceptable compressive strength and suitable flowability. SF enhances both compressive and splitting tensile strength of PAC.

- Inclusion of GGBS and SF enhances resistance to chloride ion penetration of PAC. Although incorporation of GGBS and/or SF increases drying shrinkage of PAC, drying shrinkage of PAC incorporating 40% GGBS and 10% SF is comparable to that of conventional concrete without any GGBS or SF.
- Exclusion of sand (S/B=0) improves flowability and compressive strength of grout but reduces compressive strength of PAC. This indicates that influence of sand on PAC is unique to that of grout. Removal of sand from grout enabled successful reduction in W/B ratio and coarse aggregate size to 0.33 and 10 mm, respectively, and improves strength, durability, and dimensional stability of PAC.
- Conventional concrete displays higher bond strength than that of PAC. Unlike other PAC properties, bond strength of PAC decreases with the reduction in coarse aggregate size. To achieve better bond properties using PAC, larger-size coarse aggregates is recommended (20 mm in this case), with grout supplemented with SF.
- Steel fibers improves compressive strength and splitting tensile strength of PAC. Drying shrinkage of PAC was significantly reduced with increasing steel fiber content.
- By combined test data and other data from literature review, an empirical relationship between compressive strength of PAC and its constituent materials was developed. A binder factor Beta was introduced to account for the change

in compressive strength of PAC due to incorporation of GGBS and/or SF. Results have shown that the empirical equation provides reasonable prediction of compressive strength of PAC

8.2 Further studies

PAC is unique in placement and production techniques. Even with very high potential to durability and dimensional stability, PAC fails to receive the deserved recognition. More research on PAC is essential for its wide acceptance and development as user-friendly repair and construction material.

- Flowability of grout is an important factor in filling the voids between preplaced coarse aggregates. However, research on microstructure of PAC is still limited. The study has indicated the importance of filling the voids between coarse aggregates with flowable grouts. As an alternative, expansive chemicals may be applied to fill the voids. This may help to enhance the potential of producing PAC with superior properties attributing to efficient filling of voids.
- With high mechanical property and dimensional stability on the use of steel fibers in the study, further research on optimization of types of fibers and their aspect ratio is important for development of PAC reinforced with fibers.

REFERENCES

A

Abdelgader, H. S. (1995). Polcrete economical method for dams. In: MWA international conference on dam engineering, Kuala Lumpur, Malaysia, 1-4.

Abdelgader, H. S. (1996). Effect of the quantity of sand on the compressive strength of two-stage concrete. Magazine of Concrete Research, 48(177), 353-360.

Abdelgader, H. S. (1998). Applications of two-stage concreting methods. Zeszyty Naukowe Politechniki Gdańskiej, Budownictwo Lądowe, 89-96.

Abdelgader, H. S. (1999). How to design concrete produced by a two-stage concreting method. Cement and Concrete Research, 29(3), 331-337.

Abdelgader, H. S. and El-Baden, A. S. (2015). Effect of silica fume on two-stage concrete strength. In IOP Conference Series: Materials Science and Engineering, 96(1).

Abdelgader, H. S. and Elgalhud, A. A. (2008). Effect of grout proportions on strength of two-stage concrete. Structural Concrete, 9(3), 163-170.

Abdelgader, H. S. and Górski, J. (2002). Influence of grout proportions on modulus of elasticity of two-stage concrete. Magazine of Concrete Research, 54(4), 251-255.

Abdelgader, H. S. and Górski, J. (2003). Stress-strain relations and modulus of elasticity of two-stage concrete. Journal of Materials in Civil Engineering, 15(4), 329-334.

Abdelgader, H. S. and Górski, J. (2015). Concrete repair using two-stage concrete method. Materiały Budowlane, (8), 66-68.

Abdelgader, H. S., El-Baden, A. S., Abdurrahman, H. A., and Awal, A. A. (2018). Two-stage concrete as a sustainable production. In MATEC Web of Conferences, EDP Sciences, 149.

Abdelgader, H. S., Górski, J., Khatib, J., and El-Baden, A. S. (2016). Two-stage concrete: effect of silica fume and superplasticizers on strength. Concrete Plant and Precast Technology, 82(3), 38-47.

Abdelgader, H. S., Najjar, M. F., and Azabi, T. M. (2010). Study of underwater concrete using two-stage (preplaced aggregate) concrete in Libya. Structural Concrete, 11(3), 161-165.

Abdelgader, H. S., Saud, A. F., and El-Baden, A. S. (2013). Flexural strength of two-stage concrete. In Proceedings of the Third International Conference on Sustainable Construction Materials and Technologies (SCMT3), Kyoto, Japan.

Abdelgader, H.S. and Górski, J. (2002). Influence of grout proportions on modulus of elasticity of two-stage concrete. Magazine of Concrete Research, 54(4), 251-255.

Abdelgader, H.S., Fediuk, R.S., Kurpinska, M., Khatib, J., Murali G., Baranov, A.V., and Timokhin, R.A. (2019). Mechanical properties of two-stage concrete modified by silica fume. Magazine of Civil Engineering, 89(5), 26-38.

Abdul Awal, A. S. (1984). Manufacture and properties of prepacked aggregate concrete (Master's thesis), University of Melbourne, Melbourne, Australia.

Abdul Awal, A. S. (1988). Failure mechanism of prepacked concrete. Journal of Structural Engineering, 114(3), 727-732.

Abdul Awal, A. S. (1992). Creep recovery of prepacked aggregate concrete. Journal of Materials in Civil Engineering, 4(3), 320-325.

ACI 116 (1999). Cement and concrete terminology. American Concrete Institute, ACI Committee, Michigan.

ACI 209.2R (2008). Guide for modeling and calculating shrinkage and creep in hardened concrete. American Concrete Institute, ACI Committee, Michigan.

ACI 211.1 (1996). Standard practice for selecting proportions for normal, heavyweight, and mass concrete. American Concrete Institute, ACI Committee, Michigan.

ACI 233R (1995). Ground granulated blast-furnace slag as a cementitious constituent in concrete. American Concrete Institute, ACI Committee, Michigan.

ACI 237R-07 (2007). Self-consolidating concrete. American Concrete Institute, ACI Committee, Michigan.

ACI 304.1 (2005). Guide for the use of preplaced aggregate concrete for structural and mass concrete applications. American Concrete Institute, ACI Committee, Michigan.

ACI 318 (1999). Building code requirements for structural concrete and commentary. American Concrete Institute, ACI Committee, Michigan.

ACI 363 (1997). State-of-the-art report on high-strength concrete. American Concrete Institute, ACI Committee, Michigan.

ACI E706 (2010). Field guide to concrete repair application procedures: spall repair the preplaced aggregate method. ACI RAP Bulletin, ACI Committee, Michigan.

Ajamu, S. O. and Ige, J. A. (2015). Effect of coarse aggregate size on the compressive strength and the flexural strength of concrete beam. International Journal of Engineering Research and Applications, 5(1), 67-75.

Alexander, K. M. and Wardlaw, J. (1960). Dependence of cement-aggregate bond-strength on size of aggregate. Nature, 187(4733), 230.

Ali, Y. Z. and Ambalavanan, R. (1999). Flexural behaviour of reinforced concrete beams repaired with styrene-butadiene rubber latex, silica fume and methylcellulose repair formulations. Magazine of Concrete Research, 51(2), 113-120.

An, X., Wu, Q., Jin, F., Huang, M., Zhou, H., Chen, C., and Liu, C. (2014). Rock-filled concrete, the new norm of SCC in hydraulic engineering in China. Cement and Concrete Composites, 54, 89-99.

Antony, J. (2003). Design of experiments for engineers and scientists. Elsevier.

ASTM C 1202 (2012). Standard test method for electrical indication of concrete's ability to resist chloride ion penetration. Annual Book of ASTM Standards. ASTM, West Conshohocken.

ASTM C 150 (2001). Standard specification for Portland cement. Annual Book of ASTM Standards, ASTM, West Conshohocken.

ASTM C 157 (2004). Standard test method for length change of hardened hydraulic-cement mortar and concrete. Annual Book of ASTM Standards. ASTM, West Conshohocken.

ASTM C 157 (2008). Test method for length change of hardened hydraulic cement mortar and concrete. Annual Book of ASTM Standards. ASTM, West Conshohocken.

ASTM C 1583 (2004). Standard test method for tensile strength of concrete surfaces and the bond strength or tensile strength of concrete repair and overlay materials by direct tension (pull-off method). Annual Book of ASTM Standards, ASTM, West Conshohocken.

ASTM C 29 (2009). Standard test method for bulk density ("unit weight") and voids in aggregate. Annual Book of ASTM Standards. ASTM, West Conshohocken.

ASTM C 33 (2008). Standard specification for concrete aggregates. Annual Book of ASTM Standards, ASTM, West Conshohocken.

ASTM C 39 (2005). Standard test method for compressive strength of cylindrical concrete specimens. Annual Book of ASTM Standards. ASTM, West Conshohocken.

ASTM C 496 (2011). Standard test method for splitting tensile strength of cylindrical concrete specimens. Annual Book of ASTM Standards, ASTM, West Conshohocken.

ASTM C 939 (2002). Standard test method for flow of grout for preplaced aggregate concrete (flow cone method). Annual Book of ASTM Standards. ASTM, West Conshohocken.

ASTM C 940-R03 (2016). Standard test method expansion and bleeding of freshly mixed grout for preplaced-aggregate concrete in the laboratory. Annual Book of ASTM Standards. ASTM, West Conshohocken.

ASTM C 942 (2008). Standard test method for compressive strength of grouts for preplaced-aggregate concrete in the laboratory. Annual Book of ASTM Standards, ASTM, West Conshohocken.

Austin, S., Robins, P., and Pan, Y. (1999). Shear bond testing of concrete repairs. Cement and Concrete Research, 29(7), 1067-1076.

B

Babalola, O. E., Awoyera, P. O., Tran, M. T., Le, D. H., Olalusi, O. B., Viloria, A., and Ovallos-Gazabon, D. (2020). Mechanical and durability properties of recycled aggregate concrete with ternary binder system and optimized mix proportion. Journal of Materials Research and Technology, 9(3), 6521-6532.

Barr, B. and El-Baden, A. (2003). Shrinkage properties of normal and high strength fibre reinforced concrete. Proceedings of the Institution of Civil Engineers-Structures and Buildings, 156(1), 15-25.

Bayer, I. R., Turanli, L., and Mehta, P. K. (2019). Mass concrete construction using self-compacting mortar. Turkish Journal of Engineering, ISSN 2587-1366, 3(3), 110-119.

Bayer, R. (2004). Use of preplaced aggregate concrete for mass concrete applications (Master's thesis), Middle East Technical University, Ankara, Turkey, 160.

Bentur, A. and Mindess, S. (1986). The effect of concrete strength on crack patterns. Cement and Concrete Research, 16(1), 59-66.

Bentur, A. and Mindess, S. (2006). Fibre reinforced cementitious composites. CRC Press.

Beushausen, H. and Alexander, M. G. (2008). Bond strength development between concretes of different ages. Magazine of Concrete Research, 60(1), 65-74.

Bisschop, J. and Van Mier, J. G. M. (2002). How to study drying shrinkage microcracking in cement-based materials using optical and scanning electron microscopy?. Cement and Concrete Research, 32(2), 279-287.

Bloem, D. L. and Gaynor, R. D. (1963). Effects of aggregate properties on strength of concrete. ACI Journal Proceedings, 60(10), 1429-1456.

BS EN 1881-122 (1998). Testing Concrete-Part 122: Method for Determination of Water Absorption. British Standard Institution, London.

BS EN 12504-1 (2009). Testing Concrete in Structures. Cored Specimens, Taking, Examining and Testing in Compression. British Standard Institution, London.

BS EN 13791 (2019). Assessment of in-situ compressive strength in structures and precast concrete components. British Standard Institution, London.

BS ISO 1920-8 (2009). Determination of drying shrinkage of concrete for samples prepared in the field or in the laboratory. British Standard Institution, London.

BS EN 8500 (2002). Concrete Complementary-British Standard to BSEN206-1 Part 1: Method of specifying and guidance for the specifier, Part 2: Specification for constituent materials and concrete. British Standard Institution, London.

Bu, J., Tian, Z., Zheng, S., and Tang, Z. (2017). Effect of sand content on strength and pore structure of cement mortar. Journal of Wuhan University of Technology-Mater. Sci. Ed., 32(2), 382-390.

Bungey, J. H. and Madandoust, R. (1992). Factors influencing pull-off tests on concrete. Magazine of Concrete Research, 44(158), 21-30.

C

Casson, R. B. J. and Davies, I. L. (1986). Performance of concrete backfilling materials for shafts and tunnels in rock formations. Commission of the European Communities, Directorate- General Science, 1, No. EUR 10383EN/1, 91.

Champion, S. and Davis, L. (1958). Grouted concrete construction. Reinforced Concrete Rev, 569-608.

Chen, S. G., Zhang, C. H., Jin, F., Cao, P., Sun, Q. C., and Zhou, C. J. (2019). Lattice Boltzmann-Discrete element modeling simulation of SCC flowing process for rock-filled concrete. Materials, 12(19), 3128.

Cheng, A., Huang, R., Wu, J. K., and Chen, C. H. (2005). Influence of GGBS on durability and corrosion behavior of reinforced concrete. Materials Chemistry and Physics, 93(2-3), 404-411.

Cheng, A., Huang, R., Wu, J. K., and Chen, C. H. (2005). Influence of GGBS on durability and corrosion behavior of reinforced concrete. Materials Chemistry and Physics, 93(2-3), 404-411.

Cheng, Y., Liu, S., Zhu, B., Liu, R., and Wang, Y. (2019). Preparation of preplaced aggregate concrete and experimental study on its strength. Construction and Building Materials, 229, 116847.

Choi, S. Y., Park, J. S., and Jung, W. T. (2011). A study on the shrinkage control of fiber reinforced concrete pavement. Procedia Engineering, 14, 2815-2822.

Cohen, M. D., Goldman, A., and Chen, W. F. (1994). The role of silica fume in mortar: transition zone versus bulk paste modification. Cement and Concrete Research, 24(1), 95-98.

Cohen, M. D., Goldman, A., and Chen, W. F. (1994). The role of silica fume in mortar: transition zone versus bulk paste modification. Cement and Concrete Research, 24(1), 95-98.

Coo, M. and Pheeraphan, T. (2015). Effect of sand, fly ash, and coarse aggregate gradation on preplaced aggregate concrete studied through factorial design. Construction and Building Materials, 93, 812-821.

Coo, M. and Pheeraphan, T. (2016). Effect of sand fly ash and limestone powder on preplaced aggregate concrete mechanical properties and reinforced beam shear capacity. Construction and Building Materials, 120, 581-592.

Cordon, W. A. and Gillespie, H. A. (1963). Variables in concrete aggregates and Portland cement paste which influence the strength of concrete. ACI Journal Proceedings, 60(8), 1029-1052.

Courard, L., Piotrowski, T., and Garbacz, A. (2014). Near-to-surface properties affecting bond strength in concrete repair. Cement and Concrete Composites, 46, 73-80.

D

Das, K. K. and Lam, E. S.S. (2019). Feasibility of producing two-stage (preplaced aggregate) concrete by gravity process. Structural Concrete, 21(3), 1157-1163.

Davis, H., Troxell, G., and Wiskocil, C. (1955). The testing and inspection of engineering materials. 3rd Ed., McGraw-Hill Book Company, New York.

Davis, R. E. (1960). Prepakt method of concrete repair. ACI Materials Journal, 57(8), 155-172.

Davis, R. E. and Haltenhoff, C. E. (1956). Mackinac bridge pier construction. ACI Journal Proceedings, 53(12), 581-595.

Davis, R. E., Johnson, G. D., and Wendell, G. E. (1955). Kemano penstock tunnel liner backfilled with prepacked concrete. In ACI Journal Proceedings, 52(3), 287-308.

Delatte, N. J., Williamson, M. S., and Fowler, D. W. (2000). Bond strength development of high-early-strength bonded concrete overlays. ACI Materials Journal, 97(2), 201-207.

Dixon, A. G. (1988). Correlations for wall and particle shape effects on fixed bed bulk voidage. The Canadian Journal of Chemical Engineering, 66(5), 705-708.

Du, Q., Sun, Q., Lv, J., and Yang, J. (2017). Use of preplaced casting method in lightweight aggregate concrete. Advances in Materials Science and Engineering. 1-7.

E

Ede, A. N., Bamigboye, G. O., Olofinnade, O. M., and Shittu, K. K. (2016). Influence of portland cement brands and aggregates sizes on the compressive strength of normal concrete. In Materials Science Forum, Trans Tech Publications, 866, 78-82.

Elchalakani, M., Aly, T., and Abu-Aisheh, E. (2014). Sustainable concrete with high volume GGBFS to build Masdar City in the UAE. Case Studies in Construction Materials, 1, 10-24.

Emborg, M., Jonasson, J. E., Nilsson, M., Utsi, S., and Simonsson, P. (2005). Designing robust SCC for industrial construction with cast in place concrete. In North American Conference on the Design and Use of Self Consolidating Concrete, 1251-1257.

Emmons, P. (1993). Concrete repair and maintenance illustrated. Kingston, M.R.S. Means Company, Kingston, Massachusetts.

Espeche, A. D. and León, J. (2011). Estimation of bond strength envelopes for old-to-new concrete interfaces based on a cylinder splitting test. Construction and Building Materials, 25(3), 1222-1235.

F

Folliard, K. J. and Berke, N. S. (1997). Properties of high-performance concrete containing shrinkage-reducing admixture. Cement and Concrete Research, 27(9), 1357-1364.

Fu, T., Deboodt, T., and Ideker, J. H. (2016). Development of shrinkage limit specification for high performance concrete used in bridge decks. Cement and Concrete Composites, 72, 17-26.

Furnas, C. C. (1931). Grading aggregates, mathematical relations for beds of broken solids of maximum density. Industrial and Engineering Chemistry, 23(9), 1052-1058.

G

Gao, J., Sun, W., and Morino, K. (1997). Mechanical properties of steel fiber-reinforced, high-strength, lightweight concrete. Cement and Concrete Composites, 19(4), 307-313.

Goodier, C. I. (2003). Development of self-compacting concrete. Proceedings of the Institution of Civil Engineers-Structures and Buildings, 156(4), 405-414.

Grünewald, S. and Walraven, J. C. (2001). Parameter-study on the influence of steel fibers and coarse aggregate content on the fresh properties of self-compacting concrete. Cement and Concrete Research, 31(12), 1793-1798.

Guo, Y., Wu, J., Wang, C., and Zhang, F. (2020). Study on the influence of the shape and size of coarse aggregate on the strength of concrete. In IOP Conference Series: Materials Science and Engineering, 780(4), 42.

H

Holschemacher, K., Mueller, T., and Ribakov, Y. (2010). Effect of steel fibres on mechanical properties of high-strength concrete. Materials and Design, 31(5), 2604-2615.

Hu, J. (2005). A study of effects of aggregate on concrete rheology. Iowa State University, Iowa.

Huang, M., An, X., Zhou, H., and Jin, F. (2008). Rock-fill concrete, a new type of concrete. Proceeding of International fib Symposium, 1047-1049.

Hughes, B. P. and Chapman, G. P. (1966). The deformation of concrete and micro-concrete in compression and tension with particular reference to aggregate size. Magazine of Concrete Research, 18(54), 19-24.

I

ICRI Project Award (2015). Regency house condominium plaza parking garage repairs. Phoenix, Arizona, Concrete Repair Bulletin, retrieved from: https://www.icri.org/resource/resmgr/CRB/2015NovDec/CRBNovDec15_RegencyHouse.pdf

IS 10262 (2009) Guidelines for concrete mix design proportioning. Bureau of Indian Standards, Delhi.

J

Johari, M. M., Brooks, J. J., Kabir, S., and Rivard, P. (2011). Influence of supplementary cementitious materials on engineering properties of high strength concrete. Construction and Building Materials, 25(5), 2639-2648.

K

Kankam, C. K. (1997). The influence of palm kernel fibers on crack development in concrete. Journal of Ferrocement, 27(1), 1-6.

Khan, M. I. and Siddique, R. (2011). Utilization of silica fume in concrete: Review of durability properties. Resources, Conservation and Recycling, 57, 30-35.

Khatib, J. M. and Hibbert, J. J. (2005). Selected engineering properties of concrete incorporating slag and metakaolin. Construction and Building Materials, 19(6), 460-472.

Kozul, R. and Darwin, D. (1997). Effects of aggregate type, size, and content on concrete strength and fracture energy. University of Kansas Center for Research, Inc.

Kuroda, M., Watanabe, T., and Terashi, N. (2000). Increase of bond strength at interfacial transition zone by the use of fly ash. Cement and Concrete Research, 30(2), 253-258.

Kwan, A. K. and Ng, I. Y. (2010). Improving performance and robustness of SCC by adding supplementary cementitious materials. Construction and Building Materials, 24(11), 2260-2266.

L

Lam, S. S. E., Wong, V., and Lee, R. S. M. (2019). Bonding assessment of semi-precast slabs subjected to flexural load and differential shrinkage. Engineering Structures, 187, 25-33.

Lee, I. W., Pyo, S., and Jung, Y. H. (2016). Development of quick-hardening infilling materials for composite railroad tracks to strengthen existing ballasted track. Composites Part B: Engineering, 92, 37-45.

Lee, K. M., Lee, H. K., Lee, S. H., and Kim, G. Y. (2006). Autogenous shrinkage of concrete containing granulated blast-furnace slag. Cement and Concrete Research, 36(7), 1279-1285.

Li S. E., Geissert D. G., Frantz G. C., and Stephens J. E. (1999). Freeze-thaw bond durability of rapid-setting concrete repair materials. ACI Materials Journal, 96(2), 241-249.

Li, G. (2003). A new way to increase the long-term bond strength of new-to-old concrete by the use of fly ash. Cement and Concrete Research, 33(6), 799-806.

Li, G., Xie, H., and Xiong, G. (2001). Transition zone studies of new-to-old concrete with different binders. Cement and Concrete Composites, 23(4-5), 381-387.

Li, M. and Li, V. C. (2006). Behaviour of ECC/concrete layered repair system under drying shrinkage conditions. Restoration of Buildings and Monuments, 12, 143-160.

Littlejohn, G. S. (1984). Grouted pre-placed aggregate concrete. Concrete in the Ground Conference, the Concrete Society, London.

Littlejohn, G. S. and Crawley, J. D. (1983). Pre-placed aggregate foundations for Korean nuclear power plant. Concrete (London), 17(10), 17-20.

Littlejohn, GS and Swart, A. (2006). Design of permanent intruded plugs at South Deep Gold Mine. Journal of the Southern African Institute of Mining and Metallurgy, 106(5), 331-341.

Lura, P. (2003). Autogenous deformation and internal curing of concrete. (Ph.D. dissertation), Technical University Delft, Delft, Netherlands.

Lv, J., Zhou, T., and Li, K. (2020). Development and investigation of a new low-cement-consumption concrete-preplaced aggregate concrete. Sustainability, 12(3), 1080.

Lv, J., Zhou, T., Du, Q., Li, K., and Jin, L. (2020). Research on the bond behavior of preplaced aggregate concrete-filled steel tube columns. Materials, 13(2), 300.

M

Marke, M. O. A. and Marke, A. I. (2010). Comparative evaluation of the flexural strength of concrete and colcrete. Nigerian Journal of Technology, 29(1), 13-22.

Mohammadhosseini, H., Awal, A. A., and Sam, A. R. M. (2016). Mechanical and thermal properties of prepacked aggregate concrete incorporating palm oil fuel ash. Sādhanā, 41(10), 1235-1244.

Momayez, A., Ehsani, M. R., Ramezanianpour, A. A., and Rajaie, H. (2005). Comparison of methods for evaluating bond strength between concrete substrate and repair materials. Cement and Concrete Research, 35(4), 748-757.

Momayez, A., Ramezanianpour, A. A., Rajaie, H., and Ehsani, M. R. (2004). Bi-surface shear test for evaluating bond between existing and new concrete. Materials Journal, 101(2), 99-106.

Montgomery D. C. (2017). Design and analysis of experiments. John Wiley and Sons.

Morgan, D. R. (1996). Compatibility of concrete repair materials and systems. Construction and Building Materials, 10(1), 57-67.

Morohashi, N., Meyer, C., and Abdelgader, H.S. (2013). Concrete with recycled aggregates -two-stage production method. CPI-Concrete Plant International, (4), 34-41.

N

Najjar, M. F. (2016). Innovating two-stage concrete with improved rheological, mechanical and durability properties (Ph.D. dissertation), Dept. Civil and Environmental Engineering, The University of Western Ontario, Ontario, USA.

Najjar, M. F., Soliman, A. M., and Nehdi, M. L. (2014). Critical overview of two-stage concrete: properties and applications. Construction and Building Materials, 62, 47-58.

Najjar, M. F., Soliman, A. M., and Nehdi, M. L. (2016). Two-stage concrete made with single, binary and ternary binders. Materials and Structures, 49(1-2), 317-327.

Narrow, L. (1954). Barite aggregate and grout intrusion method used in shield for materials testing reactor. Civil Engineering, 24(5), 46-49.

Nehdi, M. L., Najjar, M. F., Soliman, A. M., and Azabi, T. M. (2017). Novel eco-efficient two-stage concrete incorporating high volume recycled content for sustainable pavement construction. Construction and Building Materials, 146, 9-14.

Nehdi, M. L., Najjar, M. F., Soliman, A. M., and Azabi, T. M. (2017). Novel steel fibre-reinforced preplaced aggregate concrete with superior mechanical performance. Cement and Concrete Composites, 82, 242-251.

Nehdi, M. L., Najjar, M. F., Soliman, A. M., and Azabi, T. M. (2017). Novel eco-efficient two-stage concrete incorporating high volume recycled content for sustainable pavement construction. Construction and Building Materials, 146, 9-14.

Neville, A. and Brooks, J. (1987). Concrete technology. 8th Ed., Longman Scientific and Technical, England.

Neville, A. M. (2011). Properties of concrete. 4th Ed., London Pearson Education Limited, London.

Nguyen, D. T., Sahamitmongkol, R., Trong, L. N., Tongaroonsri, S., and Tangtermsirikul, S. (2010). Prediction of shrinkage cracking age of concrete with and without expansive additive. Songklanakarin Journal of Science and Technology, 32(5), 469-480.

Nochaiya, T., Wongkeo, W., and Chaipanich, A. (2010). Utilization of fly ash with silica fume and properties of Portland cement-fly ash-silica fume concrete. Fuel, 89(3), 768-774.

Noushini, A., Vessalas, K., Arabian, G., and Samali, B. (2014). Drying shrinkage behaviour of fibre reinforced concrete incorporating polyvinyl alcohol fibres and fly ash. Advances in Civil Engineering, 1-10.

Nowek, A., Kaszubski, P., Abdelgader, H., and Górski, J. (2007). Effect of admixtures on fresh grout and two-stage (pre-placed aggregate) concrete. Structural Concrete, 8(1), 17-23. DOI:10.1680/stco.2007.8.1.17.

O

O'Malley, J. and Abdelgader, H. S. (2010). Investigation into viability of using two-stage (pre-placed aggregate) concrete in Irish setting. Frontiers of Architecture and Civil Engineering in China, 4(1), 127-132.

Oluokun, A. F. and Haghayeghi, A. R. (1998). Flexural behavior of reinforced concrete beams retrofitted or repaired with slurry infiltrated mat concrete. Structural Journal, 95(6), 654-664.

Omar, B., Fattoum, K., Maissen, B., and Farid, B. (2010). Influence of the roughness and moisture of the substrate surface on the bond between old and new concrete. Contemporary Engineering Sciences, 3(3), 139-147.

Omidi, M. F., Rajabi, A. M., Abdelgader, H. S., Kurpińska, M., and Wilde, K. (2019). Effect of coarse grain aggregate on strength parameters of two-stage concrete. Materiały Budowlane, 3(559), 2-4.

Oner, A. and Akyuz, S. (2007). An experimental study on optimum usage of GGBS for the compressive strength of concrete. Cement and Concrete Composites, 29(6), 505-514.

Orchard, D. (1973). Concrete Technology. 3rd Ed., 2, Applied Science Publishers Ltd, London, 409-416.

P

Poon, C. S., Kou, S. C., and Lam, L. (2006). Compressive strength, chloride diffusivity and pore structure of high performance metakaolin and silica fume concrete. Construction and Building Materials, 20(10), 858-865.

R

Rao, G. A. (2001). Long-term drying shrinkage of mortar—influence of silica fume and size of fine aggregate. Cement and Concrete Research, 31(2), 171-175.

Rashid, M. A. and Mansur, M. A. (2009). Considerations in producing high strength concrete. Journal of Civil Engineering, 37(1), 53-63.

Reis, J. M. L. and Ferreira, A. J. M. (2003). Fracture behavior of glass fiber reinforced polymer concrete. Polymer Testing, 22(2), 149-153.

REMR TN CS-MR-9.4 (1992). Specialized repair technique: preplaced-aggregate concrete. REMR Technical Note CS-MR-9.4, Suppl 5, Army Corps of Engineers, Vicksburg, Mississippi.

Roussel, N. and Le Roy, R. (2005). The Marsh cone: a test or a rheological apparatus?. Cement and concrete research, 35(5), 823-830.

S

Sakata, K. and Shimomura, T. (2004). Recent progress in research on and code evaluation of concrete creep and shrinkage in Japan. Journal of Advanced Concrete Technology, 2(2), 133-140.

Saluja, S., Kaur, K., Goyal, S., and Bhattacharjee, B. (2019). Assessing the effect of GGBS content and aggregate characteristics on drying shrinkage of roller compacted concrete. Construction and Building Materials, 201, 72-80.

Samad, S. and Shah, A. (2017). Role of binary cement including Supplementary Cementitious Material (SCM), in production of environmentally sustainable concrete: A critical review. International Journal of Sustainable Built Environment, 6(2), 663-674.

Saud, A. F., Abdelgader, H. S., and El-Baden, A. S. (2014). Compressive and tensile strength of Two-stage concrete. In Advanced Materials Research, 893, 585-592.

Shumuye, E. D. and Jun, Z. (2018). A review on ground granulated blast slag (GGBS) in concrete. In Proceedings of Eighth International Conference On Advances in Civil and Structural Engineering-CSE, Kuala Lumpur, Malaysia, 5-10.

Siddique, R. (2011). Utilization of silica fume in concrete: Review of hardened properties. Resources, Conservation and Recycling, 55(11), 923-932.

Silfwerbrand, J. (1990). Concrete bond in repaired bridge decks. Concrete International, 12(9), 61-66.

Silfwerbrand, J. and Beushausen, H. (2005). Bonded concrete overlays-bond strength issues. In Proceedings ICCRRR 2005 International Conference on Concrete Repair, Rehabilitation and Retrofitting, Cape Town, South Africa, 19-21.

Song, P. S. and Hwang, S. (2004). Mechanical properties of high-strength steel fiber-reinforced concrete. Construction and Building Materials, 18(9), 669-673.

Strzelecki, Z. and Kohutek, Z. (1979). Research on possible application of 'polcrete' concrete for supporting long openings (in Czech). International Journal of Rock Mechanics and Mining Sciences and Geomechanics Abstracts, 18(4), 73.

Suhad M.A., Dunya, K. I., and Dhamya G. (2018). Mechanical properties of the light weight foam concrete with steel fiber of different aspect ratio. 1st International Scientific Conference of Engineering Sciences-3rd Scientific Conference of Engineering Science (ISCES), 305-310.

T

Takahashi, T., Itou, K., and Fuchigami, S. (2012). Development of pre-packed concrete trackbed for Shinkansen. Railw Tech Res Inst Rep, 26, 19-24.

Talbot C., Pigeon M., Beaupre´ D., and Morgan D. R. (1994). Influence of surface preparation on long-term bonding of shotcrete. ACI Materials Journal, 91(6), 560-566.

Tang, K., Khatib, J., and Beattie, G. (2017). Effect of partial replacement of cement with slag on the early-age strength of concrete. Proceedings of The Institution of Civil Engineers-Structures and Buildings, 170(6), 451-461.

Tayeh, B. A., Bakar, B. A., Johari, M. M., and Ratnam, M. M. (2013). The relationship between substrate roughness parameters and bond strength of ultra high-performance fiber concrete. Journal of Adhesion Science and Technology, 27(16), 1790-1810.

Tirpak, E. G. (1954). Design and placement techniques of barytes concrete for reactor biological shields (No. ORNL-1739). Oak Ridge National Lab, Oak Ridge, USA.

Toutanji, H. A. and El-Korchi, T. (1995). The influence of silica fume on the compressive strength of cement paste and mortar. Cement and Concrete Research, 25(7), 1591-1602.

Trottier, J. F., Mahoney, M., and Forgeron, D. (2002). Can synthetic fibers replace welded-wire mesh in slabs-on-ground?. Concrete International, 24(11), 59-68.

Tumidajski, P. J. and Gong, B. (2006). Effect of coarse aggregate size on strength and workability of concrete. Canadian Journal of Civil Engineering, 33(2), 206-213.

Tuyan, M., Zhang, L. V., and Nehdi, M. L. (2020). Development of sustainable alkali-activated slag grout for preplaced aggregate concrete. Journal of Cleaner Production, 277.

V

Varghese, L., Rao, V. V. L. K., and Parameswaran, L. (2017). Effect of nanosilica on drying shrinkage and creep properties of cement concrete. In Advance Materials Proceedings, 2(1), 56-60.

Vieira, M., Bettencourt, A., Camelo, A., and Ferreira, J. (2010). Self-compacting mortar for mass concrete application with PAC technology. Proceedings of SCC2010, Montreal, Canada.

Vizini, V. O. S., Cacciari, P. P., and Futai, M. M. (2020). Numerical assessment of factors influencing the tensile strength of rocks via pull-off test. International Journal of Geomechanics, 20(7).

W

Wang, B., Jin, F., Zhou, H., Huang, D., Liu, N., Wang, W., and Wang, Y. (2019). Pilot study on vibrated rock-filled concrete. Journal of Advanced Concrete Technology, 17(10), 559-570.

Warner, J. (2005). Preplaced-aggregate concrete. Concrete International, 27(9), 34-38.

Wei, H., Zhang, G., Sun, F., Wang, M., Li, W., and Xu, J. (2019). Experimental research on the properties of rock-filled concrete. Applied Sciences, 9(18), 3767.

Y

Yeau, K. Y. and Kim, E. K. (2005). An experimental study on corrosion resistance of concrete with ground granulate blast-furnace slag. Cement and Concrete Research, 35(7), 1391-1399.

Yildirim, H., Ilica, T., and Sengul, O. (2011). Effect of cement type on the resistance of concrete against chloride penetration. Construction and Building Materials, 25(3), 1282-1288.

Yoon, J. Y., Kim, J. H., Hwang, Y. Y., and Shin, D. K. (2015). Lightweight concrete produced using a two-stage casting process. Materials, 8(4), 1384-1397.

Yousefieh, N., Joshaghani, A., Hajibandeh, E., and Shekarchi, M. (2017). Influence of fibers on drying shrinkage in restrained concrete. Construction and Building Materials, 148, 833-845.

Yuan, C., Chen, W., Pham, T. M., and Hao, H. (2019). Effect of aggregate size on bond behaviour between basalt fibre reinforced polymer sheets and concrete. Composites Part B: Engineering, 158, 459-474.

Yuan, Y. S. and Marosszeky, M. (1991). Major factor influence on the performance of structural repair. Evaluation and Rehabilitation of Concrete Structures and Innovations in Design. In Proceedings of ACI international conference, Hong Kong, 820-837.

Z

Zollo, R. F. (1997). Fiber-reinforced concrete: an overview after 30 years of development. Cement and Concrete Composites, 19(2), 107-122.